The role of G protein-coupled receptor kinases in modulating γ-secretase activity and amyloid-β generation

by

Nicholas Kuzma Todd

B.S, University of Maryland, College Park, 2015

Submitted to the Graduate Faculty of the

School of Medicine in partial fulfillment

of the requirements for the degree of

Doctor of Philosophy

University of Pittsburgh

2021

UNIVERSITY OF PITTSBURGH

School of Medicine

This dissertation was presented

by

Nicholas Kuzma Todd

It was defended on

October 28, 2021

and approved by

Dr. Elias Aizenman, Professor, Department of Neurobiology

Dr. Jeffrey Brodsky, Professor, Department of Biological Sciences

Dr. Peter Friedman, Professor, Department of Pharmacology and Chemical Biology

Dr. Radosveta Koldamova, Professor, Department of Environmental and Occupational Health

Dissertation Director: Dr. Amantha Thathiah, Assistant Professor, Department of Neurobiology

The role of G protein-coupled receptor kinases in modulating γ-secretase activity and amyloid-β generation

Nicholas Kuzma Todd, PhD

University of Pittsburgh, 2021

Pathological changes in the Alzheimer's disease (AD) brain begin up to 20 years prior to the clinical onset of dementia, initially with the aggregation of amyloid-β (Aβ) peptides generated via processive proteolytic cleavage of the amyloid precursor protein (APP) by β-secretase followed by γ-secretase. The γ-secretase complex is a four-subunit aspartyl protease complex that consists of a catalytic presenilin 1 or 2 (PS1 or PS2) subunit, nicastrin (NCT), presenilin enhancer 2 (PEN2), and anterior pharynx-defective 1 (APH1) A or B (APH1A or APH1B). The orphan G protein-coupled receptor (GPCR) GPR3 is a regulator of γ-secretase activity and Aβ generation in AD. GPR3-mediated γ-secretase activity requires GPR3 C-terminal phosphorylation and recruitment of the multifunctional scaffolding protein β-arrestin 2 (βarr2). Canonical GPCR phosphorylation is regulated via the family of kinases known as GPCR kinases (GRKs). Interestingly, βarr2 has been shown to interact directly with the APH1A subunit of γ-secretase, independent of a specific GPCR, to regulate γ-secretase activity. Furthermore, emerging evidence suggests that GRKs regulate both Aβ and tau pathology in AD. Similar to GPCRs, APH1A contains seven transmembrane domains and putative phosphorylation sites in intracellular loop 2 and the carboxy-terminus. Therefore, we hypothesized that the GRK family of kinases can directly regulate γ-secretase activity via modulating non-canonical APH1A phosphorylation and interaction with βarr2 and that specific GRKs can regulate GPR3-mediated Aβ via canonical regulation of the GPCR GPR3. Here, we uncover a novel and constitutive role of the GRK family

of kinases in regulating APH1A phosphorylation and βarr2 interactions. We determine that distinct GRK-mediated phosphorylation barcodes differentially regulate βarr2 binding and γ-secretase cleavage of APP. Computational docking and molecular dynamic simulations reveal that βarr2 binds to APH1A in a similar fashion as a GPCR. Additionally, we discover that GRK2 kinase activity specifically regulates GPR3-mediated Aβ generation. While the exact downstream mechanisms of GPR3-βarr2 signaling that regulate Aβ generation are still undetermined, we propose a model whereby both GPR3 trafficking and regulation of APH1A-βarr2 interaction are involved. Together, this work suggests that drugs targeting the APH1A-βarr2 interaction and GPR3 biased ligands may be therapeutically beneficial in AD.

Table of Contents

1.0 Introduction 1

1.1 Alzheimer's Disease 1

1.1.1 Overview and Clinical Symptoms of Alzheimer's Disease 1

1.1.2 Alzheimer's Disease Pathology 3

1.1.2.1 Amyloid Plaque Pathology 3

1.1.2.2 γ-Secretase 6

1.1.2.3 Tau Pathology 9

1.2 G Protein-Coupled Receptors 12

1.2.1 Overview of GPCR Signaling 13

1.2.2 GPCR Functional Selectivity – Conformation is Key 16

1.2.2.1 GPCR Kinases (GRKs) 18

1.2.2.2 GPCR Phosphorylation Barcodes 21

1.3 GPCR signaling in Alzheimer's Disease 26

1.3.1 GRKs in Alzheimer's Disease 26

1.3.2 G Protein-Coupled Receptor 3 (GPR3) 29

1.4 Dissertation Goal 32

2.0 GPCR kinases mediate an APH1A phosphorylation barcode to regulate amyloid-β generation 34

2.1 Introduction 34

2.2 Results 37

2.2.1 APH1A is phosphorylated in the 2nd intracellular loop (ICL2) and C-terminus 37

2.2.2 Chemical inhibition of GRKs affects βarr2 recruitment and Aβ generation in a physiological model of AD 40

2.2.3 GRKs differentially regulate γ-secretase activity and Aβ generation 42

2.2.4 GRKs differentially regulate APH1A phosphorylation.....48

2.2.5 Site-specific APH1A phosphorylation mediates interaction with βarr2 and γ-secretase activity 51

2.2.6 Structural modeling and MD simulations reveal βarr2 finger loop domain engagement with APH1A cytoplasmic loops.....55

2.2.7 βarr2 finger loop engagement with APH1A ICL2 and ICL3 facilitates binding and γ-secretase activity 61

2.3 Discussion 66

2.4 Materials and Methods 74

2.4.1 Antibodies and Compounds 74

2.4.2 Plasmid Construction.....75

2.4.3 Cell Lines 75

2.4.4 Cell Culture 75

2.4.5 Generation of HEK293 GRK Knockout Monoclonal Cell lines by CRISPR/Cas9.....76

2.4.6 Mass Spectrometry.....77

2.4.7 Aβ enzyme-linked immunosorbent assay (ELISA).....77

2.4.8 β-arrestin PathHunter Assay 78

2.4.9 Co-immunoprecipitation Assays....78

2.4.10 Generation of a βarr2-APH1A complex based on structural alignment 79

2.4.11 Generation of structural models for βarr2-APH1A complex using docking simulations....80

2.4.12 MD simulations of the βarr2-APH1A complex (WT and mutated) 81

3.0 GRK2 orchestrates GPR3-mediated amyloid-β generation.... 84

3.1 Introduction 84

3.2 Results.... 86

3.2.1 GRK2 regulates GPR3-mediated Aβ generation in HEK293 cells....86

3.2.2 GRK2 regulates GPR3-mediated Aβ generation in fAD neurons 87

3.2.3 GRK2 regulates βarr2 recruitment to GPR3 92

3.2.4 GPR3-βarr2 signaling regulates βarr2 interaction with γ-secretase 93

3.3 Discussion 95

3.4 Materials and Methods 99

3.4.1 Antibodies and Compounds 99

3.4.2 Plasmid Construction....99

3.4.3 Cell Lines 99

3.4.4 Cell Culture 100

3.4.5 Aβ enzyme-linked immunosorbent assay (ELISA)....101

3.4.6 Bioluminescence Resonance Energy Transfer (BRET) Assay 101

3.4.7 β-arrestin PathHunter Assay 102

3.4.8 Co-immunoprecipitation Assay 103

3.4.9 Immunostaining and Confocal Microscopy....104

4.0 Discussion..... 106

4.1 APH1 C-terminal phosphorylation in β-arrestin binding and γ-secretase activity 109

4.2 Mechanisms of GPR3-mediated γ-secretase activity and Aβ generation 111

4.3 Exploring GPR3 as a putative regulator of the APH1A phosphorylation barcode 117

4.4 Evaluating the APH1A-βarr2 interaction as a therapeutic target..... 121

4.5 Concluding Remarks..... 123

Appendix A..... 125

Appendix B..... 126

References..... 131

List of Tables

Table 1 DNA sequences for each sgRNA used to generate the CRISPR GRK KO cell lines 82

Table 2 Sequencing primers used to validate the CRISPR GRK KO cell lines 83

List of Figures

Figure 1. APP processing by secretases generates Aβ peptide 6

Figure 2. GRKs mediate a GPCR phosphorylation barcode 25

Figure 3. LC-MS/MS analysis identifies sites of APH1A phosphorylation in HEK293 cells 38

Figure 4. The APH1A subunit of the γ-secretase complex is phosphorylated in ICL2 and the C-terminus 39

Figure 5. Schematic diagram of the βarr2 recruitment to APH1A PathHunter assay 41

Figure 6. Chemical inhibition of GRK2 and GRK3 increases βarr2 recruitment to APH1A and Aβ generation 42

Figure 7. GRK expression in CRISPR GRK KO cell lines 44

Figure 8. γ-secretase subunit expression in GRK KO cell lines 45

Figure 9. Expression of C99-FLAG in GRK KO cell lines corresponding to Aβ ELISAs in Figure 10 46

Figure 10. Genetic deletion of each GRK differentially regulates γ-secretase activity and Aβ generation 47

Figure 11. Differential APH1A phosphorylation is mediated by GRKs and regulates interaction with βarr2 and γ-secretase activity 49

Figure 12. LC-MS/MS analysis identifies novel APH1 S105 phosphorylation in GRK2 KO 51

Figure 13. Expression of APH1A-PK and C99-FLAG corresponding to PathHunter and Aβ ELISA assays in Figure 11 54

Figure 14. Modeling of the APH1A-βarr2 complex based on structural alignment against the complex resolved for rhodopsin..... 57

Figure 15. Structural modeling of the interaction between APH1A and βarr2 and the time evolution of the most stable interfacial contacts for the Alignment and DOCK1 models..... 58

Figure 16. Structural modeling of the interaction between APH1A and βarr2 and the time evolution of the most stable interfacial contacts 60

Figure 17. βarr2 finger loop engagement with APH1A ICL3 and ICL2 facilitates binding and γ-secretase activity 64

Figure 18. Expression of C99-FLAG and βarr2 or APH1A corresponding to Aβ ELISA and PathHunter assays in Figure 17..... 66

Figure 19. GRKs differentially regulate γ-secretase activity by mediating an APH1A phosphorylation barcode..... 73

Figure 20. Representative Western blot images for Aβ ELISA assays corresponding to Figure 21..... 89

Figure 21. GRK2 regulates GPR3-mediated Aβ generation..... 90

Figure 22. 4 week-differentiated fAD neuron characterization..... 91

Figure 23. GRK2 regulates βarr2 recruitment to GPR3..... 93

Figure 24. GPR3- βarr2 signaling regulates βarr2 interaction with γ-secretase 95

Figure 25. Proposed mechanism GPR3-mediated Aβ generation and regulation by GRK2 116

Figure 26. Proposed mechanism of GPR3 modulation of the APH1A phosphorylation barcode in normal physiology and in Alzheimer's disease and GRK2 regulation of these mechanisms 120

Appendix Figure 1. Preliminary evidence of reduced GPR3 Golgi localization and co-localization with APP in a GRK2 KO cell line. 125

Acknowledgements

I would first like to thank my advisor Dr. Amantha Thathiah for her mentorship and guidance throughout my time at the University of Pittsburgh and would like to acknowledge her important role in my growth as a scientist. I am especially grateful for her time and dedication in helping me develop my experiments, my writing, and my communication skills.

I would like to thank all of my research collaborators, especially the members of the MacDonald lab and the Bahar lab. Completion of this dissertation would not have been possible without your excellent work and collaboration. I would like to thank Dr. Matt MacDonald in particular for his additional scientific mentorship and training me in the field of mass spectrometry. I would also like to thank my thesis committee – Dr. Elias Aizenman, Dr. Peter Friedman, Dr. Jeff Brodsky, and Dr. Rada Koldamova – for their guidance and their insightful feedback.

Thank you to all of the current and former members of the Thathiah laboratory. In particular, I would like to thank Dr. Yunhong Huang, Bryan Hurtle, and Thais Guimaraes, who have spent many hours over the years in the lab with me assisting on experiments and sharing many laughs. I wish you all the very best in your careers. I would also like to acknowledge all of the research technicians in the Thathiah lab over the years who have helped me over the course of my graduate career.

Finally, I would like to thank my family, friends, and loved ones for their encouragement and support throughout my years in graduate school. I would like to especially thank my parents, Anita and Bill, for their love, their support, and for always reminding me that no matter what I was frustrated with, at least I didn't have to complete my Ph.D. before computers existed like they both did.

1.0 Introduction

1.1 Alzheimer's Disease

1.1.1 Overview and Clinical Symptoms of Alzheimer's Disease

Alzheimer's disease (AD) is a progressive neurodegenerative disease and is the most prevalent form of dementia, accounting for between 60-80% of cases. In the United States, AD is the sixth leading cause of death. More than one-third of the population over the age of 75 is living with AD and this number is expected to rise as the population ages (1). Clinically, AD is characterized by episodic memory loss, followed by loss of other higher-order cognitive functions. AD can be broadly segmented into two types: early-onset AD (before the age of 65) or late-onset AD (after the age of 65) (2–5). Early-onset AD accounts for around 5% of total cases. Of these patients, 10% suffer from autosomal dominant AD or familial AD (fAD), caused by rare and 100% penetrant mutations in three different genes coding for the amyloid precursor protein (*App*), presenilin-1 (*Psen1*), or presenilin-2 (*Psen2*) (6). Late-onset or sporadic AD accounts for the majority of cases. Women also have a higher likelihood of developing AD than men. The biggest risk factor associated with late-onset AD is age. Additionally, a multitude of environmental, social, lifestyle, and genetic risk factors all contribute to the development of AD (7,8). The most significant genetic risk factor associated with AD is the allelic status of *ApoE* encoding the apolipoprotein E protein involved in regulating lipid homeostasis and lipid/cholesterol transport in the brain (9–11). Of the three polymorphic *ApoE* alleles, namely ε2 (ApoE2), ε3 (ApoE3), and ε4 (ApoE4), individuals carrying one or two copies of ApoE4 have between a 3-to-9-fold increased

likelihood of developing AD than those carrying the more prevalent ApoE3 alleles. Conversely, the rarer ApoE2 allele is protective against AD. In total, over 75 loci have been identified as risk loci for AD (9,10,12).

Clinically, AD is divided into three stages: the preclinical phase, mild cognitive impairment (MCI) due to Alzheimer's disease, and Alzheimer's dementia (4,5,13). The preclinical phase of AD begins up to 20 years prior to clinical onset. During this period, molecular and cellular changes in the brain lead to the accumulation of disease pathology and, while patients do not experience any cognitive symptoms, ultimately is the trigger for neuron death and clinical dementia (14,15). During the MCI stage, patients begin to exhibit impairments in one or more cognitive domains and are characterized by evidence of neuronal death, reduced brain volume, and decreased brain glucose metabolism (16,17). A patient with Alzheimer's dementia experiences the inability to remember new information and exhibits impaired reasoning, impaired ability to function normally and perform normal daily activities, and may experience behavioral changes. The AD brain at the macroscopic level exhibits symmetrical atrophy in the cortex and hippocampus and enlargement or dilation of the lateral ventricles. Cortical atrophy is observed particularly in the medial temporal lobes while generally sparing the motor, sensory, and visual cortices (18). Overall, AD is a devastating neurodegenerative disorder that presents a large burden to society, both emotionally for patients and their families as well as the economically on the healthcare system. Further research is still needed to develop a therapeutic strategy to prevent or reverse clinical dementia in AD patients.

1.1.2 Alzheimer's Disease Pathology

AD is characterized by two main pathological hallmarks – extracellular plaques consisting of amyloid-β (Aβ) peptides and intra-neuronal neurofibrillary tangles (NFTs) composed of post-translationally modified and mislocalized microtubule-binding protein tau (18–20). In addition to the two main pathologies, the majority of AD brains contain additional co-existing, non-AD pathologies. The main co-existing pathologies include inclusions of the TAR DNA-binding protein 43 (TDP-43), observed in 20-50% of all AD patients and 75% in severe AD cases, and α-synuclein (21,22), observed in ~25% of AD patients. The incidence of comorbidities increases with age. Furthermore, AD brains can be characterized by dystrophic neurites and an increase in activated microglia and reactive astrocytes (23).

1.1.2.1 Amyloid Plaque Pathology

Amyloid pathology in the brain begins up to 20 years prior to the clinical onset of dementia and precedes the observation of tau pathology (24). Amyloid plaque pathology is first observed in the associative cortex and progressively spreads from the neocortex to the allocortex as the disease progresses (18,23). In 1992, Dr. John Hardy and Dr. Gerald Higgins first proposed the amyloid cascade hypothesis of Alzheimer's disease in which they posit that amyloid precursor protein (APP) cleavage to generate Aβ peptides, the main component of amyloid plaques, is a causative agent in a pathogenic cascade which results in NFT pathology, vascular damage, neuron death, and ultimately, clinical dementia (25). The strongest support for this hypothesis is genetic evidence from early-onset AD. fAD point mutations in *APP, PSEN1*, or *PSEN2* which increase Aβ production or the generation of more aggregation-prone Aβ species results in 100% penetrant AD.

Additionally, Down's Syndrome patients with trisomy 21, the chromosome encoding *App*, results in Alzheimer's dementia as well as fAD caused by an *App* gene duplication (2,26,27).

Amyloid plaques consist of aggregated Aβ peptides which are generated from the sequential proteolytic processing of APP by the secretase family (Figure 1). APP is a single-pass type I protein that primarily localizes to the Golgi and plasma membrane (PM) (28). At the plasma membrane, APP can undergo endocytosis and recycling back to the Golgi or to the PM. Depending on the initial secretase, APP can be cleaved through either a non-amyloidogenic or amyloidogenic pathway. APP predominantly undergoes non-amyloidogenic processing through cleavage by α-secretase (ADAM10/ADAM17) at the plasma membrane within the Aβ sequence of APP, generating a membrane-imbedded 83 amino acid α-C-terminal fragment (APP-CTF_α/APP-C83) and releasing a soluble N-terminal APP fragment ($sAPP_\alpha$). The APP-C83 fragment is further cleaved by γ-secretase to release a p3 fragment into the extracellular space and an APP intracellular domain (AICD) into the cytosol. Besides the lack of Aβ generation, non-amyloidogenic processing of APP has beneficial physiological effects in neurons. Notably, $sAPP_\alpha$ has been shown to have multiple neuroprotective and neurogenic effects including promoting neurite outgrowth and synaptogenesis, modulating long-term potentiation (LTP), and improving synaptic plasticity (29,30). Conversely, APP can traffic into endosomes where β-secretase (BACE1) can cleave APP at the β-site. β-secretase cleavage of APP generates a longer, 99 amino acid CTF (APP-CTF_β/APP-C99) and releases a soluble N-terminal APP fragment ($sAPP_\beta$) which, contrary to $sAPP_\alpha$, does not potentiate LTP. The APP-C99 CTF fragment can further be cleavaged by γ-secretase following trafficking back to lipid raft domains at the PM to generate an AICD and release Aβ species ranging from 37-43 amino acids into the extracellular space.

Longer Aβ species are more hydrophobic and thus, more prone to aggregate. As such, an increased ratio of $A\beta_{42}/A\beta_{40}$ is used as a biomarker for AD (31). Although insoluble amyloid plaques are a defining pathology of AD, research has shown that the soluble oligomeric Aβ aggregates are neurotoxic while the larger insoluble plaques are rather benign (32–34). Aβ oligomers have many cellular binding partners that mediate toxicity in AD. For example, oligomeric Aβ interacts with both the cellular prion protein (PrP^C) and the metabotropic glutamate receptor subtype 5 (mGluR5) to form a ternary signaling complex that potentiates mGluR5 signaling (35–37). Increased mGluR5 signaling results in an increase in intracellular Ca^{2+} release that leads to an increase in reactive oxygen species (ROS) and inhibition of autophagy pathways that ultimately result in cell death. Additionally, oligomeric Aβ interaction with PrP^C/mGluR5 increases tau aggregation via increased phosphorylation by Fyn kinase (37,38). Another oligomeric Aβ receptor integral in mediating toxicity in AD is the receptor for advanced glycation end products (RAGE). Oligomeric Aβ binding to RAGE on neurons increases ROS production, and binding to RAGE on microglia and astrocytes triggers neuroinflammation. Furthermore, Aβ-RAGE interaction is a key regulator of Aβ transport across the blood brain barrier (BBB) and critically, the concentration of toxic Aβ species in the brain (39,40). Overall, despite amyloid plaques being a defining pathologic feature of AD, oligomeric Aβ species seem to be the driving Aβ player in AD pathogenesis.

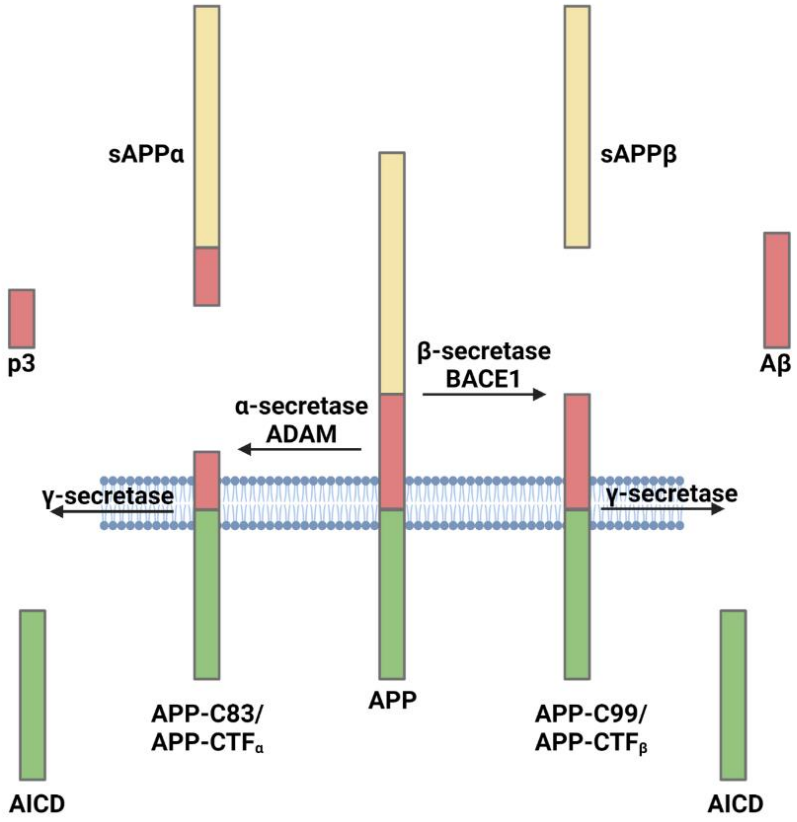

Figure 1. APP processing by secretases generates Aβ peptide

APP cleavage by the α-secretase generates $sAPP_{\alpha}$ and APP-C83/CTF_{α}. APP-C83 is further cleaved by γ-secretase to yield the AICD and p3. APP cleavage by the β-secretase generates $sAPP_{\beta}$ and APP-C99/CTF_{β}. Processive APP-C99 cleavage by the γ-secretase yields the AICD and Aβ peptides ranging from 37-43 amino acids in length.

1.1.2.2 γ-Secretase

The final enzyme involved in APP enzymatic cleavage to generate Aβ is γ-secretase. γ-secretase is a 4 subunit, aspartyl protease complex with over 90 known substrates involved in regulating cell adhesion, neurite outgrowth, cell migration, synaptic transmission, among others (41). A functional γ-secretase complex consists of anterior pharynx-defective 1 (APH1), nicastrin (NCT), presenilin enhancer 2 (PEN2), and a catalytic presenilin subunit (PS1 or PS2). All four

subunits are translated in the endoplasmic reticulum (ER) and assemble together as they traffic through the ER and to the Golgi (42–44). APH1 and NCT first interact early following translation, followed by association with presenilin and finally PEN2 before being trafficked to the Golgi. In order for presenilin to be enzymatically active, it must first undergo endoproteolytic cleavage within its third intracellular loop following complex assembly in the ER. Additionally, once at the Golgi, the large ectodomain of NCT is glycosylated (45).

In humans, there are two APH1 proteins, APH1A and APH1B. There are two isoforms of APH1A: -long ($APH1A_L$) and -short ($APH1A_S$), which lacks the last 18 amino acids on the C-terminus of $APH1A_L$. APH1 is a necessary component for the assembly of γ-secretase and as such, genetic deletion of all *Aph1* genes in mice (*Aph1a*, *Aph1b*, and *Aph1c*) results in embryonic lethality (46). In mice, *Aph1a* is homologous to the human *APH1A* gene. Due to an *Aph1b* gene duplication in rodents, mice have an *Aph1b* and *Aph1c* gene homologous to human *APH1B* and thus, genetic deletion of both *Aph1b* and *Aph1c* in mice (*Aph1b/c*$^{-/-}$) is used as a model for human *APH1B* deficiency. Furthermore, γ-secretase complexes with different APH1 and presenilin subunits exhibit differential affinities for substrates (47–49). For example, γ-secretase complexes with an APH1B protein are shown to favor cleavage of APP over complexes containing an APH1A protein. APH1B-containing γ-secretase complexes also generate longer Aβ species compared to APH1A-containing complexes (50). While distinct complexes exhibit a preference for one substrate over another, there is still redundancy of substrates between unique γ-secretase complexes. Nonetheless, γ-secretase exhibits distinct mechanisms for recognizing substrate. In fact, all APH1 proteins contain two conserved histidine residues H171 and H197 in the 5th and 6th transmembrane domains (TM5/TM6), respectfully, which regulate complex assembly as well as direct binding to γ-secretase substrates (51–53). Studies have shown that the positive charge of

H171 and H197 play critical roles in complex assembly. Furthermore, histidine-to-lysine mutagenesis of H171 and H197 (H171K and H197K) maintains the negative charge and complex assembly but significantly reduces direct APH1A binding to APP and APP-C99 and reduces overall γ-secretase/PS1 catalytic activity (51,52), thus suggesting the positioning of H171 and H197 may play key roles in overall substrate recognition and proteolytic activity.

Another critical regulator of γ-secretase activity and Aβ generation is via post-translational modifications. To date, post-translational modifications to both NCT and PS1 have been shown to regulate the stability and activity of the γ-secretase complex. NCT can serve as a 'gatekeeper' for γ-secretase substrates, and the extent of NCT amino-terminal (N-terminal) glycosylation can regulate the binding of substrates and overall catalytic activity of γ-secretase (54). NCT can also be phosphorylated at S437 in the carboxy-terminal (C-terminal) cytoplasmic domain by serum/glucocorticoid regulated kinase 1 (SGK1) and Akt. NCT S437 phosphorylation results in NCT degradation via proteasomal and lysosomal pathways and, as a result, decreases overall γ-secretase activity (55,56). Extracellular signal-regulated kinase 1/2 (ERK1/2) interacts directly with NCT to downregulate expression and γ-secretase activity; however, no direct phosphorylation of NCT by ERK 1/2 has been demonstrated (57). In addition to NCT, PS1 phosphorylation has been shown. Over a dozen phospho-sites have been identified on PS1 (58), but phosphorylation at each site does not always regulate activity. However, Maesako *et al.* find that PS1 phosphorylation at T74, S313, S365, S366, or S367 alters PS1's conformation into a 'closed' conformation which increases the ratio of $A\beta_{42}/A\beta_{40}$ (59). Conversely, another study found that S367 phosphorylation of PS1 by casein kinase 1 isoform γ2 ($CS1_{\gamma}2$) decreases overall Aβ generation by activating autophagy-mediated degradation of APP-C99 and γ-secretase (59,60). Despite conflicting evidence of the pathogenicity of PS1 phosphorylation at S367, it is clear that phosphorylation of

γ-secretase subunits plays an important role in regulating overall complex stability, activity, and generation of pathogenic Aβ peptides.

1.1.2.3 Tau Pathology

In addition to Aβ plaques, post-translationally modified, misfolded, and mislocalized intracellular inclusions of the microtubule-associated protein tau comprise the second major pathological hallmark of AD (61,62). Adult humans express 6 isoforms of the Tau protein, generated by differential splicing of the *MAPT* gene. Alternative splicing of Exon 2 or Exon 3 results in Tau having 0, 1, or 2 N-terminal inserts (0N, 1N, or 2N tau) while alternative splicing of Exon 10 results in tau with either 3 or 4 C-terminal repeat domains (3R or 4R tau), which bind microtubules and have high propensity to self-assemble (63,64). Tau is a cytoplasmic protein expressed in neurons, predominantly in the axons, and binds microtubules to facilitate assembly, regulate dynamics, and aid in axonal transport. In addition, tau can be localized to the nucleus where it serves to maintain the integrity of DNA (65,66). Tau is overall a basic protein; however, it contains concentrated regions of charged residues, aromatics, and polar residues with both negative and positive charges at physiological pH. Due to these features, tau is highly soluble and is considered an 'intrinsically disordered' or natively unfolded protein. Nonetheless, at high local concentrations, tau can self-assemble into 'droplets' which aid in stabilizing microtubules during polymerization, but in diseases such as AD, may serve to generate seeds that initiate further pathological aggregation and results in cellular dyshomeostasis (64,67,68).

Tau exhibits prion-like properties by which small, ordered, tau aggregates or seeds act as templates to exacerbate a chain-reaction of further tau misfolding and aggregation (69,70). As such, disruptions in cellular homeostasis that initiate tau misfolding to generate initial seeds is an

essential step in AD pathology. The pathogenic spread of tau throughout the brain follows interconnected neuronal connections (71–73). Initial detection of pathological tau can be observed in the locus coeruleus (LC) and spreads early in progression to the entorhinal cortex (EC). Pathologic tau then spreads to the limbic areas including the hippocampus in patients with MCI due to AD. Further spread into the neocortex occurs later in AD dementia (61,70,74).

Pathologic tau is typically characterized by the presence of specific phosphorylated residues found in NFTs and paired helical filament (PHF) tau aggregates in the AD brain or by staining for or imaging tau amyloid and PHF structures directly (75–79). Tau contains many phosphorylation sites (Serine, Threonine, and Tyrosine) with up to 85 putative phosphorylation sites on the 2N4R Tau isoform. To date, around 45 sites have been identified to be phosphorylated and many tau kinases have been identified (64). Serine/Threonine tau kinases include glycogen synthase kinase 3β (GSK3β), cyclin-dependent kinase 5 (CDK5), mitogen-activated protein kinase (MAPK), protein kinase A (PKA), calcium/calmodulin-dependent protein kinase II (CaMKII), and c-Jun N-terminal kinase (JNK), among others. Tau tyrosine kinases include Src family kinases Fyn, Lck, and Syk (77). Phosphorylation of tau regulates normal physiological function. For example, phosphorylation at S262 within the first repeat domain by MAPK, PKA, or CaMKII reduces tau's affinity for microtubules (80). However, in AD brains, tau can be found to be hyperphosphorylated, although there is some debate over whether this phosphorylation triggers aggregation, is protective against aggregation, or is an artifact of prolonged post-mortem intervals following tissue collection and processing (81,82). In addition to phosphorylation, other post-translational modifications such as acetylation are found in the AD brain (64). Acetylated tau has been shown to mislocalize to the axon initial segment (AIS), where it induces destabilization of

the cytoskeleton, decreased tau turnover, and mislocalizes tau to the somatodendritic compartment (83–85).

While some reports suggest initial tau seeding or aggregation due to normal aging may occur prior to the detection and onset of amyloid plaque pathology in AD, Aβ pathology is an essential driver which transforms and accelerates subcortical tau pathology into full NFT pathology and results in the advancement and progression throughout the limbic and neocortical regions in AD (86–89). To date, a few main hypotheses have arisen on the mechanisms of Aβ-induced tau aggregation. Firstly, Aβ binding or activating neuronal receptors may trigger intracellular signaling cascades resulting in tau phosphorylation by kinases. For example, Aβ binding to RAGE can increase tau phosphorylation via activating GSK3β and Aβ interactions with N-methyl-D-aspartate (NMDA) receptors and α7 nicotinic acetylcholine receptors (α7nAchR) can induce tau phosphorylation via activating CDK5 and GSK3β (39,90). Secondly, Aβ-induced neuroinflammation can trigger tau aggregation via the release of cytokines such as IL-1β, which has been shown to regulate tau pathology in the 3x-Tg mouse models of AD (91,92). Lastly, Aβ oligomers and aggregates themselves may be able to act as templates to 'cross-seed' for intracellular tau aggregation. This hypothesis is supported by research measuring intracellular Aβ either via cellular uptake of Aβ species or low level of γ-secretase cleavage of APP-C99 in intracellular compartments such as endosomes and by studies demonstrating the ability of Aβ aggregates to potentiate tau aggregation (43,87,93–95). In addition, some research has demonstrated that in the absence of tau expression, toxic effects of Aβ to cells are mitigated (96), thus further establishing a critical relationship between these two proteins in AD.

1.2 G Protein-Coupled Receptors

G protein-coupled receptors (GPCRs) are the largest class of cell surface receptors. There are over 800 genes in the human genome encoding for GPCRs, encompassing approximately 1-2% of the entire genome (97,98). GPCRs share a common seven transmembrane (TM) helical structure that is conserved in mammals, insects, plants, and protozoa. Despite the common 7TM helical domains, GPCRs display great variability in their amino acid sequences, thus giving rise to the vast array of stimuli that can activate GPCRs including neurotransmitters, hormones, small molecules, and light. Based on phylogenetic origin, GPCRs are classified into 5 classes by the GRAFS system. These classes include the glutamate (class C), rhodopsin (class A), adhesion (class B2), frizzled (class F), and secretin (class B1) classes of GPCRs (99). Receptors in each class share structural and physiological similarities. Nonetheless, all GPCRs function to communicate extracellular stimuli intracellularly to initiate signaling cascades in response to such stimuli by binding to and activating intracellular signaling transducers. Common to the GPCR family, GPCRs couple to and activate heterotrimeric guanine-nucleotide binding proteins (G-proteins). Activated G-proteins act as signal transducers and interact with a multitude of downstream effector proteins to initiate signaling cascades to elicit a physiological response via intrinsic GTPase activity and structural scaffolding. Given the widespread cell-type and tissue distribution of GPCRs, it is no surprise that GPCR function (and dysfunction) is highly implicated in many diseases including cancer, pain, cardiovascular disease, neurological and neurodegenerative disease, endocrine disorders, inflammation, among many more (100–106). The cell plasma membrane localization, diverse tissue expression, and the dynamic conformational states that GPCRs adopt make GPCRs an ideal therapeutic target. As such, ~35% of all currently FDA-approved drugs target GPCRs (107,108).

1.2.1 Overview of GPCR Signaling

GPCRs are conformationally dynamic proteins and shift constantly between multiple 'inactive-like' and 'active-like' states (109,110). In the absence of ligand, the most energetically favorable state that a GPCR predominantly occupies is an inactive state. The initial step in a GPCR signaling cascade is ligand binding or the presence of an extracellular stimulus such as light. While the exact location of the orthosteric ligand binding site differs between classes of GPCRs and specific GPCRs, most orthosteric ligands bind to GPCRs forming interactions within the 7TM bundle near the extracellular side of the plasma membrane (111,112). Agonist binding to a GPCR lowers the energy barrier needed for the receptor to occupy an 'active' state, and therefore there is a high probability a GPCR will shift to occupy an active state. This is done via structural rearrangement of the TM domains, including a conserved outward movement of the transmembrane helix 6 (TM6) to expose interfacial residues that interact with G-protein transducers (109,110). Common to class A GPCRs, TM3 and TM7 also undergo conserved movement upon agonist binding to allow for G-protein interaction and activation. G-protein affinity for a GPCR is increased upon agonist binding and, reciprocally, agonist binding to a GPCR is increased by pre-coupling of a GPCR/G-protein complex (98). For full G-protein engagement with a GPCR, the α5 helix of a G-protein positions into the intracellular cavity of the TM domains. This conformation is needed for full activation of G-protein (110,113).

G-proteins are plasma membrane-bound heterotrimeric signal transducers made up of a G_{α} subunit and a G_{β} and G_{γ} subunit that function as an obligate heterodimer. Inactive G-proteins are bound to guanosine diphosphate (GDP). G-protein binding to an agonist-bound GPCR and α5 helix-engagement with the TM core reduces GDP affinity from G-protein and, due to the high concentration of GTP in cells, GDP is exchanged for GTP. This guanine-nucleotide exchange

reduces G-protein affinity for GPCR and the G_{α} and $G_{\beta\gamma}$ subunits dissociate from one another and interact with various downstream effectors (98). There are 16 G_{α} subunits, 5 G_{β} subunits, and 13 G_{γ} subunits, leading to a wide array of possible heterotrimeric G-proteins in cells (114). Given the large number of different GPCRs, a single G-protein can couple to many different GPCRs. Likewise, a given GPCR can couple to and activate multiple G-proteins. G_{α} subunits contain intrinsic GTPase activity and independently regulate downstream effectors. Commonly, $G_{\alpha S}$ subunits activate adenylate cyclase to increase cellular concentrations of the signaling molecule cyclic adenosine monophosphate (cAMP) and conversely, $G_{\alpha i}$ subunits inhibit adenylate cyclase activity to lower cellular cAMP levels. Additionally, $G_{\alpha q}$ subunits can activate phospholipase C (PLC) which increases intracellular calcium (Ca^{2+}) concentration. Liberated $G_{\beta\gamma}$ subunits can interact with and regulate ion channels including G-protein-gated inward rectifying potassium channels (GIRKs) and Ca^{2+} channels as well as protein kinases (115). In addition, free $G_{\beta\gamma}$ subunits at the plasma membrane recruit specific members of the GPCR kinase (GRK) family of kinases, which downregulate GPCR signaling (116).

Following agonist binding, G-protein activation, and initiation of downstream signaling cascades, GPCR signaling is downregulated via a series of phosphorylation events, scaffolding interactions, and receptor trafficking. The family of AGC kinases known as GRKs are recruited to activated GPCRs and phosphorylate serine/threonine residues in the intracellular loops (ICLs) and carboxy terminus (C-terminus) of the receptor (117). (GRK-mediated GPCR phosphorylation and regulation of GPCR signaling is discussed in detail in section 1.2.2) The multifunctional scaffolding proteins known as arrestins are recruited to phosphorylated GPCRs. Arrestin-1 and arrestin-4 (visual arrestins) are expressed in the eye and have a high affinity for light-activated and phosphorylated rhodopsin. Arrestin-2 and Arrestin-3, more commonly referred to as β-arrestin 1

(βarr1) and β-arrestin 2 (βarr2) respectively, are expressed throughout tissues in the body and bind with high affinity to many different phosphorylated GPCRs (118,119). GPCR C-terminal and ICL phosphorylation initiate β-arrestin recruitment to the receptor where β-arrestins can occupy multiple binding conformations, depending on the phosphorylated GPCR residues (120,121) (discussed more in section 1.2.2). β-arrestin binding to a GPCR sterically precludes further G-protein coupling to a GPCR, thus terminating additional signaling from a ligand-bound GPCR. Furthermore, β-arrestins bound to GPCRs can interact with proteins involved in intracellular signaling cascades and act as scaffolds to initiate signaling pathways independent of G-protein activation (122). Specific ligands can activate or favor 'G-protein' or 'β-arrestin' signaling pathways (123–125). This mechanism is termed functional selectivity and is discussed in detail in the subsequent section. Additionally, β-arrestins classically function as molecular scaffolds to recruit endocytosis machinery (clathrin and AP-2) to internalize receptors. In the endosome, the acidic environment of the endosomal lumen (pH ~4.5-6.5) results in the dissociation of ligand from the GPCR. Depending on the receptor, the GPCR-containing endosome can be recycled back to the plasma membrane where it can bind to a new ligand and continue signaling, or conversely, can be trafficked to the Golgi or a lysosome for degradation. Interestingly, some GPCRs can maintain functional signaling complexes upon endocytosis and can result in prolonged and/or functionally distinct signaling events from the plasma membrane (126–131). This type of endosomal signaling is common with class B1 (secretin-type) GPCRs since the GPCR- β-arrestin interactions are more stable than class A GPCR- β-arrestin interactions.

Overall, GPCR signaling and downstream physiological responses can be regulated at different points through the signaling process: ligand binding, G-protein coupling and activation, receptor phosphorylation, β-arrestin binding and signaling, and receptor trafficking. As such, the

ability to manipulate and modulate specific steps in GPCR signaling pathways provides a great opportunity to fine-tune physiological responses. Indeed, therapeutic drug design has recently aimed at identifying specific GPCR ligands to manipulate or bias signaling for more precise targeting of pathways to treat disease (122,123,132,133).

1.2.2 GPCR Functional Selectivity – Conformation is Key

Both endogenous and synthetic GPCR agonists can promote G-protein and/or β-arrestin signaling. However, different GPCR ligands for a given receptor have the ability to preferentially activate distinct downstream signaling pathways. This concept is referred to as functional selectivity or commonly, biased signaling (123). The first evidence of 'biased' GPCR agonists demonstrated that different ligands for a receptor exhibited different efficacies in activating downstream signaling pathways (134). Today, evidence supports the notion that GPCR signaling bias comes from multiple 'active' conformational states of a single receptor/transducer/scaffold complex and that different ligands for a given receptor can differentially stabilize unique active conformations (98).

Different ligands can initiate GPCR signaling bias via inducing 1) different conformations of the receptor, 2) different conformations of the G-protein transducer, or 3) different conformations of scaffold (β-arrestins) (98). As discussed in the previous section, GPCR ligand binding induces conformational rearrangement on the intracellular GPCR interface to allow for interaction with G-protein or β-arrestin scaffolds. Unique ligands will cause distinct structural rearrangements within the GPCR cytoplasmic interface, thus favoring a conformation either conducive to increased G-protein binding and activation or a conformation more favorable for β-arrestin scaffolding interactions at the expense of G-protein activation. These ligands are said to

exhibit G-protein or β-arrestin signaling bias, respectively. Structural studies have shown that for class A GPCRs, the movement/positioning of TM7 and a conserved NPXXY motif in TM7 in particular, is critical for efficient β-arrestin-coupling and activation of β-arrestin signaling pathways (135). For example, one ^{19}F-NMR study on the β_2-adrenergic receptor (β_2AR) found that strong agonists that activate both G-protein and β-arrestin signaling pathways (isoproterenol and formoterol) induce large shifts in both TM6 (important for G-protein binding) and TM7. As expected, partial agonists (tulobuterol and clenbuterol) resulted in less pronounced TM6 movement. Additionally, the β_2AR β-arrestin-biased agonists carvedilol and isoetharine primarily altered TM7 movement to favor β-arrestin engagement (136). Similarly, stimulation of the 5-hydroxytryptamine receptors 5HT1B and 5HT2B by the agonist ergotamine demonstrate a functional role of TM7 movement in β-arrestin bias. Ergotamine can activate both G-protein and β-arrestin pathways downstream of 5HT1B; however, ergotamine administration to 5HT2B receptors induces primarily β-arrestin signaling and exhibits much greater TM7 movement than in the 5HT1B receptor (137).

Additionally, specific GPCR ligands may alter the conformation of the specific G-protein bound to the receptor. These different G-protein conformations can lead to different rates of G-protein activation and GTP-GDP exchange and result in different downstream signaling efficacies (138). For example, if a ligand induces strong G-protein binding and rapid GTP-GDP exchange, the cell will undergo quantitatively more downstream signaling per given unit of time than a ligand that causes weaker G-protein binding and slower GTP-GDP exchange.

Finally, different ligands can induce GPCR structural rearrangements to ultimately bind to β-arrestin scaffolds in different conformations. Different ligands can promote unique GRK-mediated phosphorylation patterns, or phosphorylation barcodes, on the C-terminus and ICLs of

the GPCR, thus resulting in differential β-arrestin binding modes to the GPCR (139–141). As such, β-arrestins will adopt different conformations to scaffold for distinct intracellular signaling cascades. The concept of a GRK-mediated GPCR phosphorylation barcode is discussed in detail in section 1.2.2.2.

1.2.2.1 GPCR Kinases (GRKs)

Once an external stimulus has relayed a message to a cell, the cell needs a mechanism to stop signaling. For GPCRs, this is accomplished via GPCR phosphorylation within the ICLs and C-terminus followed by β-arrestin binding to sterically hinder further G-protein coupling, recruit endocytosis machinery, and initiate arrestin-signaling pathways. GRKs are members of the AGC family of serine-threonine kinases and are the predominant family of kinases responsible for phosphorylating GPCRs. Other kinases including protein kinases A (PKA) and C (PKC), Akt, and casein kinases 1 (CK1) and 2 (CK2) have also been shown to selectively phosphorylate certain GPCRs (142–144).

GRKs are grouped into three classes based on structural homology. The GRK1-family includes GRK1 and GRK7. These two kinases are visual GRKs and are expressed in the retina. The GRK2-family includes GRK2 and GRK3 and the GRK4-family includes GRK4, GRK5, and GRK6. GRK4 is primarily expressed in the testes, whereas GRK2, GRK3, GRK5, and GRK6 are ubiquitously expressed throughout the body (144); however, different tissues and cell-types can exhibit different expression patterns of the ubiquitously expressed GRKs, which may play a key role in regulating GPCR signaling in normal physiology and in disease (145,146). Furthermore, changes in GRK expression levels occur during normal development (146). The specific changes in GRK expression during development are tissue specific. For example, only expression level of

GRK5 was found to change in rat brain tissue from embryonic day 14 to birth (103). In some instances, however, changes in GRK expression levels in specific tissues with age contribute to disease progression. For example, decreased GRK2 expression with age in cardiac tissue is linked to heart failure (146). In humans, there are 4 *Grk4* splice variants (GRK4α, GRK4β, GRK4γ, and GRK4δ) and 3 *Grk6* splice variants (GRK6A, GRK6B, and GRK6C). All GRKs share a conserved catalytic kinase domain and a regulator of G-protein signaling (RGS) homology (RH) domain at the N-terminus that has been shown to be involved in membrane and GPCR binding. GRK RH domains exhibit very low GTPase activity that is observed in other RGS proteins. GRKs are soluble proteins and therefore require mechanisms to bring them into the vicinity of membrane-bound GPCRs following GPCR activation. The visual GRKs (GRK1/GRK7) are prenylated at the C-terminus and are retained in membranes. The GRK2-family of GRKs contains a C-terminal plexstrin homology (PH) domain that binds to free $G_{\beta\gamma}$ subunits. Following G-protein activation, GRK2/3 are recruited to the membrane environment of the activated GPCR via PH-$G_{\beta\gamma}$ binding. GRK4 and GRK6 are palmitoylated at the C-terminus to ensure membrane localization. GRK5 contains a C-terminal poly-basic region that allows for interaction with negatively charged phospholipids at membranes. GRK5 also contains a nuclear localization sequence (NLS) and a DNA-binding motif.

The GRK family of kinases differs from other AGC kinases in that their kinase domain is constitutively in an open conformation, which is not typical of AGC kinases (147). This suggests that GRKs require structural rearrangement to occupy an active conformation of the kinase domain. Evidence suggests that GRK binding to a GPCR allows for GRK structural rearrangement to become active. Recent structural data of GRK1-bound rhodopsin suggests that the N-terminal domain of GRKs is intrinsically disordered until it binds to an activated GPCR (148). To bind,

the N-terminal region forms an αN-helix and inserts into the GPCR core, a process which the authors call ‘molecular fly-casting.’ Additionally, basic residues in the RH domain interact with negatively charged phospholipids in the membrane. GRK engagement with a GPCR allows for kinase domain closure and receptor phosphorylation. The study also suggests that partial disengagement of GRK from GPCR may allow for more efficient adenine nucleotide exchange and allow for consecutive phosphorylation events (148). Overall, the structural data support the idea that ligand-induced changes in GPCR conformations could select for specific GRK phosphorylation and distinct phosphorylation barcodes and downstream signaling events.

In addition to phosphorylating GPCRs, GRKs can phosphorylate non-canonical substrates (non-GPCR proteins) including receptor tyrosine kinases, single-pass transmembrane domain serine-threonine kinases, death receptors, toll-like receptors, transcription factions, and adaptor proteins. For example, GRK2 can phosphorylate platelet-derived growth factor receptor-β (PDGFRβ) to regulate downstream transcription that induces cell proliferation (149). GRK2 and GRK5 phosphorylate tubulin to regulate cytoskeleton structure (150). GRK2/3 and GRK5 can phosphorylate histone deacetylases (HDACs) to regulate DNA transcription (151,152). To date, it is unknown whether GRKs must be in a GPCR-bound state to phosphorylate non-GPCR substrates in close proximity to these GPCR-GRK complexes or if GRKs simply exhibit low, intrinsic/basal activity for non-GPCR substrates. Studies with purified GRKs have shown that GRKs can phosphorylate purified, non-GPCR substrates in *in vitro* kinase assays (such as p53) (153) suggesting GRKs do possess some intrinsic ability to phosphorylate other substrates. However, GRKs cannot fully adopt the closed kinase domain conformation needed for full activity unless GPCR-bound (144,147). Given that non-GPCR GRK substrates are both cytosolic proteins and

membrane-bound, it seems likely that both explanations may be correct and most likely depends on the specific substrate.

GRKs are also able to regulate signaling pathways independent of the kinase function by functioning as molecular scaffolds (116). The most notable non-kinase function of GRK2/3 is the ability of these kinases to bind to liberated $G_{\alpha q}$ G-protein subunits to regulate GPCR G-protein signaling, particularly metabotropic glutamate receptor 5 (mGluR5) signaling. GRK2/3 RH domain interaction with activated $G_{\alpha q}$ subunits has been shown to downregulate mGluR5 signaling, independent of GRK2/3 kinase activity (154,155). Similarly, the RH domain of GRK5 can interact with the cytosolic protein IκBα to increase nuclear localization of IκBα to inhibit NFκB transcriptional activity (156). Given the diverse functions and widespread distribution of the GRK family of proteins, GRK function and dysfunction has been implicated in a wide range of diseases including cardiovascular disease, pain, depression, inflammation, multiple cancers, and neurodegenerative disease including Parkinson's disease (PD) and Alzheimer's disease (discussed in 1.3.2) (106,157–162).

1.2.2.2 GPCR Phosphorylation Barcodes

Not only can distinct GPCR ligands induce signaling via β-arrestin pathways in addition to classical G-protein signaling cascades, but different ligands can selectively modulate the specific β-arrestin-dependent functional outcome(s), (e.g. receptor endocytosis, GPCR desensitization, or β-arrestin-dependent signaling pathways such as ERK1/2 activation or Src activation). Original studies investigating this phenomenon utilizing the chemokine receptor CCR7 and the two endogenous CCR7 ligands CCL19 and CCL21 suggested that CCL19 and CCL21 impart distinct functional consequences downstream of βarr2 via differentially recruiting

specific GRKs to phosphorylate CCR7 (124). Further reports with the chemokine receptor CXCR4 (163), muscarinic acetylcholine M3 receptor (M3R) (164), and the β_2AR (140) further established the concept of a GRK-mediated, GPCR phosphorylation barcode which differentially regulates β-arrestin signaling outcomes (Figure 2). Importantly, Nobles et al. mapped GRK2 and GRK6 phosphorylation sites on β_2AR and demonstrated that GRK2 and GRK6 differentially affect βarr2 conformation using a bioluminescence resonance energy transfer (BRET) – based intramolecular βarr2 biosensor (140).

A common feature of GRK regulation of a GPCR phosphorylation barcode is hierarchical phosphorylation by GRKs at specific sites on a receptor. In other words, there is a particular order of GRK phosphorylation and some sites, termed primary site(s), on a GPCR allow for further phosphorylation at other residues. For example, GRK phosphorylation at S375 of the μ-OR occurs first and is necessary for additional GRK phosphorylation of the μ-OR C-terminus (165). Dopamine D1 receptor (D1R) C-terminal phosphorylation is necessary for D1R ICL3 phosphorylation by GRKs (166,167). Hierarchical phosphorylation has been reported in multiple other GPCRs including rhodopsin (168) the adenosine A3 receptor (A3R) (169), delta-opioid receptor (δ-OR) (170), cannabinoid receptors (171), CXCR4 (172), and the bitter taste receptor TAS2R14 (173). Two hypotheses exist to explain the mechanism of hierarchical phosphorylation, and both may prove to hold true depending on the GPCR and/or GRK. First, phosphorylation of a GPCR at certain sites may make the receptor more of an attractive substrate for GRKs, perhaps by increasing the GRKs affinity for the receptor. Secondly, primary site phosphorylation of a GPCR induces conformational changes in the C-terminus and/or ICLs which make other sites accessible for phosphorylation by GRKs. Overall, due to the interdependence of specific phosphorylated residues by GRKs, it is reasonable to believe that tissue and cell-type-specific changes in GRK

expression or activity in disease may result in significantly altered GPCR phosphorylation, downstream signaling, and contribute to many disease etiologies.

Structural studies investigating β-arrestin interactions with phosphorylated GPCRs have further supported a mechanism of a GPCR phosphorylation barcode where GPCR phosphorylation patterns function as a 'code' that is read by β-arrestins to dictate the GPCR-β-arrestin binding conformation and downstream functional consequence. These studies have identified biphasic interaction modes between βarr2 and GPCRs – each with distinct downstream consequences (174–177). β-arrestins can interact with a GPCR C-terminus alone forming a partially engaged conformation or with the C-terminus plus the TM cytoplasmic GPCR core in a fully engaged conformation. In one particular study using a GPCR chimera composed of the β_2AR extracellular and TM domains and the vasopressin V2 receptor (V_2R) intracellular domains (β_2V_2R), the authors determined that a partially engaged β_2V_2R-βarr2 complex could functionally induce receptor endocytosis as well as activate ERK1/2, but the fully engaged β_2V_2R-βarr2 complex was required for receptor desensitization (176).

Initial recruitment of β-arrestins is mediated by GPCR C-terminal phosphorylation. Phosphorylated GPCR C-termini bind to the N-domain of arrestins and induce conformational shifts in β-arrestin that function as switches, allowing for full β-arrestin engagement with the GPCR TM core. Importantly, two of these switches include the disruption of an 'ionic lock' by negatively charged phosphates in the GPCR C-terminus that results in the outward movement of a conserved region in β-arrestins known as the finger loop domain, and disruption of the β-arrestin polar core (175,178–180). Specific arrangements of these β-arrestin domains will differ depending on the phosphorylation pattern and location of phosphates on a GPCR C-terminus. Therefore,

different GPCR phosphorylation patterns on unique GPCRs will induce different GPCR-bound β-arrestin conformations with distinct signaling functions and efficacies for interacting partners.

In further support of GPCR phosphorylation barcodes, one group investigated how βarr1 conformation changed upon binding to 4 distinct phosphorylated V_2R C-termini. The authors determined that small changes in V_2R C-terminal phosphorylation were able to induce significant conformational rearrangements in distal regions of βarr1. Significantly, the authors found that alterations in the V_2R C-terminal phosphorylation status altered the conformation and position of residues on βarr1 known to interact with the small GTPase Raf-1 and the protein kinase MEK-1 to mediate downstream signaling cascades (181). Intriguingly, a recent report utilizing a combination of computational and spectroscopic methods found that GPCR phosphorylation patterns that favor β-arrestin binding are not necessarily those that favor arrestin signaling-associated conformational changes. Also, the authors note that the extent of β-arrestin binding and conformation depend more on the arrangement of phosphates rather than on the total number of phosphorylated residues (121). Collectively, the current literature provides evidence that the extent of β-arrestin binding, GPCR internalization, GPCR desensitization, and downstream arrestin-mediated signaling events are separate functional outcomes downstream of GPCR phosphorylation and that specific GPCR phosphorylation barcodes can differentially regulate these events.

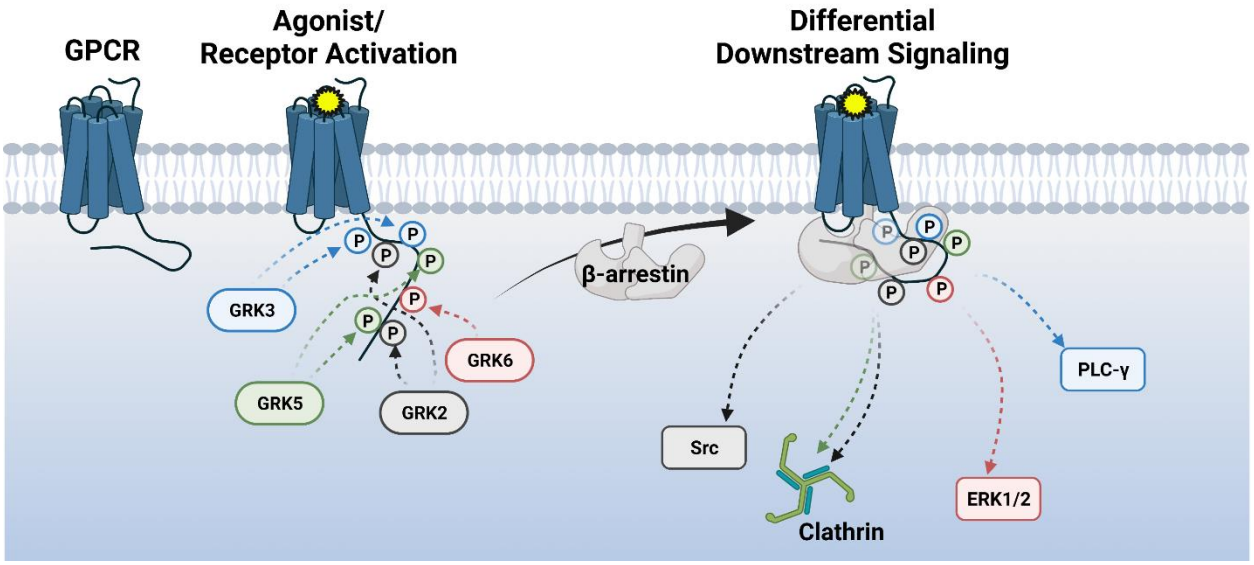

Figure 2. GRKs mediate a GPCR phosphorylation barcode

Following the activation of a GPCR and release of a heterotrimeric G-protein, GRKs are recruited to the C-terminus and ICLs of a receptor. Multiple GRKs can phosphorylate a single receptor and at multiple sites. Different GPCR ligands can induce differential phosphorylation patterns by specific GRKs. GPCR C-terminal and ICL phosphorylation induce the recruitment of the multifunctional GPCR adaptor proteins β-arrestin 1 (βarr1) and/or β-arrestin 2 (βarr2). A fully engaged β-arrestin interacts with both the GPCR C-terminus and transmembrane cytoplasmic core to preclude further G-protein coupling and signaling. In addition, β-arrestins can interact with a multitude of additional proteins such as Src, ERK1/2, PLC-γ, and clathrin, to act as a scaffold for signaling cascades and receptor endocytosis. Depending on the specific GRK-mediated phosphorylation pattern or 'barcode', β-arrestins will adopt distinct conformations that favor interactions with one signaling molecule or the other. Therefore, specific GRK phosphorylation patterns of a GPCR will allow for conformationally-distinct GPCR-β-arrestin complexes to functionally select for one signaling pathway over another.

1.3 GPCR signaling in Alzheimer's Disease

1.3.1 GRKs in Alzheimer's Disease

Despite the expansive literature surrounding GPCR dysfunction in AD, there are only a handful of studies investigating the specific role of GRKs in AD pathogenesis. Initial reports of GRK dysfunction in AD suggested that GRK2 and GRK5 displayed altered cellular localization upon aging in the TgCRND8 AD transgenic mouse model expressing mutant human $APP_{Swe/Ind}$. GRK2 is localized in the cytosol, whereas GRK5 is membrane-bound; however, the researchers found that with age, $APP_{Swe/Ind}$-expressing mice exhibited a much greater cytosolic GRK5 pool and a slightly higher GRK2 cytosolic fraction prior to the onset of cognitive decline (182). Because GPCRs are membrane-bound proteins, a decreased membrane fraction of GRKs (in particular GRK5 or GRK6) may result in decreased binding to, and regulation of GPCRs and their signaling cascades. Furthermore, treatment of cells with $A\beta_{40}$ or $A\beta_{42}$ induced GRK5 translocation from the membrane to the cytosol (182). Functionally, this resulted in reduced recruitment to the protease activated receptor 1 (PAR1), a GPCR involved in synaptic plasticity and memory (183), upon addition of the PAR1 agonist thrombin. Additional studies have also primarily focused on GRK2 and GRK5 in the regulation of AD pathology and confirmed a reduced membrane fraction of GRK5 in another AD transgenic mouse model (APP/PS1) and upon treatment with $A\beta_{42}$ (184–186).

GRK5 membrane deficiency has been linked to increased amyloid plaque pathology by multiple mechanisms. Loss of membrane GRK5 results in dysregulation of the M2 and M4 mAChRs. The M2 and M4 mAChRs are primarily localized pre-synaptically in the hippocampus, and activation of these receptors negatively regulates acetylcholine (ACh) release into the synapse

(187). Reduced ACh release upon M2 and M4 activation will result in a loss of cholinergic signaling and cognitive deficits. Additionally, reduced ACh release pre-synaptically will reduce postsynaptic M1 mAChR signaling, a receptor known to reduce amyloidogenic processing of APP (188). In Tg2576 mice expressing human APP_{Swe}, *Grk5* deficiency (*Grk5*$^{+/-}$ or *Grk5*$^{-/-}$) results in multiple phenotypes. Tg2576/*Grk5*$^{-/-}$ mice exhibit increased amyloid plaque burden and soluble Aβ in the brain (185). Additionally, these mice exhibit a significant increase in neuroinflammation (189). The authors of these studies argue that the increase in Aβ pathology is due to impaired cholinergic signaling, but do not account for putative changes in Aβ clearance from altered microglia and astrocytic signaling as well as potential neuroinflammatory-induced changes in APP processing and Aβ generation. Because GRK5 regulates many GPCRs, it is difficult to point to one mechanism for the observed increase in plaque burden in these transgenic mice.

In addition to Aβ and plaque pathology, there is evidence implicating GRKs in mediating tau pathology as well. Non-transgenic *Grk5*$^{-/--}$ mice present with swollen axonal clusters – a phenotype that is age-dependent and more pronounced in female mice. In the APP/PS1 AD transgenic mouse, genetic deletion of *Grk5* increases tau phosphorylation at S396, an AD-associated phospho-tau epitope (190). Further evidence of a functional role of GRK5 mediating tau S396 phosphorylation comes from two G*rk5* single nucleotide polymorphisms (SNPs) identified in the population encoding for GRK5 Q41L and R304H point mutations (186). GRK5 Q41L exhibits increased membrane localization. Q41 is located in the N-terminal phosphatidylinositol 4,5-bisphosphate (PIP_2) binding domain and substitution with a non-polar residue likely results in the increased membrane binding. In SH-SY5Y human neuroblastoma cells expressing GRK5 Q41L, treatment with $A\beta_{42}$ for 24 hours did not alter GRK5 membrane localization compared to wild-type GRK5-expressing cells. In addition, the GRK5 Q41L cells

exhibited less pS396 tau than in wild-type GRK5-expressing cells. Conversely, GRK5 R304H-expressing cells displayed reduced membrane-bound GRK5 and higher $A\beta_{42}$-induced pS396 tau. In the population, GRK5 Q41L is associated with a lower risk of developing AD (186). GRK5 has also been shown to regulate the activity of the tau kinase GSK3β. In mice, *Grk5* deficiency reduces inhibitory S9 phosphorylation of GSK3β. In turn, GSK3β is more active and increases tau phosphorylation at multiple epitopes (191).

In addition to GRK5, GRK2 has been implicated in tau pathology in AD as well. GRK2 has been shown to co-localize with NFTs stained with a pS202 tau antibody (CP13) or the amyloid dye thioflavin S (ThioS) in the AD hippocampus. However, only about 40-50% of CP13 or ThioS positive NFTs contained GRK2, suggesting the GRK2 positive NFTs may be a distinct subpopulation. No GRK5 positive NFTs were identified in the AD brains from this study (192). GRK2 can also regulate tau pathology via regulating specific GPCRs. Monomeric $A\beta_{42}$ treatment of SH-SY5Y cells increased tau phosphorylation at S214 via activating the β_2AR. GRK2 is a known β_2AR kinase, and inhibition of GRK2 by co-expression of a truncated dominant-negative GRK2 (βARKct) decreased $A\beta_{42}$-induced tau S214 phosphorylation (193). Because inhibition of GRK2 could increase β_2AR G-protein signaling, the positive effect of Aβ42 treatment on tau S214 phosphorylation may be β-arrestin signaling-dependent. Additionally, βARKct would inhibit all GRK2 and GRK3 activity in the cells and could be affecting tau phosphorylation via additional, off-target pathways.

Until recently, a comprehensive analysis of GRKs in the AD brain has been missing. A recent study from our lab analyzed the cell-type and brain region-specific expression of each ubiquitously expressed GRK in human AD brains and non-AD aged-matched control brains as well as characterized the association between each GRK and amyloid and tau pathology using

immunostaining and confocal microscopy techniques (146). The analysis revealed that in late-stage AD brains, expression levels of GRK2, GRK5, and GRK6 are decreased in the CA1 region of the hippocampus. GRK2 was found to positively correlate with soluble tau and co-localize with phosphorylated NFT tau in AD brains. GRK3 was found to be associated with both total tau level and soluble tau levels in AD brains. GRK5 was also found to be associated with total tau levels in AD brains. GRK6 expression positively correlated with soluble tau levels and co-localized with phosphorylated NFT tau in AD brains. Interestingly, both GRK3 and GRK5 levels co-localized significantly with amyloid in AD brains, including ThioS positive NFTs and amyloid plaques. Interestingly, an older report characterizing GRK expression in Parkinson's disease with dementia (PDD) brains that exhibited both tau and amyloid AD pathologies showed increased expression of GRK3 and GRK5 (194). Collectively, these studies provide a connection between the GRK family of kinases and AD pathologies. As such, further investigation into the precise mechanisms by which specific GRKs regulate AD pathogenesis is warranted.

1.3.2 G Protein-Coupled Receptor 3 (GPR3)

G protein-coupled receptor 3 (GPR3) is an orphan GPCR with no known ligand. GPR3 is a member of the class A GPCR family (rhodopsin-family) and exhibits high constitutive $G_{\alpha S}$ signaling resulting in high constitutive production of cAMP (195,196). GPR3 is mainly expressed in the central nervous system (CNS) (197,198), testes (199), oocytes (200), and to a lesser extent, brown adipose tissue (BAT) (201). In the CNS, GPR3 is expressed highly in the medial habenular nucleus, hippocampus, cerebral cortex, olfactory bulb, striatum, and hypothalamus (197,199,201). GPR3 plays an important role in reproductive function. In mice, *Gpr3* genetic deletion (*Gpr3*$^{-/-}$ mice) exhibit reduced fertility with age (202). This is attributed to the disruption of meiotic arrest

caused by the loss of constitutive $G_{\alpha S}$ signaling and cAMP production in oocytes. Additionally, constitutive GPR3 signaling has recently been shown to be an important regulator of thermogenesis. In BAT, lipolysis induces increased GPR3 expression which results in a greater thermogenic effect (201). The authors of this study also suggest that a GPR3 N-terminal peptide consisting of GPR3 amino acid residues 18-27 (GPR3aa18-27) can stimulate GPR3 $G_{\alpha S}$ signaling, potentially acting as a constitutive tethered agonist. However, their data suggests the EC_{50} of GPR3aa18-27 on cAMP generation is ~31μM, and the authors did not measure any effects on β-arrestin recruitment following GPR3aa18-27 treatment. Nonetheless, GPR3aa18-27 showed no effect on the cannabinoid 1 receptor (CB1 receptor), the closest structural relative to GPR3 (201). In the brain, GPR3 signaling has been linked to reward processes and anxiolytic behavior. *Gpr3*$^{-/-}$ mice exhibit enhanced responsiveness to cocaine reward (203), high levels of avoidance of novel environments, and increased stress reactivity and anxiety-like behaviors (204).

GPR3 is upregulated in sporadic AD brains (205). High GPR3 expression in the cortex and hippocampus coincides with Aβ plaque load in brains. Overexpression of GPR3 induces an increase in Aβ without altering β-secretase activity, suggesting the effect of GPR3 on Aβ is downstream of β-secretase processing of APP. Indeed, co-expression of GPR3 with APP-C99 (CTF_{β}), a direct substrate of γ-secretase, results in increased Aβ generation. This effect is blocked by treatment with the selective γ-secretase L-685,458 (205). Overexpression of GPR3 increases localization of active γ-secretase complex in detergent-resistant membrane (DRM) or lipid raft domains where it is more catalytically active (206). Furthermore, the GPR3-mediated effect on γ-secretase appears to be at least partially selective for APP-C99 cleavage, as GPR3 expression does not alter the proteolysis of the Notch receptor, another γ-secretase substrate (205). Furthermore, genetic deletion of *Gpr3* in four different AD transgenic mouse models reduced amyloid plaque

burden and rescued cognitive deficits in these mice, highlighting GPR3 as a putative therapeutic target in AD (207).

Our lab has previously demonstrated that the GPR3-mediated increase in γ-secretase activity and Aβ generation is dependent on β-arrestin signaling and is independent of $G_{\alpha S}$ signaling (208). Expression of GPR3 with a $G_{\alpha S}$ dominant negative mutant, the PKA inhibitor H89, or adenylate cyclase inactivation via 2',5'-dideoxyadenosine failed to reduce GPR3-mediated Aβ, suggesting an alternative (β-arrestin) pathway may be involved (208). To measure β-arrestin recruitment to GPR3, we utilized a PathHunter β-arrestin recruitment assay. In the PathHunter assay, a split β-galactosidase (β-gal) complementation assay, cells stably expressing βarr2 tagged with an inactive β-gal are transfected with GPR3 (wild-type or mutant) with a ProLink (PK) tag attached at the C-terminus. Upon βarr2 binding to GPR3-PK, β-gal is activated. When a β-gal substrate is added, luminescence can be measured and is proportional to βarr2-GPR3 binding. Utilizing the PathHunter β-arrestin recruitment assay, our lab determined a high basal level of βarr2 recruitment to GPR3. Preventing G-protein coupling by mutating a conserved DRY-motif on the 3rd transmembrane domain resulted in increased βarr2 recruitment as well as increased GPR3-mediated Aβ generation. Conversely, serine-to-alanine mutagenesis of six C-terminal serine residues on GPR3 reduced βarr2 recruitment to GPR3 and completely prevented the GPR3-mediated γ-secretase activity and Aβ generation. Further experiments using siRNAs to silence the expression of βarr2 in cells co-expressing GPR3 and APP-C99 reduced $A\beta_{40}$ and $A\beta_{42}$ generation (208). Collectively, these studies indicate that βarr2 is required for the GPR3-mediated increase in γ-secretase activity and Aβ generation and GPR3 C-terminal phosphorylation is a critical regulator of this mechanism.

In addition, βarr2 can independently increase γ-secretase activity by stabilizing active γ-secretase complexes in DRM domains (208). βarr2 directly interacts with the APH1A subunit of the γ-secretase complex. Interestingly, *Gpr3*$^{-/-}$ mice display reduced βarr2 interaction with APH1A in the cortex (208), suggesting GPR3 may modulate γ-secretase activity by regulating βarr2/APH1A interaction.

A critical role of the GPR3 C-terminus in βarr2 binding was confirmed by another group as well. Expression of GPR3 with a truncated C-terminus (GPR3 Q302*) exhibited reduced βarr2 binding and reduced Aβ generation (209). Interestingly, the researchers also observed a direct interaction between GPR3 and APP. They determined that GPR3/APP interaction positively correlates with βarr2 binding to GPR3 as well as Aβ generation. Additionally, βarr2 co-transfection with GPR3 increased GPR3/APP interaction and Aβ production. Surprisingly, preventing phosphorylation at S237 on the 3rd intracellular loop (ICL3) using a S237A mutant increased βarr2 recruitment to GPR3. Overall, GPR3-mediated Aβ generation involves multiple protein-protein interactions between βarr2, APP, and γ-secretase although mechanistically, many unanswered questions remain.

1.4 Dissertation Goal

Alzheimer's disease is a progressive neurodegenerative disease with currently no successful therapeutic strategy to prevent or slow disease progression. In AD, Aβ dyshomeostasis acts as an initial trigger for neuroinflammation, tau posttranslational modifications, tau aggregation, and eventual cell death and clinical dementia (18,74,86,210). As such, investigation into the basic cellular mechanisms that regulate Aβ pathology is paramount to better understand

AD etiology and to develop successful disease-modifying therapeutics. The GPCR family of cell surface receptors is a well-studied class of receptors in regulating AD pathology and in particular, Aβ pathology. However, much less is known in AD about the GRK family of serine-threonine kinases which are critical in modulating GPCR function and GPCR-independent cellular signaling pathways in normal physiology and disease.

The overall goal of this dissertation is to determine if, and how, the GRK family of kinases regulate Aβ generation. Specifically, we sought to determine 1) if GRKs directly regulate the activity of the γ-secretase complex and APP processing and 2) if GRK regulation of a specific GPCR, i.e., GPR3, can modulate Aβ generation. Our findings reveal that APH1A is a non-canonical GRK substrate and that the ubiquitously expressed GRKs regulate a phosphorylation barcode on APH1A to mediate βarr2 binding and functionally, γ-secretase activity and Aβ generation. This novel finding expands the concept of a GRK-mediated phosphorylation barcode beyond GPCRs and to a 7TM-domain protein that is not classified as a GPCR. Furthermore, we determine that GRK2 specifically regulates GPR3-mediated γ-secretase activity and Aβ generation via its kinase function and determine that GRK2 regulation of GPR3 may modulate γ-secretase activity via multiple, distinct cellular mechanisms.

2.0 GPCR kinases mediate an APH1A phosphorylation barcode to regulate amyloid- β generation

Chapter 2 is a modified version of:
Todd, N.K, Huang, Y, Lee, J.Y, Doruker, P, Krieger, J.M, Salisbury, R, MacDonald, M, Bahar, I, and Thathiah, A. GPCR kinases mediate an APH1A phosphorylation barcode to regulate amyloid-β generation. *Manuscript in Review* (2021).

2.1 Introduction

Alzheimer's disease (AD) is a progressive neurodegenerative disorder characterized pathologically by the deposition of extracellular plaques composed of the β-amyloid (Aβ) peptide and intracellular inclusions of the misfolded and post-translationally modified microtubule associated protein tau (18,20). Sequential cleavage of the amyloid precursor protein (APP) by BACE1 (β-secretase) and γ-secretase yields Aβ peptides, which range in length from 37-46 amino acids (211). γ-secretase is a 4-subunit complex consisting of nicastrin (NCT), anterior pharynx-defective (APH)1A or APH1B, presenilin-enhancer 2 (PEN2), and presenilin 1 (PS1) or presenilin 2 (PS2), the catalytic core of the complex (43,206,212). Our lab previously determined that the G protein-coupled receptor (GPCR) scaffolding protein β-arrestin 2 (βarr2) interacts with the APH1A subunit of the γ-secretase complex and stabilizes localization of the γ-secretase complex in lipid raft, or detergent-resistant membrane (DRM), domains where it is more catalytically active (43,206,208,212). Thus, βarr2 interaction with the APH1A subunit of the γ-secretase complex is a critical mediator in the pathogenic cascade of Aβ accumulation.

The β-arrestin family of proteins (βarr1 and βarr2) recognize and bind to phosphorylated serine or threonine residues on the carboxy-terminus (C-terminus) or intracellular loops (ICLs) of GPCRs following receptor activation (213,214). GPCR kinases (GRKs) are serine/threonine kinases that are primarily responsible for GPCR phosphorylation (144). Evidence within the past decade suggests that multiple GRKs can phosphorylate a single receptor at distinct sites. The specific phosphorylation pattern or barcode generated by GRKs leads to differential β-arrestin binding conformations and downstream signaling events (120,121,139,140,215,216). Additionally, recent structural studies suggest multiple functional binding conformations of β-arrestins with a GPCR. Specifically, the N-terminal domain of β-arrestins can interact with the phosphorylated C-terminus of a GPCR or, alternately, a small region on β-arrestin known as the finger loop domain can engage with the intracellular cytoplasmic loops (ICLs) of a GPCR transmembrane (TM) core (175,177,179,180). These conformationally distinct complexes differentially regulate downstream signaling pathways and are regulated by unique GRK-mediated phosphorylation barcodes (176,181). Furthermore, GRKs can phosphorylate a growing list of non-GPCR substrates to regulate GPCR-independent signaling cascades (116,144). Accordingly, we postulated that APH1A may be a non-canonical GRK substrate.

APH1 is a subunit of the γ-secretase complex and is required for active complex assembly and stability (49,212). APH1 is a 7TM-domain protein and despite sharing structural similarities to 7 transmembrane-domain receptors (7TMRs) or GPCRs, has not been shown to couple to or activate heterotrimeric G proteins. In humans, two genes (*APH1A* and *APH1B*) encode for the two APH1 proteins, APH1A and APH1B, respectively. Similar to GPCRs, APH1A has been shown to bind to βarr2 to mediate downstream functional outcomes. We hypothesized that GRK

phosphorylation of APH1A regulates βarr2 recruitment to APH1A and catalytic activity of the γ-secretase complex.

In the present study, we utilize a combination of label-free quantitative liquid chromatography-tandem mass spectrometry (LC-MS/MS), *in vitro* biochemical assays, structural modeling, and molecular dynamics (MD) simulations to investigate the molecular determinants that regulate βarr2 interaction with APH1A and how regulation of this critical protein-protein interaction mediates Aβ generation. We determine that GRKs 2, 3, 5, and 6 impart unique APH1A phosphorylation patterns within the second intracellular loop (ICL2) and C-terminus of APH1A to differentially regulate γ-secretase activity and Aβ generation. Furthermore, our MD simulation studies reveal that the βarr2 finger loop region engages with ICL2 and ICL3 of APH1A to facilitate the interaction between βarr2 and APH1A. Our structural analysis of βarr2 binding to APH1A suggests a conformation that closely resembles a fully engaged GPCR-β-arrestin complex. We demonstrate that mutagenesis of specific residues in the βarr2 finger loop region or ICL3 of APH1A significantly reduces binding and Aβ generation, thus confirming a critical role of this interaction in regulating γ-secretase activity. Overall, we propose that GRK-mediated phosphorylation barcodes on the APH1A subunit of the γ-secretase complex lead to conformationally-distinct APH1A-βarr2 complexes, which differentially affect γ-secretase activity and Aβ generation.

2.2 Results

2.2.1 APH1A is phosphorylated in the 2nd intracellular loop (ICL2) and C-terminus

β-arrestins are canonically involved in GPCR desensitization and internalization via recognition and binding to phosphorylated serine and threonine residues in the ICLs and/or C-terminus of GPCRs (213,217). We previously demonstrated that APH1A interacts with βarr2 in cells and in mouse brain tissue (208). Similar to GPCRs, APH1A contains putative phosphorylation sites in ICL2 and the C-terminus based on a phosphorylation-site prediction algorithm (218). To determine whether APH1A is indeed phosphorylated, we expressed APH1A in HEK293 cells and performed label-free LC-MS/MS analysis on phosphopeptide-enriched trypsin digests. LC-MS/MS analysis confirms that APH1A is phosphorylated at S103 and S110 in ICL2 and S251 and S257 in the C-terminus (Fig. 3 and Fig. 4).

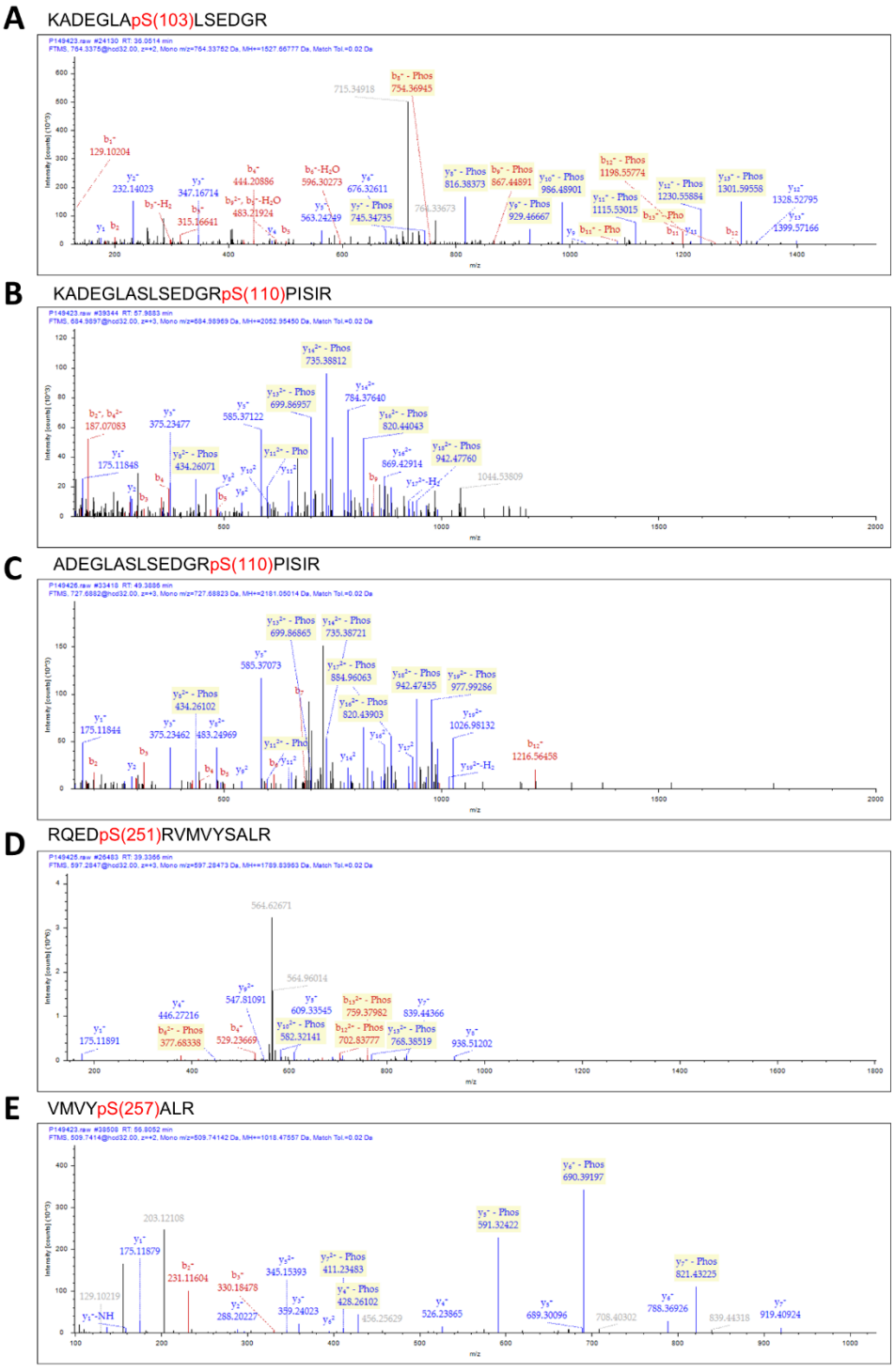

Figure 3. LC-MS/MS analysis identifies sites of APH1A phosphorylation in HEK293 cells

MS2 spectra of identified APH1A phosphorylated peptides correspond to **(A)** S103, **(B)** S110 **(C)** S110, **(D)** S251 **(E)** S257.

A

Region	Site	Annotated Peptide Sequence	Theoretical MH+ [Da]
ICL2	Ser103	KADEGLApS(103)LSEDGR	1527.67
	Ser110	KADEGLASLSEDGRpS(110)PISIR	2181.05
		ADEGLASLSEDGRpS(110)PISIR	2052.96
C-terminus	Ser251	RQEDpS(251)RVMVYSALR	1789.84
	Ser257	VMVYpS(257)ALR	1018.50

B

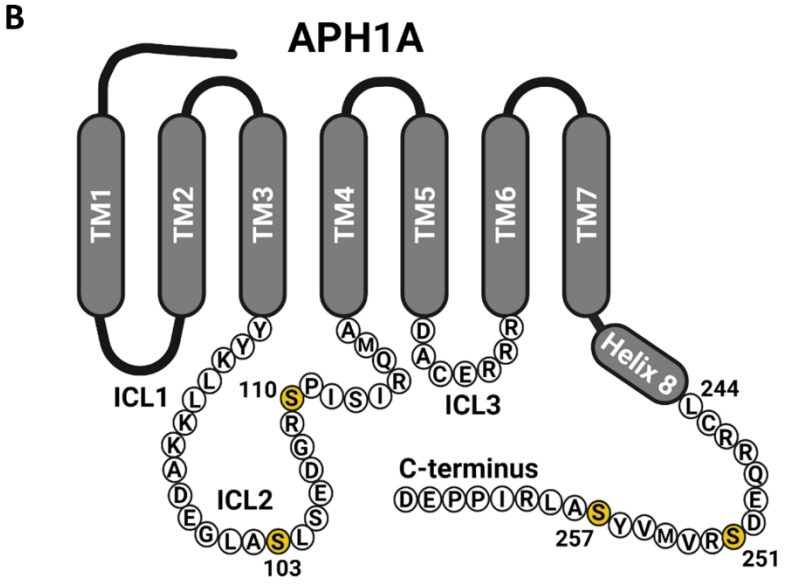

Figure 4. The APH1A subunit of the γ-secretase complex is phosphorylated in ICL2 and the C-terminus

(A) Table of identified phosphorylated peptides on APH1A determined by label-free LC-MS/MS on trypsin-digested and phosphorylation-enriched HEK293 cells following expression of APH1A. **(B)** Snake diagram of APH1A. The phosphorylated amino acids in ICL2 and the C-terminus are indicated in *yellow*.

2.2.2 Chemical inhibition of GRKs affects βarr2 recruitment and Aβ generation in a physiological model of AD

GRKs are serine/threonine kinases primarily responsible for phosphorylating the ICLs and C-termini of GPCRs to initiate β-arrestin recruitment. GRKs are also capable of phosphorylating non-GPCR substrates (117,144). GRK2, GRK3, GRK5, and GRK6 are ubiquitously expressed in tissues throughout the body and in the brain (144,219). We hypothesized that GRK activity is involved in mediating the βarr2 interaction with APH1A. To initially test this hypothesis and gain preliminary insight into whether GRKs regulate βarr2 recruitment to APH1A and γ-secretase activity, we utilized the commercially available Takeda Compound 101 (CMPD101), which inhibits the kinase activity of both GRK2 and GRK3 with an IC_{50} ~32-34nM (220). To measure βarr2 recruitment to APH1A, we utilized a PathHunter βarr2 recruitment assay (Fig. 5). Surprisingly, we determined that treatment of cells that express APH1A with 10μM CMPD101 results in a significant increase in βarr2 recruitment to APH1A in comparison to vehicle-treated cells (Fig. 6A). To determine whether GRK2 and GRK3 are also involved in regulating Aβ generation, we turned to a more biologically and AD-relevant system. As such, we treated a human neural progenitor cell (NPC) line, ReN, which harbor familial AD (fAD) mutations in APP (221,222), with 10μM CMPD101. Significantly, CMPD101 treatment leads to an increase in both $Aβ_{40}$ and $Aβ_{42}$ generation in the human fAD NPCs (Fig. 6B). Collectively, our data demonstrate that chemical inhibition of GRK2/3 enhances βarr2 interaction with APH1A and Aβ generation. Additionally, the studies with the human fAD NPCs suggest a putative pathogenic role of the GRK family of kinases in AD.

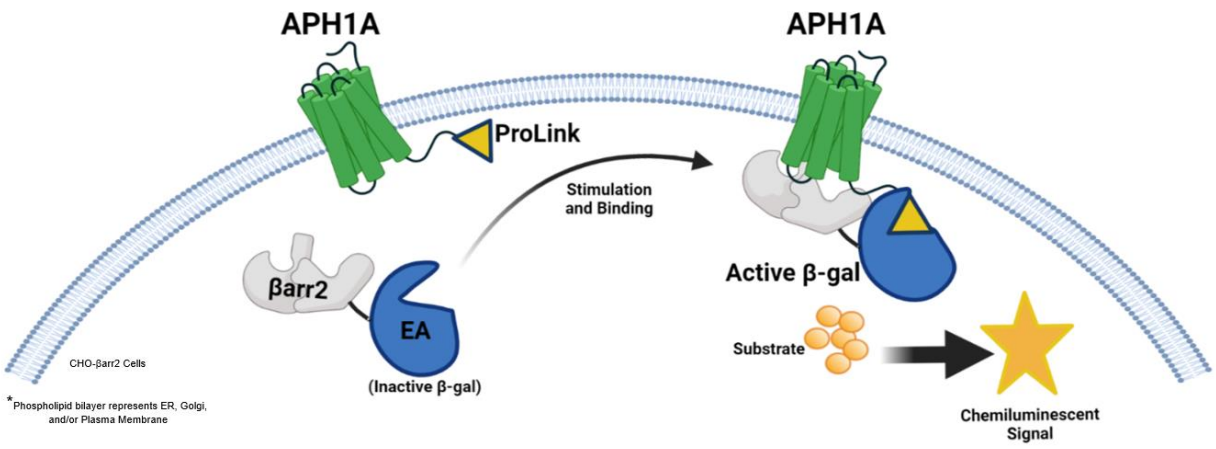

Figure 5. Schematic diagram of the βarr2 recruitment to APH1A PathHunter assay

Schematic diagram depicting the principle of the PathHunter assay used to detect the βarr2 interaction with APH1A. The CHO-βarr2 cells stably express βarr2 covalently attached to a portion of β-galactosidase (enzyme acceptor (EA)) and were transfected with ProLink (PK)-tagged APH1A (APH1A-PK). Upon βarr2 binding to APH1A, the EA and PK form an active β-galactosidase enzyme. Upon addition of a β-galactosidase substrate, the interaction between βarr2 and APH1A is detected by a chemiluminescent signal.

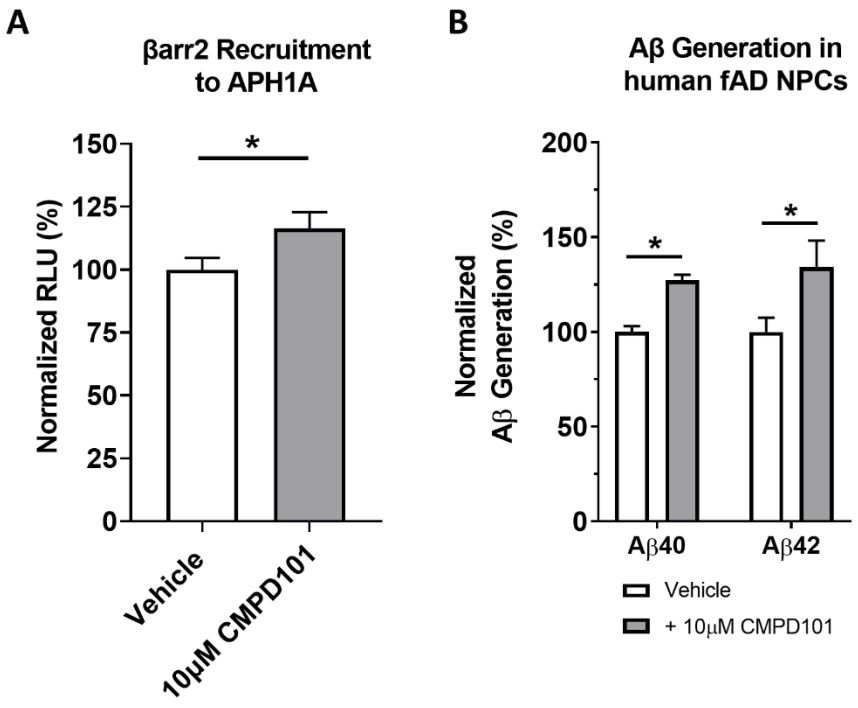

Figure 6. Chemical inhibition of GRK2 and GRK3 increases βarr2 recruitment to APH1A and Aβ generation

(A) βarr2 recruitment to $APH1A^{WT}$ in the CHO-βarr2 cell line following treatment with 10μM CMPD101 relative to vehicle (0.1% DMSO) for 30 min as measured with the PathHunter assay. ** $P < 0.01$ by unpaired t-test. **(B)** $A\beta_{40}$ and $A\beta_{42}$ generation in human fAD neural progenitor cells (NPCs) that stably express $APP_{Swe/Ind}$. * $P < 0.05$ by ANOVA with Sidak's post-test. Data are mean ± SEM of 3 independent experiments performed in triplicate or quadruplicate.

2.2.3 GRKs differentially regulate γ-secretase activity and Aβ generation

We next sought to comprehensively investigate the putative involvement of each ubiquitously expressed GRK in mediating APH1A phosphorylation and γ-secretase activity. To

accomplish this, we utilized a clustered regularly interspaced short palindromic repeats (CRISPR)/Cas9 genome editing strategy (223) to genetically delete *Adrbk1*, *Adrbk2*, *Grk5*, or *Grk6* in HEK293 cells and generate monoclonal GRK knockout (KO) cell lines, herein referred to as GRK2 KO, GRK3 KO, GRK5 KO, or GRK6 KO cells, respectively. The small guide RNAs (sgRNAs) for *Grk6* were designed to genetically delete all GRK6 isoforms. Successful genetic deletion of each *Grk* was confirmed by Western blot analysis (Fig. 7). Notably, genetic deletion of each *Grk* did not affect protein expression of the other GRKs. Furthermore, we did not detect changes in γ-secretase subunit expression in the GRK KO cell lines (Fig. 8).

We then sought to determine whether genetic deletion of each *Grk* mediates distinct functional outcomes, specifically in the regulation of γ-secretase activity and Aβ generation. We transiently expressed APP-C99 (Fig. 9), a direct substrate of γ-secretase, in each GRK KO and an unedited CRISPR control cell line and determined the levels of $A\beta_{40}$ and $A\beta_{42}$ generation by enzyme-linked immunosorbent assay (ELISA). Surprisingly, we detect a 6 to 7-fold increase in $A\beta_{40}$ and $A\beta_{42}$ generation in GRK2 KO cells in comparison to control cells (Fig. 10A). Remarkably, these results are consistent with CMPD101 treatment in human fAD NPCs (Fig. 6B). In contrast, we detect a ~50% reduction in $A\beta_{40}$ and $A\beta_{42}$ generation GRK3 KO and GRK5 KO cells (Fig. 10 B and C) and no change in $A\beta_{40}$ or $A\beta_{42}$ generation in GRK6 KO cells relative to control cells (Fig. 10D). These results establish a role for the GRKs in differential regulation of γ-secretase activity and Aβ generation.

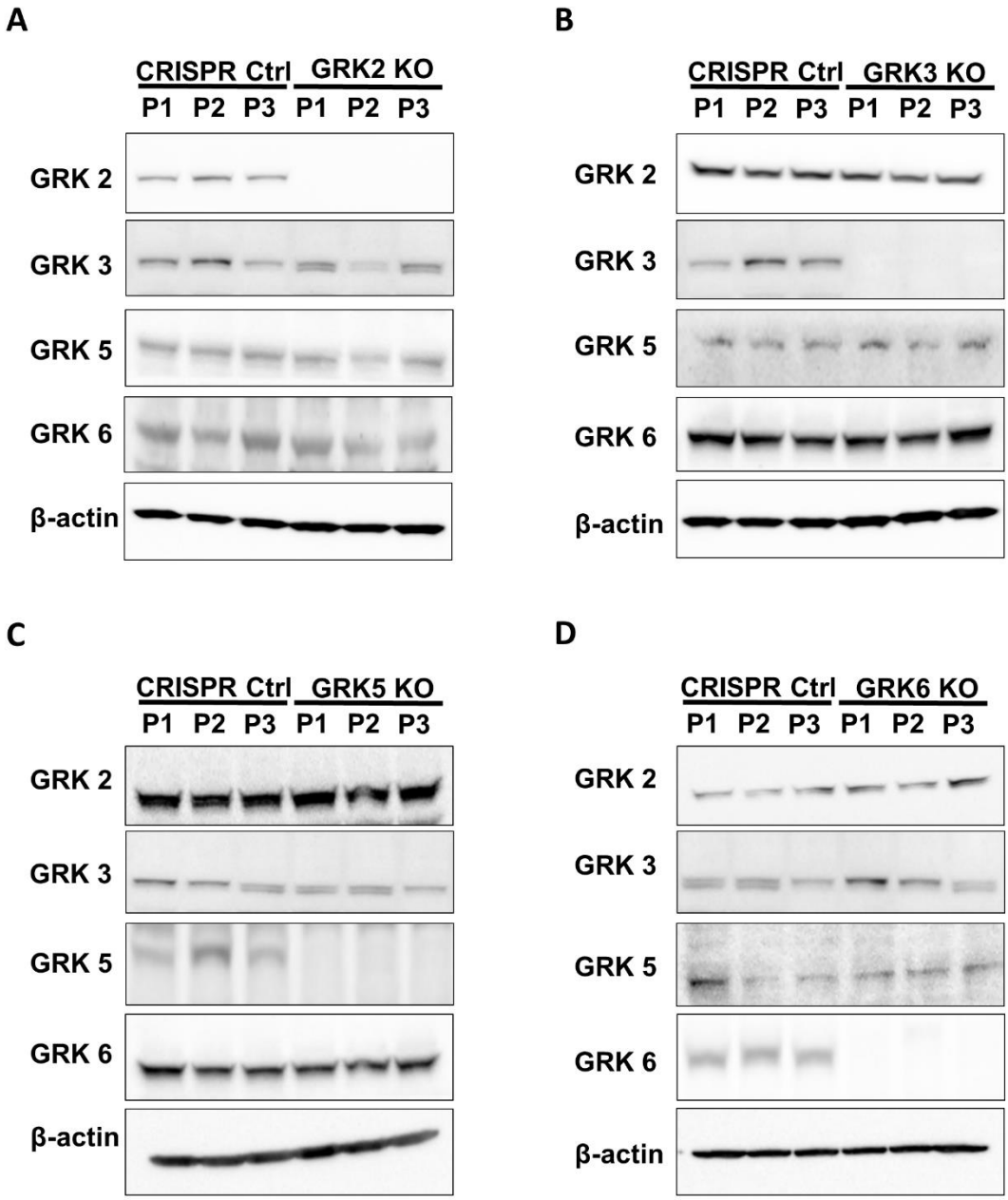

Figure 7. GRK expression in CRISPR GRK KO cell lines

Western blot characterization of GRK expression in HEK293 CRISPR Control and **(A)** GRK2 KO, **(B)** GRK3 KO, **(C)** GRK5 KO, and **(D)** GRK6 KO cell lysates from 3 different passages of cells (P1, P2, and P3).

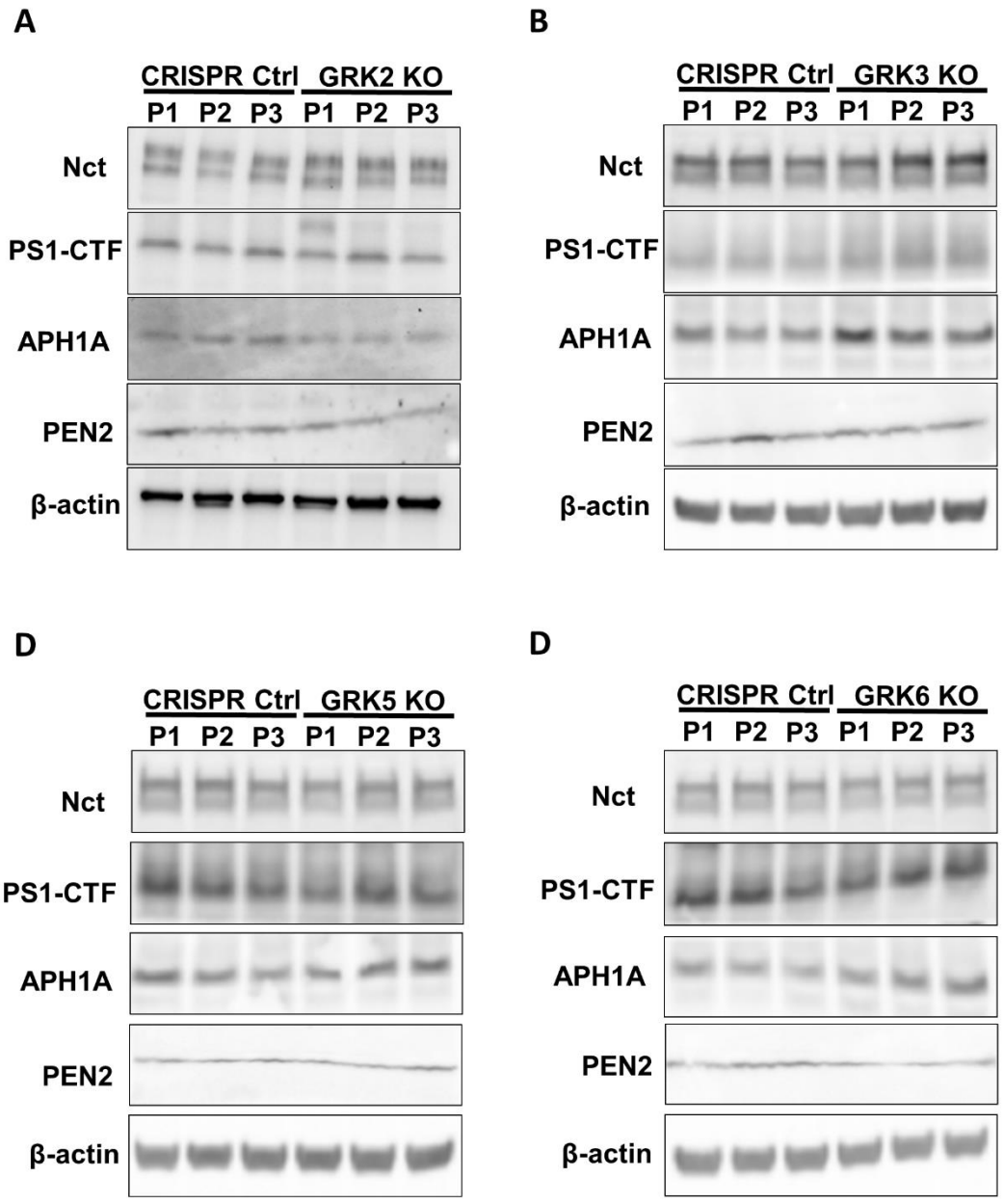

Figure 8. γ-secretase subunit expression in GRK KO cell lines

Western blot characterization of γ-secretase subunit expression in HEK293 CRISPR Control and **(A)** GRK2 KO, **(B)** GRK3 KO, **(C)** GRK5 KO, and **(D)** GRK6 KO cell lysates from 3 different passages of cells (P1, P2, and P3).

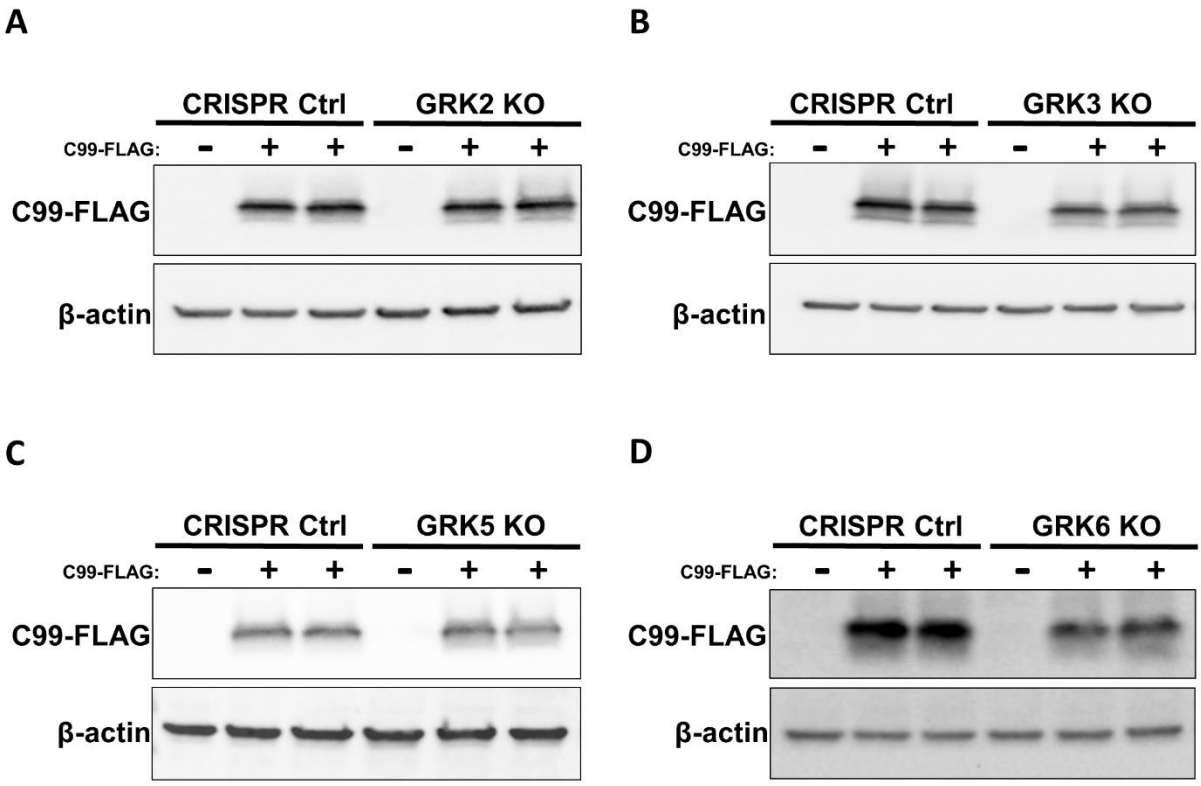

Figure 9. Expression of C99-FLAG in GRK KO cell lines corresponding to Aβ ELISAs in Figure 10

Representative Western blot of transfected C99-FLAG in HEK293 CRISPR Control and **(A)** GRK2 KO, **(B)** GRK3 KO, **(C)** GRK5 KO, **(D)** GRK6 KO cells used for Aβ ELISA in Fig. 10.

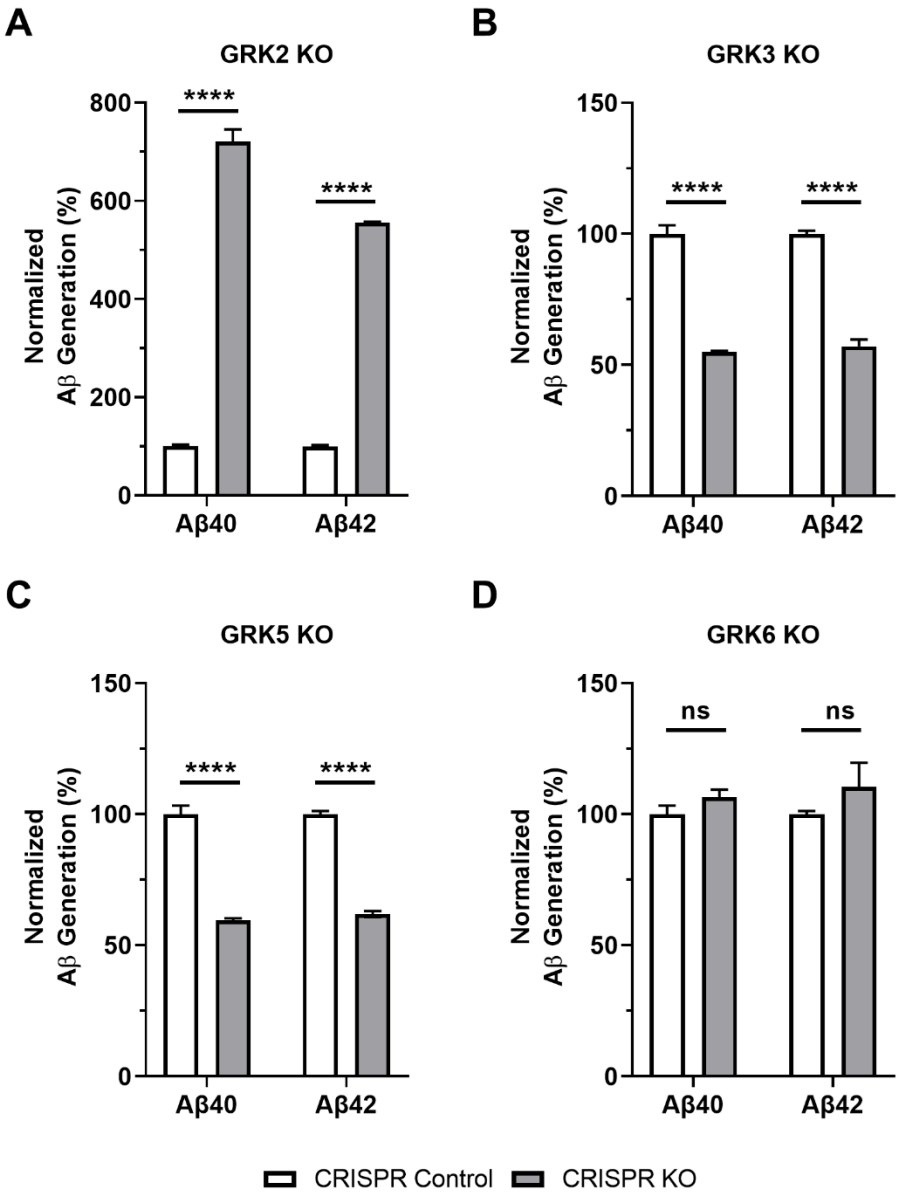

Figure 10. Genetic deletion of each GRK differentially regulates γ-secretase activity and Aβ generation

$A\beta_{40}$ and $A\beta_{42}$ generation in HEK293 cells following expression of APP-C99 in CRISPR control cells (*white bars*) and each GRK KO cell line (*grey bars*): **(A)** *Adrbk1* (GRK2), **(B)** *Adrbk2* (GRK3), **(C)** *Grk5* (GRK5), and **(D)** *Grk6* (GRK6). **** $P < 0.0001$ by ANOVA with Tukey's post-test. Data are mean ± SEM of 3 independent experiments performed in triplicate.

2.2.4 GRKs differentially regulate APH1A phosphorylation

Given the identification of phosphorylation sites in ICL2 and the C-terminus of APH1A and the differential effects of *Grk* genetic deletion on Aβ generation, we hypothesized that the GRKs generate distinct phosphorylation patterns in APH1A, which differentially affect γ-secretase activity and Aβ levels. To test this hypothesis, we first determined the phosphorylation pattern of APH1A in each GRK KO cell line. We transiently expressed equivalent amounts of APH1A in each GRK KO and control cell line and performed label-free quantitative LC-MS/MS analysis. We detect unique APH1A phosphorylation patterns in the GRK2 KO and GRK6 KO cell lines and a similar APH1A phosphorylation pattern in the GRK3 KO and GRK5 KO lines. Interestingly, we observe the most striking differential phosphorylation changes in ICL2. We identify a novel phosphorylation site at S105 and increase in phosphorylation at S110 in the GRK2 KO line (Fig. 11A and Fig. 12). Genetic deletion of *Grk6* also leads to a substantial increase in APH1A phosphorylation at S110. In contrast, phosphorylation at S103 is almost completely abolished in the GRK2, GRK3, and GRK5 KO cell lines. Genetic deletion of each *Grk* reduces, but does not eliminate, S251 and S257 C-terminal phosphorylation. We observe a greater loss of phosphorylation at S257 relative to S251 in each GRK KO cell line, suggesting that phosphorylation at S251 may affect or facilitate phosphorylation at S257. Collectively, MS analysis of APH1A phosphorylation in the GRK KO cell lines highlights unique ICL2 and C-terminal phosphorylation patterns, with ICL2 displaying the primary differential sites of phosphorylation in APH1A (Fig. 11 A and B).

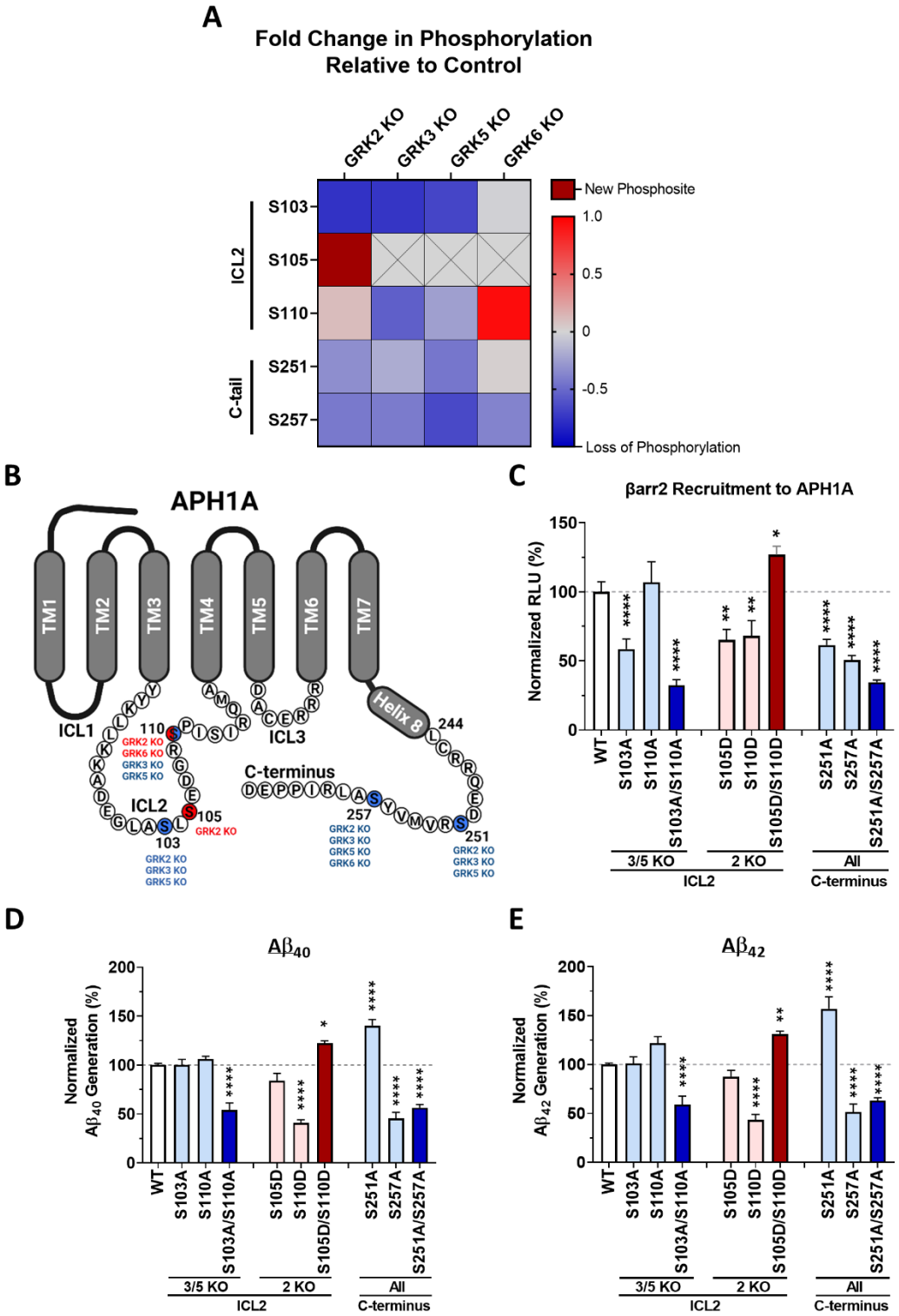

Figure 11. Differential APH1A phosphorylation is mediated by GRKs and regulates interaction with βarr2 and γ-secretase activity

(A) Heat map of the fold change in APH1A phosphorylation following expression in each GRK KO cell line relative to control cells as measured by label-free LC-MS/MS in 3 independent experiments. The "x" in specific squares indicates that phosphorylation was not detected. **(B)** Snake diagram of APH1A. The serine residues that display increased (*red*) or decreased (*blue*) levels of phosphorylation in each GRK KO cell line are indicated. **(C)** βarr2 recruitment to APH1A in the CHO-βarr2 cell line following expression of $APH1A^{WT}$ or the APH1A ICL2 and C-terminal phosphorylation-deficient or phosphorylation-mimetic mutants. * $P < 0.05$ ** $P < 0.01$, **** $P < 0.0001$, by two-way ANOVA with Tukey's post-test. **(D)** $A\beta_{40}$ and **(E)** $A\beta_{42}$ generation in cells following expression of APP-C99 and $APH1A^{WT}$, APH1A phosphorylation-deficient, or phosphorylation-mimetic mutants. * $P < 0.05$, ** $P < 0.01$, **** $P < 0.0001$ by two-way ANOVA with Tukey's post-test. Data are mean ± SEM of 3 independent experiments performed in quadruplicate.

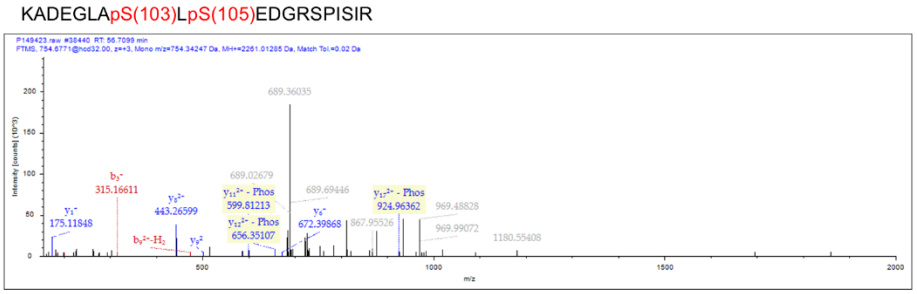

Figure 12. LC-MS/MS analysis identifies novel APH1 S105 phosphorylation in GRK2 KO

MS2 spectra of an identified APH1A S105 phosphorylated peptide in GRK2 KO cells.

2.2.5 Site-specific APH1A phosphorylation mediates interaction with βarr2 and γ-secretase activity

Our lab previously demonstrated that βarr2 interacts with APH1A to stabilize the γ-secretase complex in lipid-raft or DRM domains where the complex is more enzymatically active and can process substrates, including APP-C99 (208). As such, we hypothesized that APH1A phosphorylation patterns differentially regulate βarr2 recruitment to APH1A and consequent γ-secretase activity and Aβ generation. To test this hypothesis and establish the presence of an APH1A phosphorylation barcode, we generated individual phosphorylation-deficient ($APH1A^{S103A}$, $APH1A^{S110A}$, $APH1A^{S251A}$, and $APH1A^{S257A}$) and phosphorylation-mimetic ($APH1A^{S105D}$ and $APH1A^{S110D}$) mutants, which correspond to phosphorylation changes observed in the GRK KO cell lines relative to control cells (Fig. 11 A and B). In addition, to gain insight into a putative multi-site phosphorylation barcode on APH1A, we generated double-phosphorylation mutants in ICL2 representative of phosphorylation changes in the GRK3/GRK5

KO (APH1A$^{S103A/S110A}$) and GRK2 KO (APH1A$^{S105D/S110D}$) cell lines, and in the C-terminus (APH1A$^{S251A/S257A}$) as observed in the GRK2/GRK3/GRK5 KO cell lines. We then expressed APH1A^{WT} or the phosphorylation mutants along with APP-C99 in CHO-βarr2 cells (Fig. 13) and utilized the PathHunter assay to measure βarr2 recruitment to APH1A (Fig. 11C) and ELISAs to measure $A\beta_{40}$ and $A\beta_{42}$ generation (Fig. 11 D and E). Following expression of the individual phosphorylation-deficient APH1A^{S103A} or APH1A^{S110A} mutants, βarr2 recruitment is reduced or unaffected, respectively, relative to cells that express APH1A^{WT}. Neither the APH1A^{S103A} nor APH1A^{S110A} mutation affects γ-secretase activity. However, expression of the APH1A$^{S103A/S110A}$ double ICL2 phosphorylation-deficient mutant leads to a significant reduction (~60%) in βarr2 recruitment to APH1A and Aβ generation compared to APH1A^{WT}. These results suggest that phosphorylation at both S103 and S110 within ICL2 regulates both βarr2 recruitment and γ-secretase activity and that loss of phosphorylation at both sites, as observed in both the GRK3 KO and GRK5 KO cells (Fig. 11A), significantly hinders βarr2 recruitment and Aβ generation.

In the GRK2 KO cell line, MS analysis identified a novel phosphorylation site at S105 and an increase in phosphorylation at S110 (Fig. 11A). Interestingly, expression of the individual APH1A^{S105D} and APH1A^{S110D} phosphorylation-mimetic mutants reduces βarr2 recruitment and Aβ generation relative to APH1A^{WT}. However, expression of the APH1A$^{S105D/S110D}$ double phosphorylation-mimetic mutant results in a significant increase in both βarr2 recruitment to APH1A and $A\beta_{40}$ and $A\beta_{42}$ generation (Fig.11 C to E). These results are consistent with the effect we observe in the GRK2 KO cell line (Fig. 10A) and with CMPD101 treatment in CHO-βarr2 cells (Fig. 6A) and human fAD NPCs (Fig. 6B). Taken together, these data highlight the importance of phosphorylation at multiple ICL2 sites, i.e., a phosphorylation barcode, to mediate βarr2 recruitment to APH1A and direct the functional outcome of γ-secretase activity.

MS analysis of the GRK KO cell lines reveal a decrease in C-terminal phosphorylation at S251 and S257 in the GRK2, GRK3, and GRK5 KO lines and only a decrease in phosphorylation at S257 in the GRK6 KO line (Fig. 11A). Expression of the individual $APH1A^{S251A}$ and $APH1A^{S257A}$ or double $APH1A^{S251A/S257A}$ phosphorylation mutant reduces βarr2 recruitment to APH1A relative to $APH1A^{WT}$. Surprisingly, despite a reduction in βarr2 recruitment, the $APH1A^{S251A}$ mutant exhibits increased Aβ generation. In contrast, the $APH1A^{S257A}$ and double $APH1A^{S251A/S257A}$ mutants exhibit a decrease in βarr2 recruitment and Aβ generation relative to $APH1A^{WT}$. Given that we observe reduced C-terminal phosphorylation in each GRK KO cell line and still detect increased Aβ generation in GRK2 KO cells or equivalent Aβ generation in GRK6 KO cells relative to control cells (GRK6 KO), we can conclude that APH1A phosphorylation changes by GRKs on the C-terminus function in conjunction with ICL2 phosphorylation to dictate overall βarr2 binding and downstream functional consequences on γ-secretase activity.

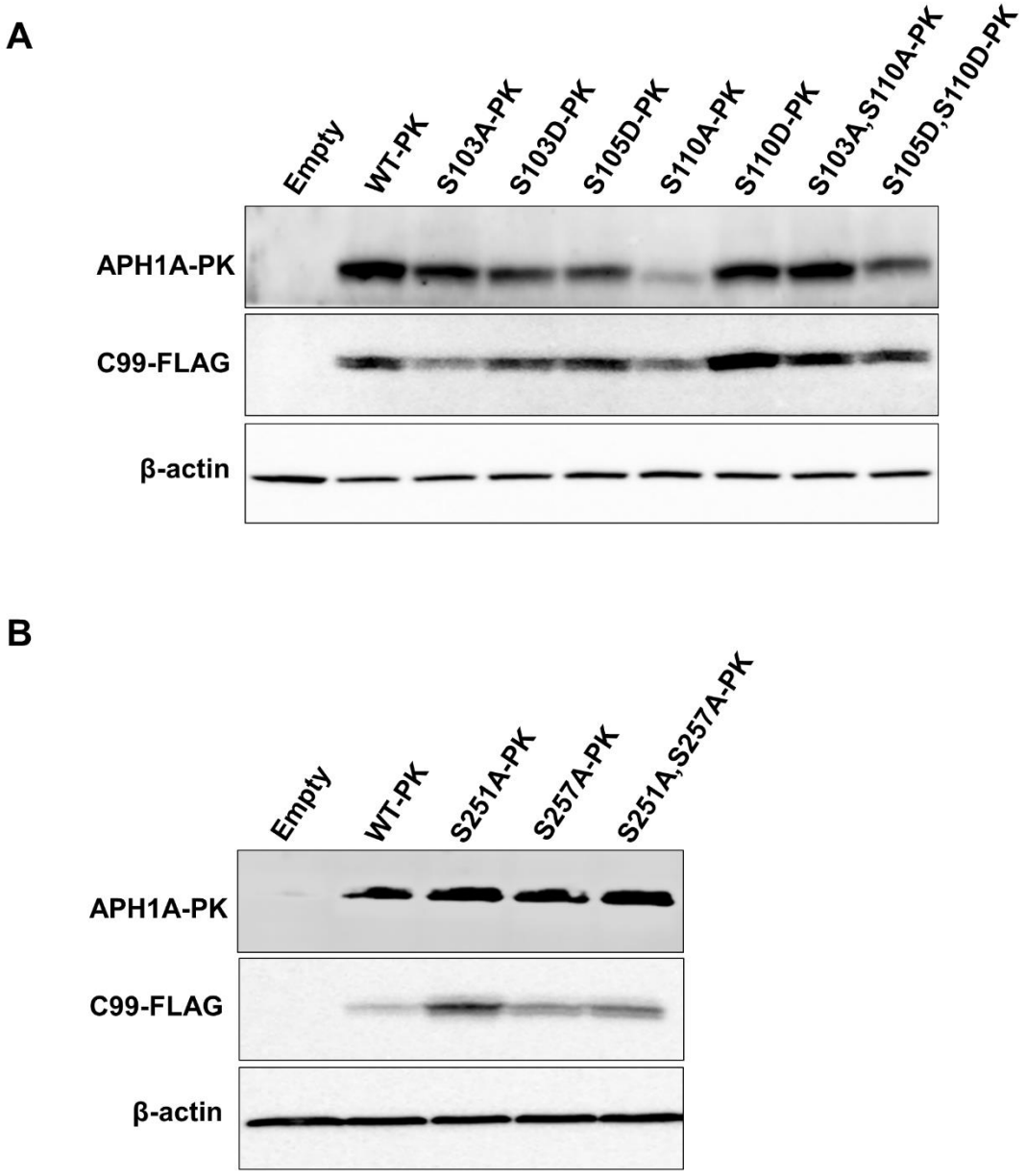

Figure 13. Expression of APH1A-PK and C99-FLAG corresponding to PathHunter and Aβ ELISA assays in Figure 11

Representative Western blot expression of C99-FLAG and APH1A^{WT}-PK and **(A)** APH1A-PK ICL2 phosphorylation-dead and phosphorylation-mimetic mutants or **(B)** APH1A-PK C-terminus phosphorylation-dead mutants used for PathHunter and Aβ ELISA experiments in Fig. 11.

2.2.6 Structural modeling and MD simulations reveal βarr2 finger loop domain engagement with APH1A cytoplasmic loops

After establishing the differential effects of the ubiquitously expressed GRKs in mediating an APH1A phosphorylation barcode and a role of each specific APH1A ICL2 and C-terminal phosphorylation site in mediating βarr2 binding and γ-secretase activation, we sought to gain additional structural insights into the mechanism of the βarr2-APH1A interaction. To this aim, we first generated a structural model for the complex formed between APH1A and βarr2 using the x-ray structure resolved for constitutively active rhodopsin (224) in the presence of visual arrestin (Fig. 14A). While the relative orientations of the TM helices exhibited some differences between APH1A and rhodopsin (Fig. 14B), TM6, TM7, and helix 8 were closely superposable, which allowed construction of a structural model for the βarr2-APH1A complex by optimally aligning the APH1A and βarr2 molecules onto their counterparts in the resolved rhodopsin-arrestin structure and refining the generated model using MD simulations (Fig. 14C). In addition to this so-called 'alignment' model, we independently generated two additional models termed DOCK1 (Fig. 15) and DOCK2 (Fig. 16), by docking simulations followed by MD refinement, to explore the possible occurrence of alternative binding poses and the robustness of interfacial contacts. Fig. 5 illustrates the results for the DOCK2 model (Fig. 16 A and B) and displays the time evolution of the corresponding interfacial contacts observed during two independent runs of 40 ns carried out for this model (Fig. 16C). Equivalent results for the other two models are presented in Fig. 15.

The three models consistently exhibited interfacial interactions at APH1A ICL2 and ICL3 and βarr2 finger loop, despite some local differences in specific residue pairs. The C-terminus of APH1A was also engaged in close contact with βarr2 in the two docking models (Fig. 16B and

Fig. 15 A and B) enclosed in the respective *yellow* (ICL2/3 interactions) and *blue* (C-terminus interactions) circles. Contacts validated by at least two independent models include the three main groups of interactions: E183 or R184 (ICL3) with G73, L74 and/or S75 (finger loop); I114-R115 (ICL2) with V71 -L72 finger loop; and E83-R184 (ICL3) with G73 and S75. Contacts observed between the C-terminus of APH1A and βarr2 in the DOCK1 and DOCK2 models involved APH1A residues R241, C245, Q248 or E249 (C-terminus) making contacts with K153, E156, E157 or R52 on βarr2. As shown in Fig. 16C and Fig. 15C, these interactions were stably maintained during extended portions of the MD runs.

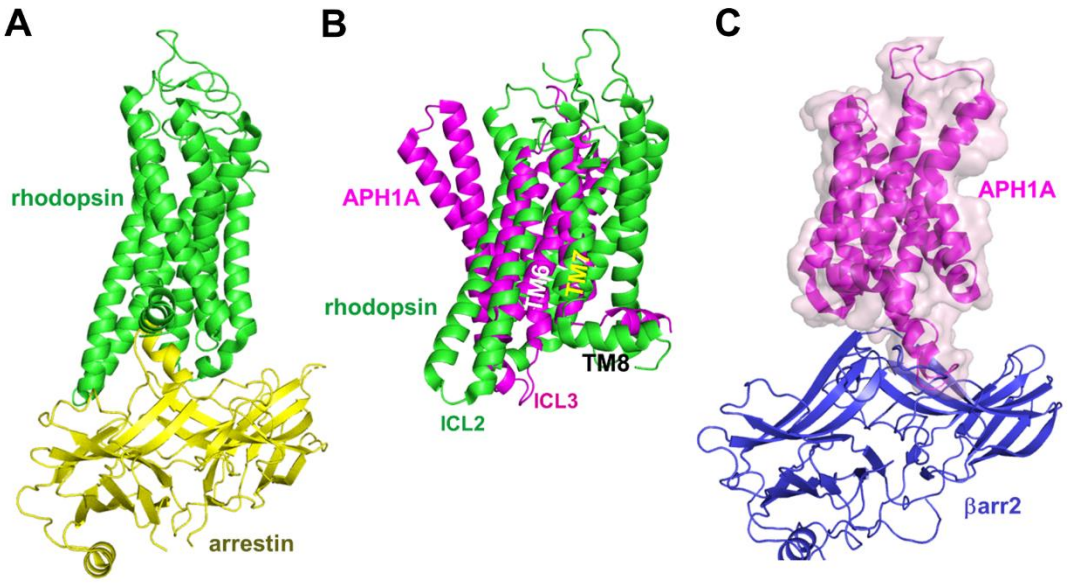

Figure 14. Modeling of the APH1A-βarr2 complex based on structural alignment against the complex resolved for rhodopsin

(**A**) The X-ray structure of rhodopsin bound to arrestin (PDB id 4zwj) used as template. The rhodopsin is in *green* and visual arrestin in *yellow*. (**B**) Alignment of APH1A (*magenta ribbon*, taken from γ-secretase complex; PDB id: 5a63) onto rhodopsin (*green ribbon;* PDB id: 4zwj) using Cealign plugin in PyMOL. The two structures exhibit structural similarity between their TM helices, especially TM6 and TM7. (**C**) Structural model of the complex between APH1A and βarr2 generated after structural alignment of APH1A against rhodopsin and further refinement to optimize interfacial interactions. Additional models generated by docking simulations and the time evolution of the corresponding interfacial contacts in MD simulations are presented in Figs 15 and 16.

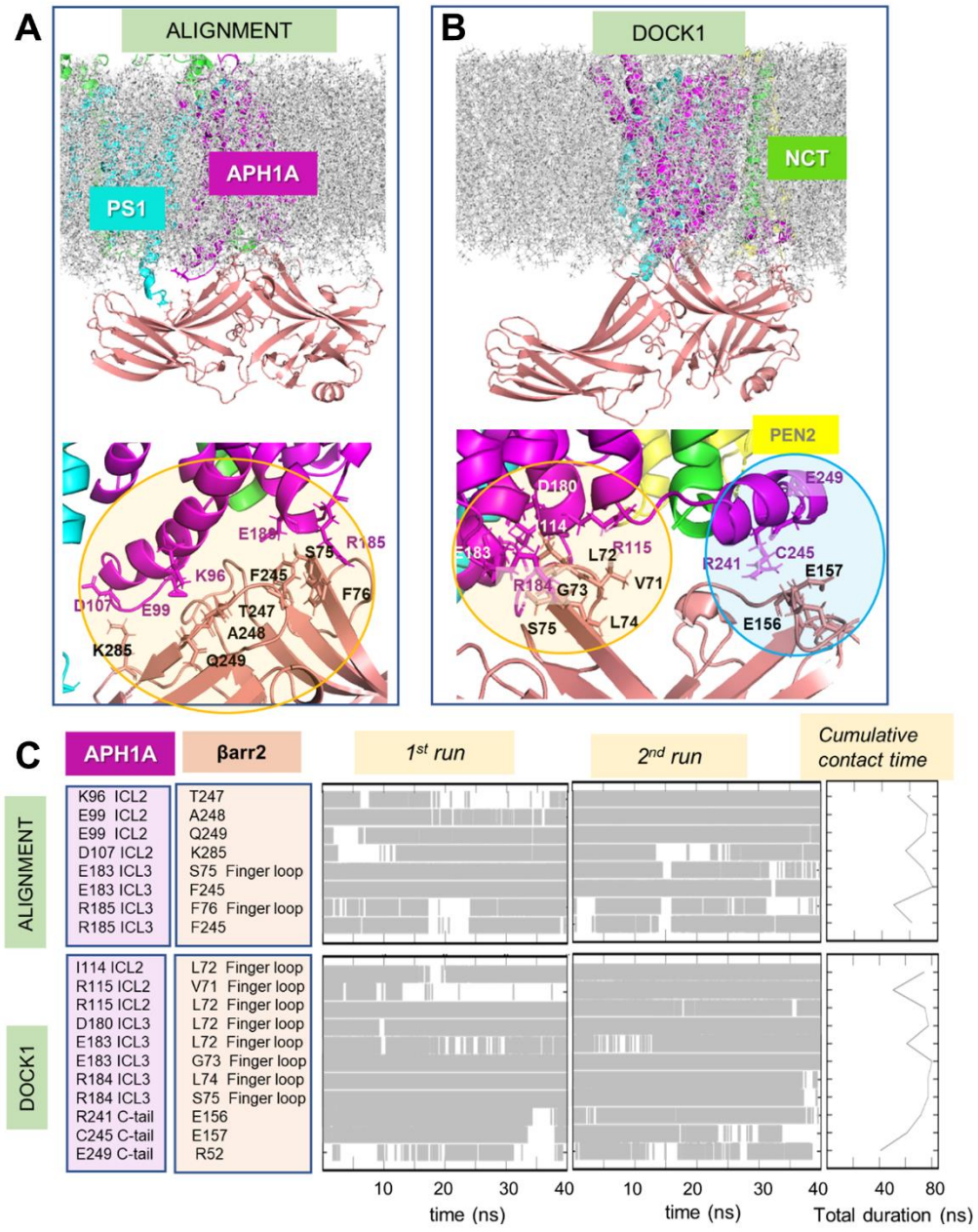

Figure 15. Structural modeling of the interaction between APH1A and βarr2 and the time evolution of the most stable interfacial contacts for the Alignment and DOCK1 models

(**A**) Alignment and **(B)** structural model DOCK1 generated by docking simulations followed by MD refinement carried out at full atomic scale in explicit membrane (shown in *gray sticks*) and water. Note that the simulations were performed for the intact γ-secretase complex that displayed tight interaction between APH1A (*magenta*) and βarr2

(*salmon*), with transient involvement of other γ-secretase complex subunits such as the PS1 (*cyan*) and NCT (*green*). (**C**) Interactions between APH1A and βarr2 for two independent runs (40 ns each) carried out for this model (the first two columns) and corresponding time-evolution of interactions for both run. The last column displays the cumulative fractional time during which those pairs made contacts. Here, interactions are defined when any pairs of heavy atoms belonging to the two respective proteins are separated by less than 5 Å.

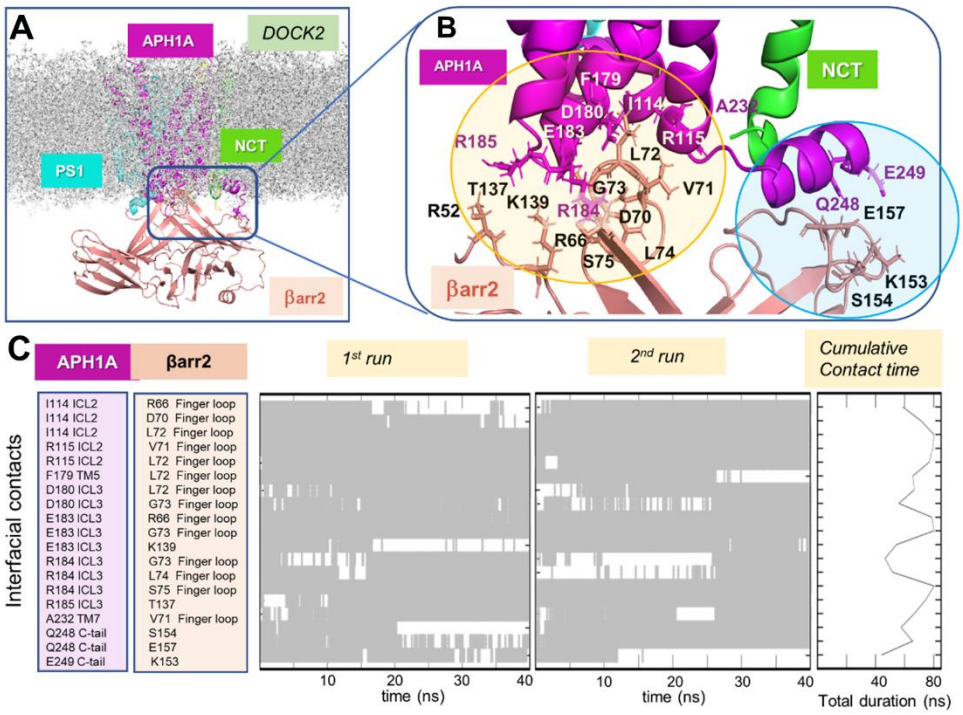

Figure 16. Structural modeling of the interaction between APH1A and βarr2 and the time evolution of the most stable interfacial contacts

(**A**) Structural model DOCK2 generated by docking simulations followed by MD refinement carried out at full atomic scale in explicit membrane (*gray sticks*) and water. The simulations were performed for the intact γ-secretase complex that displays tight interaction between APH1A (*magenta*) and βarr2 (*salmon*) and transient involvement of other γ-secretase complex subunits such as the PS1 (*cyan*) and NCT (*green*). (**B**) Detailed view of interfacial interactions robustly observed at the interface. Residues engaged in persistent interfacial contacts are shown in *sticks* and labeled. (**C**) Interactions between APH1A and βarr2 for two independent runs (40 ns each) carried out for this model (the first two columns) and corresponding time-evolution of interactions for both runs. The last column displays the cumulative fractional time during which those pairs made contacts. Here, interactions are defined when any pairs of heavy atoms belonging to the two respective proteins are separated by less than 5 Å. Equivalent results for two other models, termed Alignment and DOCK1, are presented in Supplementary Fig S9, supporting the robustness of the regions (ICL2 and ICL3 in APH1A and finger loop and C-terminus in βarr2) and residues engaged in interfacial association, despite minor redistributions of the specific pairs of residues.

2.2.7 βarr2 finger loop engagement with APH1A ICL2 and ICL3 facilitates binding and γ-secretase activity

Our computational docking and MD simulation studies indicate a putative model of βarr2 binding to APH1A that resembles a fully engaged GPCR-arrestin complex (174,175,177). As shown in Fig. 16, MD simulations indicate that the βarr2 finger loop domain engages in hydrophobic and polar interactions with ICL2 and ICL3 of the APH1A cytoplasmic core. We sought to experimentally validate these interactions and to further determine whether specific residues in these regions on βarr2 and APH1A are critical for engagement and downstream functional effects on γ-secretase activity. Guided by computational predictions, we generated βarr2 mutants containing the substitution S75R at the primary site of interaction. Importantly, S75 was consistently observed to engage in interfacial associations in all three models (Fig. 15 and Fig. 16). We also generated the βarr2 L72E mutation at a secondary site of interaction shared by DOCK1 and DOCK2 (Fig. 15 and Fig. 16). In HEK293 cells expressing APH1A^{WT} and βarr2^{WT}, βarr2^{L72E}, or βarr2^{S75R}, we utilized a co-immunoprecipitation (co-IP) assay to determine the effect of mutagenesis of L72 and S75 on the interaction between βarr2 and APH1A. Our data demonstrate that mutagenesis of the βarr2 finger loop region at L72 and S75 reduces binding to APH1A (Fig. 17A), indicating that the βarr2 finger loop domain is critical for interaction with APH1A.

Given the involvement of L72 and S75 in the βarr2 finger loop domain in interaction with APH1A, we then determined the effect of L72E and S75R mutagenesis on γ-secretase activity and Aβ generation. We expressed APP-C99 in HEK293 cells along with an empty vector, βarr2^{WT}, βarr2^{L72E}, or βarr2^{S75R} (Fig. 18A) and utilized ELISA to measure $A\beta_{40}$ and $A\beta_{42}$ generation (Fig. 17 B and C). As expected, expression of βarr2^{WT} increased Aβ generation in comparison to vector control samples. Significantly, the βarr2^{L72E} and βarr2^{S75R} finger loop mutants reduced Aβ

generation to control conditions, indicating that engagement of the βarr2 finger loop domain with APH1A is necessary for both the βarr2 interaction with APH1A and γ-secretase activity.

To further investigate the putative involvement of specific residues in ICL3 of APH1A identified by MD simulations in the interaction with βarr2, we generated an APH1A ICL3 mutant ($APH1A^{R184D}$) to disrupt interaction with the primary interaction site at S75 on βarr2. In our CHO-βarr2 cell line, we expressed APP-C99 and $APH1A^{WT}$ or the $APH1A^{R184D}$ mutant (Fig. 18B) and utilized the PathHunter assay and ELISA to determine the effect of APH1A ICL3 mutagenesis on βarr2 recruitment and the downstream functional effect on γ-secretase activity. Expression of the $APH1A^{R184D}$ mutant significantly reduced both βarr2 recruitment to APH1A (Fig. 17D) and $Aβ_{40}$ and $Aβ_{42}$ generation (Fig. 17E) compared to cells expressing $APH1A^{WT}$. These data provide evidence of critical βarr2 finger loop domain interactions with the APH1A cytoplasmic core to facilitate γ-secretase activation and Aβ generation.

Additional MD simulations for the L72E and S75R mutants corroborated the decreased binding to APH1A. As illustrated in Fig. 17F, the L72 of $βarr2^{WT}$ makes contacts with I114, R115, D180, and E183 of APH1A within a $C^{α}$-$C^{α}$ distance range of 4-10 Å (*dashed curves*) while intermolecular distances in the presence of the E72 mutant ($βarr2^{L72E}$) are shifted to longer distances (*solid curves*), indicating that the interaction becomes weaker upon substitution of L72 with E72. On the other hand, the R75 mutant ($βarr2^{S75R}$) shows a slightly weaker interactions compared to $βarr2^{WT}$, with a bimodal distribution of inter-residue distances (Fig. 17G). As such, one might anticipate a smaller reduction in binding affinity. However, we observed that L72, at the middle of the finger loop, is entropically amenable to a diversity of contacts (including those with ICL2 D184) which is impaired by the perturbations caused by the S75R mutation. The introduction of a charged amino acid R75 in the immediate neighborhood of the hydrophobic

residues, L74, and highly flexible G73, further destabilize the interfacial contacts in this region as evidenced by the distance changes presented in Fig. 17G. Furthermore, our MD simulations conducted with APH1A^{R184D} also clearly show a weakening in the interaction of D184 with finger loop residues L74 and S75 (Fig. 17H). C^{α}-C^{α} distances of R184-L74 and R184-S75 increase by about 2 Å compared to those achieved in APH1A^{WT}, demonstrating the occurrence of a looser binding. These structural and dynamic characteristics consistently support the experimentally observed decrease in binding affinity for both mutants. Overall, our data suggest a model where the GRK-mediated APH1A phosphorylation barcodes regulate βarr2 finger loop domain interactions with the cytoplasmic TM core of APH1A to differentially regulate γ-secretase activity and proteolytic cleavage of APP-C99 (Fig. 19).

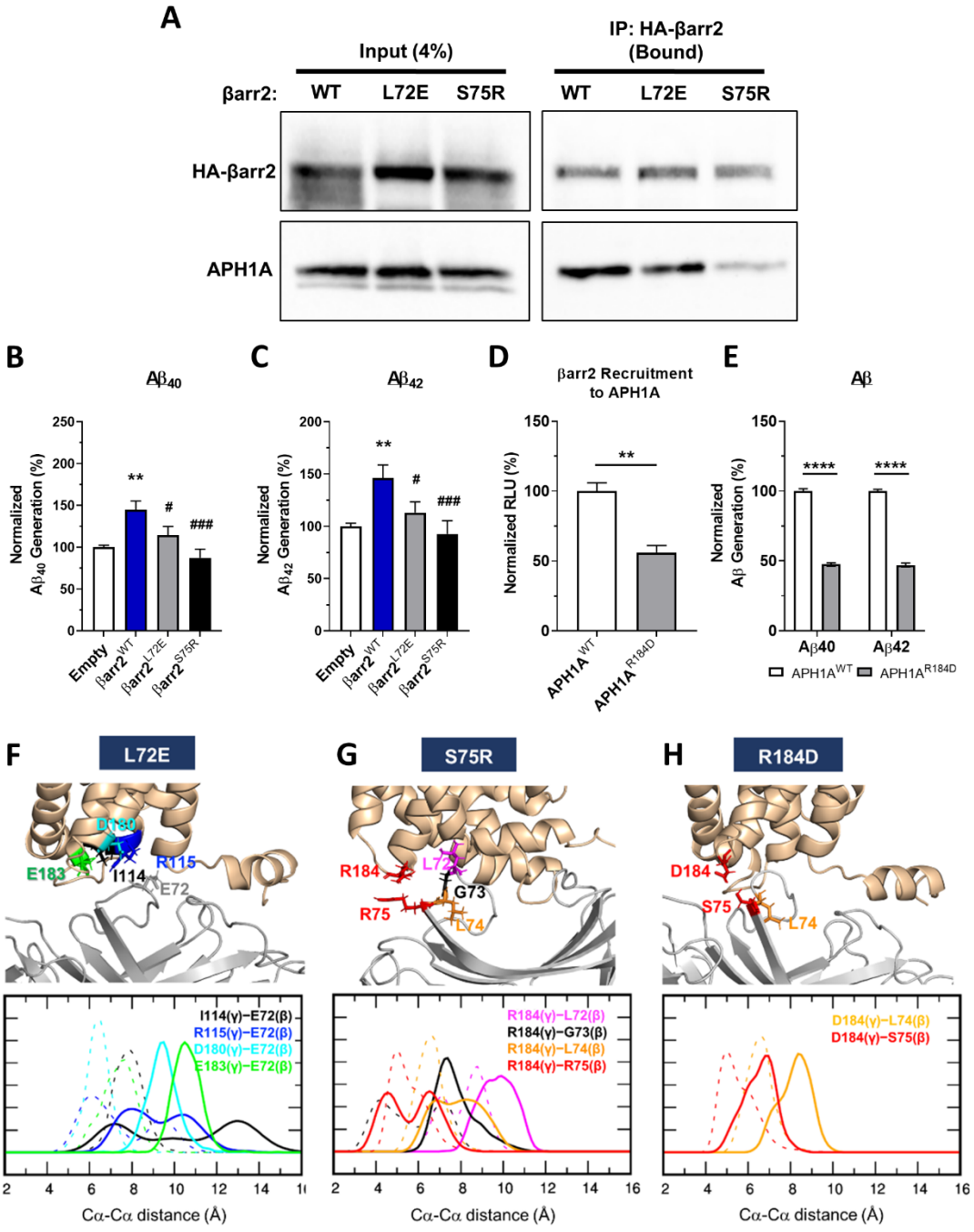

Figure 17. βarr2 finger loop engagement with APH1A ICL3 and ICL2 facilitates binding and γ-secretase activity

(A) Co-immunoprecipitation experiments in HEK293 cells expressing APH1A and $\beta arr2^{WT}$ or the βarr2 finger loop mutants ($\beta arr2^{L72E}$, $\beta arr2^{S75R}$). **(B)** $A\beta_{40}$ and **(C)** $A\beta_{42}$ generation in HEK293 cells following expression of APP-C99

and empty-vector, βarr2^{WT} or βarr2 finger loop mutants. ** $p < 0.01$ by ANOVA with Tukey's post-test (comparison to Empty). # $p < 0.05$, ### $p < 0.001$ by ANOVA with Tukey's post-test (comparison to βarr2^{WT}). **(D)** βarr2 recruitment to APH1A^{WT} or APH1A^{R184D} mutant in the CHO-βarr2 cell line. ** $P < 0.01$ by unpaired t-test. **(E)** $A\beta_{40}$ and $A\beta_{42}$ generation in the CHO-βarr2 cell line following expression of C99-FLAG and APH1A^{WT} or APH1A^{R184D}. **** $P < 0.0001$ by ANOVA with Sidak's post-test. Data are mean ± SEM from 3 independent experiments performed in triplicate or quadruplicate. Results for the βarr2 mutants **(F)** L72E and **(G)** S75R and **(H)** for the APH1A mutant R184D are presented in the respective panels using the structural model DOCK1. In each case, a representative snapshot for the complex with the mutant (*top*), and the histograms of the intermolecular C^{α}-C^{α} distances between the indicated residue pairs of APH1A and βarr2 are shown (*bottom, solid curves*) based on duplicate runs (total of 80 ns) conducted for the indicated mutant. *Dashed curves* indicate the counterparts obtained with the βarr2^{WT} or APH1A^{WT} proteins.

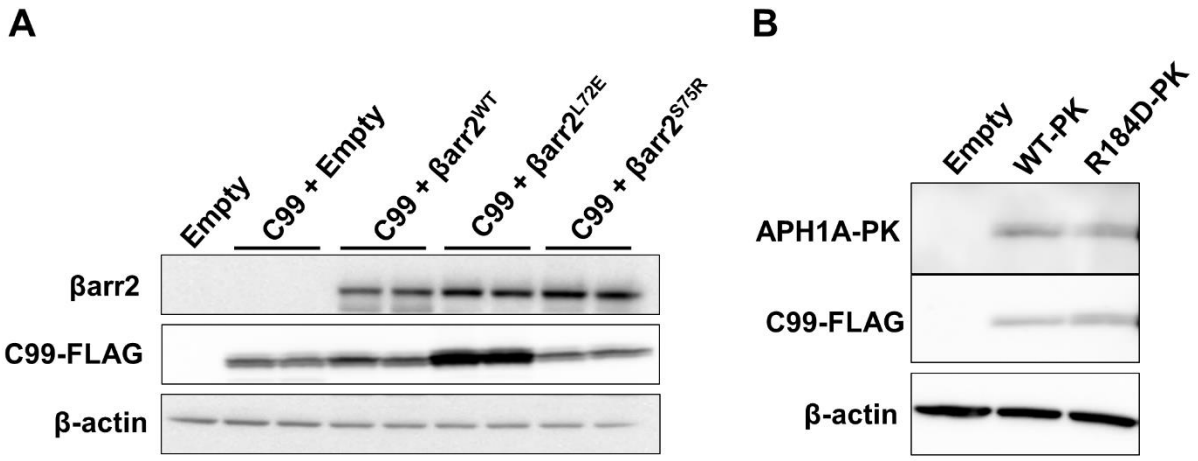

Figure 18. Expression of C99-FLAG and βarr2 or APH1A corresponding to Aβ ELISA and PathHunter assays in Figure 17

(A) Representative Western blot expression of C99-FLAG and $\beta arr2^{WT}$, $\beta arr2^{L72E}$, or $\beta arr2^{S75R}$ used in Aβ ELISAs in Fig. 6. **(B)** Representative Western blot expression of C99-FLAG and $APH1A^{WT}$-PK or $APH1A^{R184D}$-PK used in Aβ ELISA and PathHunter assays in Fig. 17.

2.3 Discussion

GRKs are a family of proteins canonically involved in GPCR phosphorylation that regulate receptor desensitization and internalization. GRK phosphorylation of GPCRs also leads to the activation of intracellular signaling cascades via G proteins and β-arrestins (144,213,214). Different ligands or stimuli initiate distinct GRK phosphorylation patterns or barcodes on GPCRs to differentially regulate cellular signaling (140,225). Here, we uncover a role for the four ubiquitously expressed GRKs in phosphorylation of a non-canonical substrate, APH1A, an integral

component of the γ-secretase complex. Quantitative LC-MS/MS analysis indicates that APH1A is phosphorylated at S103 and S110 within ICL2 and at S251 and S257 on the C-terminus. Further investigation reveals that chemical inhibition of GRK2/3 increases the direct interaction between βarr2 and APH1A as well as γ-secretase activity and Aβ generation in a human fAD NPC model. Genetic deletion of each ubiquitously expressed *Grk*, namely GRK2, 3, 5, and 6, generates unique phosphorylation patterns in ICL2 and the C-terminus of APH1A and differentially affects γ-secretase activity and Aβ generation. Intriguingly, we determine that distinct APH1A phosphorylation barcodes differentially regulate interaction with the GPCR scaffolding protein βarr2. Further structural modeling and MD simulation studies reveal that a conserved region in βarr2, known as the finger loop, interacts with the cytoplasmic TM core (ICL2/3) of APH1A. Experimental validation of the computational modeling studies indicate that the βarr2 finger loop domain and APH1A TM core interaction regulates γ-secretase catalytic activity. Collectively, these studies suggest a model whereby specific APH1A phosphorylation barcodes dictate unique βarr2-APH1A binding conformations that affect γ-secretase substrate recognition of APP-C99 and consequent proteolytic cleavage and Aβ generation (Fig. 19).

In this study, we uncover a functional role for the ubiquitously expressed GRKs in differential modulation of γ-secretase activity. In the GRK2 KO cells, we observe a substantial increase in γ-secretase activity and Aβ generation (Fig. 10A). Surprisingly, we observe an increase in ICL2 phosphorylation at S105 and S110 in the GRK2 KO cells and S110 in the GRK6 KO cells (Fig. 11 A and B), suggesting potential compensatory phosphorylation at S105 and S110 by other kinases in these cell lines and hierarchical phosphorylation of APH1A by GRKs. Indeed, GRKs are known to act in a hierarchical fashion to mediate ICL and C-terminal phosphorylation of many GPCRs to regulate downstream functional signaling outcomes (167,169–171). We also detect an

increase in Aβ generation following chemical inhibition of GRK2/3 in human fAD NPCs (Fig. 6B). These results suggest that GRK2-mediated APH1A phosphorylation precludes pathogenic phosphorylation at S105 and S110 in ICL2 by other GRKs. In agreement with these data, we observe a decrease in constitutive γ-secretase activity and Aβ generation in both the GRK3 KO and GRK5 KO cells in comparison to control cells, which suggests that GRK3 and GRK5 activity contributes to increased γ-secretase activity and Aβ generation. Interestingly, our lab recently determined that both GRK3 and GRK5 are abundantly localized around amyloid plaques in human AD brains (146). Together, these data support the hypothesis that GRK3 and GRK5 activity may contribute to pathogenic Aβ generation while GRK2 activity may act in a protective manner to regulate γ-secretase activity.

Genetic deletion of each ubiquitously expressed *Grk* reduces APH1A C-terminal phosphorylation. The APH1A phosphorylation patterns in the GRK KO cell lines also suggest hierarchical GRK phosphorylation at the C-terminus. In each GRK KO line, we detect a greater loss of phosphorylation at S257 than at S251. Accordingly, phosphorylation at S251 may dictate the level of phosphorylation at S257 by GRKs. In fact, GRK2 has been demonstrated to preferentially phosphorylate serine and threonine residues that are preceded by negatively charged amino acids (226) which may explain how loss of phosphorylation at S251 could reduce S257 phosphorylation to an even greater extent.

While individual APH1A ICL2 and C-terminal serine mutants can independently alter interaction with βarr2 and/or γ-secretase activity, the double serine-mutant results suggest that unique, multi-site APH1A phosphorylation patterns determine differential functional outcomes with regard to regulating βarr2 interaction and γ-secretase cleavage of APP-C99. Furthermore, ICL2 and C-terminal phosphorylation of APH1A appears to act in conjunction to modulate the

overall outcome of βarr2 recruitment and γ-secretase activity. For example, we measure an increase in γ-secretase activity in the GRK2 KO cells (Fig. 10A), where levels of APH1A ICL2 phosphorylation at S103 and S105 are elevated in comparison to a reduction in C-terminal S251 and S257 phosphorylation (Fig. 11A). Given that loss of S251 and S257 C-terminal phosphorylation alone ($APH1A^{S251A/S257A}$) reduces βarr2 recruitment to APH1A and γ-secretase activity (Fig. 11 C to E), our GRK2 KO data suggest an important role of ICL2 phosphorylation in determining the functional γ-secretase outcomes. Likewise, our MD simulation data reveals a critical role of APH1A ICL2 and regulating engagement with βarr2 (Fig. 15 and Fig. 16) which would be altered by the addition or removal of negatively charged phosphates. Overall, we establish the existence of an APH1A phosphorylation barcode in ICL2 and the C-terminus that regulates βarr2 recruitment and γ-secretase activity.

Our previous work demonstrated that overexpression of βarr2 stabilizes localization of the γ-secretase subunits in DRMs where the complex is catalytically active (208). In support of our previous finding, CMPD101 treatment (Fig. 6) and $APH1A^{S103D/S105D}$ expression (Fig. 11 C to E), which increase βarr2 recruitment to APH1A, result in increased γ-secretase activity and Aβ generation. Interestingly, our data in this study also reveal that phosphorylation of APH1A at distinct sites can differentially regulates βarr2 recruitment and γ-secretase activity (Fig. 11 C to E). Accordingly, APH1A phosphorylation patterns that reduce βarr2 recruitment do not necessarily reduce γ-secretase activity, as observed with the $APH1A^{S103A}$, $APH1A^{S105D}$, and $APH1A^{S251A}$ mutants. APH1A contains two histidine residues, H171 and H197 within TM5 and TM6 respectively, that have been shown to be critical for γ-secretase complex assembly and stability, APP-C99 substrate recognition, and aspartyl proteolytic cleavage (51,52). We postulate that APH1A ICL2 and C-terminal phosphorylation allows for differential βarr2 binding modes to

ICL2/3 of the APH1A TM core, which in turn, induce conformational shifts in TM5 and TM6 of APH1A to regulate APP-C99 binding and γ-secretase activity. Additionally, the binding conformation of βarr2 may also sterically prevent entry of γ-secretase substrates. Collectively, we argue that γ-secretase activity is regulated by both the extent of βarr2 recruitment and the distinct APH1A-βarr2 conformation following binding (Fig. 19).

Structural analysis of β-arrestin interaction with GPCRs indicates that there is a biphasic interaction between β-arrestin and the receptor (177). Initial β-arrestin binding to a GPCR is mediated via GPCR C-terminal phosphorylation. However, β-arrestin can also transition into a fully engaged conformation with the receptor where a small structural region in β-arrestins known as the finger loop engages with the cytoplasmic TM core of the receptor (174,175,179,180). Notably, our computational modeling data suggest a similar, critical role of the APH1A TM cytoplasmic core, i.e., ICL2 and ICL3, in binding to βarr2 finger loop residues, which resembles a fully-engaged GPCR-β-arrestin complex. Our MD simulations are supported by APH1A MS and mutagenesis studies which suggest that ICL2 phosphorylation in particular is a critical determinant of βarr2 binding and functional effect on γ-secretase activity and APP-C99 cleavage. A recent paper investigating how GPCR phosphorylation patterns direct β-arrestin signaling concluded that the position of phosphates on a GPCR is more important than the total number of phosphorylated residues in determining the outcomes of β-arrestin binding and downstream signaling. Importantly, the authors conclude that phosphorylation patterns that favor β-arrestin binding are not necessarily the same as those that favor β-arrestin signaling (121). We observe a similar mechanism with APH1A phosphorylation, βarr2 binding, and the downstream functional effect on APP-C99 cleavage by the γ-secretase complex where APH1A phosphorylation mutants that decrease βarr2 recruitment do not always reduce γ-secretase activity (Fig. 11 C to E).

We predict changes to the APH1A phosphorylation barcode may occur via direct or indirect changes in GRK activity in the brain. Our lab recently demonstrated that GRKs are differentially expressed across AD-affected regions and in different cell types in the brain. Significantly, we observed a decrease in GRK2, GRK5, and GRK6 expression in AD brain tissue relative to age-matched control samples (146). As such, changes in GRK levels across brain regions and during disease progression may directly affect constitutive GRK phosphorylation of APH1A and alter γ-secretase activity. Furthermore, we cannot rule out the possibility of unidentified, endogenous interacting partners of APH1A that can induce conformational changes in APH1A to directly recruit GRKs. Alternatively, changes in GPCR signaling in different brain regions with age and by other AD etiologies may indirectly alter the activity of GRKs, thus changing the APH1A phosphorylation barcode and effecting γ-secretase activity. Multiple GPCRs have been demonstrated to contribute to the pathophysiology of AD, including regulating APP proteolytic processing (100,227). Since both GPCR signaling complexes and the γ-secretase complex preferentially partition into DRMs (206,228,229), it is conceivable that GPCR dysregulation, e.g., changes in expression level or ligand stimulation, will alter GRK activity in cells and in the local DRM environment, which may lead to changes in APH1A phosphorylation and γ-secretase activity. Intriguingly, the constitutively active, orphan GPCR GPR3 is increased in the AD brain, and *in vitro* GPR3 expression increases DRM localization of the γ-secretase complex (205). Furthermore, genetic deletion of *Gpr3* in mice reduces βarr2 interaction with APH1A in cortical brain tissue (208), reduces γ-secretase activity and Aβ generation, and alleviates cognitive deficits in four AD transgenic mouse models (207). Thus, constitutive GPR3 activity may modulate the APH1A phosphorylation barcode by recruiting specific GRKs to the local DRM environment of the γ-secretase complex to alter the APH1A phosphorylation barcode.

Overall, our analysis opens the door for computational drug screening to identify and design small molecules or peptides to modulate βarr2 interaction with APH1A. As advances in amyloid and tau brain imaging along with AD biomarker discovery continue to be made, the opportunity to detect and intervene early in AD progression becomes more possible. The work here suggests a new avenue for therapeutic drug screening to disrupt critical APH1A-βarr2 interactions and reduce Aβ generation early in disease progression in an effort to negate the Aβ concentration-dependent pathogenic cascade cumulating in neurodegeneration and dementia.

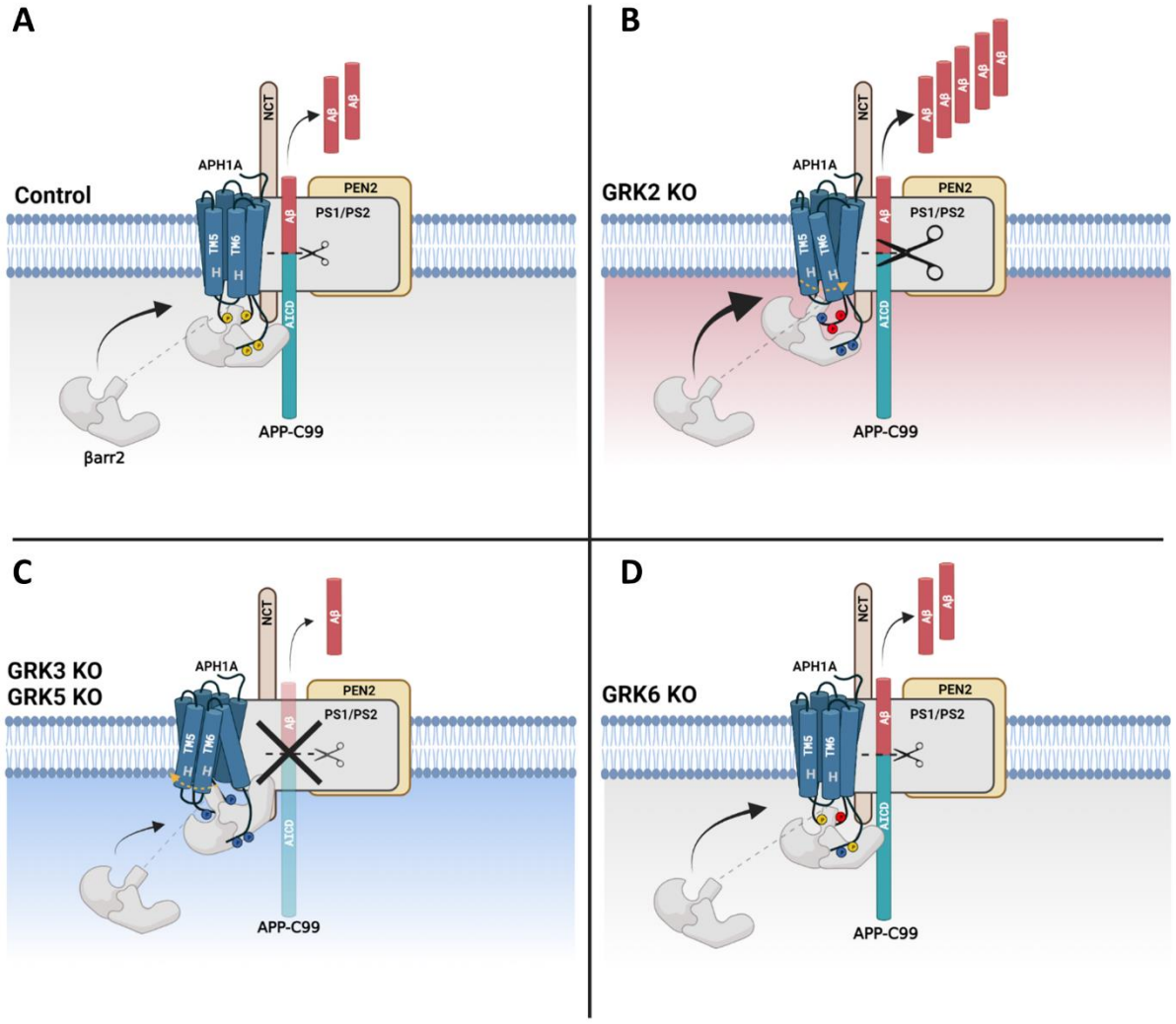

Figure 19. GRKs differentially regulate γ-secretase activity by mediating an APH1A phosphorylation barcode

GRKs mediate APH1A phosphorylation within ICL2 and the C-terminus of APH1A to regulate βarr2 recruitment via interactions between the βarr2 finger loop domain and the cytoplasmic TM core (ICL2/3) of APH1A. **(A)** In HEK293 cells, phosphorylation of APH1A leads to βarr2 recruitment and γ-secretase cleavage of APP-C99 to generate Aβ. **(B)** In GRK2 KO cells, APH1A ICL2 phosphorylation at both S105 and S110 is elevated relative to control cells. The γ-secretase complex exhibits increased activity and cleavage of APP-C99. **(C)** In GRK3 KO and GRK5 KO cells, APH1A displays reduced levels of ICL2 phosphorylation at S103 and S110 relative to control cells. The γ-secretase complex exhibits decreased activity and cleavage of APP-C99. **(D)** In GRK6 KO cells, APH1A phosphorylation at S110 alone is elevated relative to control cells. The γ-secretase activity and Aβ generation are unaffected relative to

control cells. We hypothesize that changes in the phosphorylation barcode affect both the extent of βarr2 recruitment to APH1A and the APH1A-βarr2 conformation following binding. We predict the positioning of H171 and H197 in APH1A is altered by βarr2 engagement, which affects recognition and cleavage of APP-C99. The phosphorylation sites highlighted in *red* and *blue* indicate elevated or reduced levels of phosphorylation, respectively, relative to control (or basal) levels of phosphorylation at the sites highlighted in yellow. Figure was made using BioRender.com.

2.4 Materials and Methods

2.4.1 Antibodies and Compounds

Rabbit polyclonal antibodies to human PS1-NTF (B19.3, 1:20,000), $APH1A_L$ (B82.3, 1:1,000), PEN-2 (B126.2, 1:1,000) and the APP C terminus (B63.3, 1:10,000) and the mouse monoclonal antibody 9C3 (1:3,000) directed against the C terminus of NCT have been previously described and were the gift of Dr. Bart De Strooper (VIB and KU Leuven, Leuven, Belgium; UK Dementia Research Institute and University College London, London, United Kingdom)(230,231). Antibodies to the following were purchased: GRK2 (mouse, C-9, SantaCruz Biotechnology, 1:1000), GRK3 (rabbit, D8G6V Cell Signaling Technologies, 1:1000), GRK5 (mouse, D-9, SantaCruz Biotechnology, 1:1000), GRK6 (rabbit, D1A4, Cell Signaling Technologies, 1:1000), FLAG (mouse, M2, Sigma, 1:1,000), βarr2 (mouse, H-9, SantaCruz Biotechnology, 1:1000), hemagglutinin (HA) (mouse, HA.11, BioLegend, 1:1000), hemagglutinin (HA) (rabbit, C29F4, Cell Signaling Technologies, 1:1000). Takeda Compound101 was purchased from Hello Bio, and octyl-β-D-glucopyranoside was purchased from EMD Millipore.

2.4.2 Plasmid Construction

All mutations in APH1A and βarr2 were generated with the XL II Site-Directed Mutagenesis Kit (Agilent Technologies) according to manufacturer's instructions.

2.4.3 Cell Lines

The HEK293 cell line was purchased from American Type Culture Collection. The CHO-KI β-arrestin 2 cell line (CHO-βarr2) was purchased from DiscoveRx. The ReNCell GA2 familial Alzheimer's disease (fAD) human neural progenitor cell (hNPC) line was a kind gift From Dr. Rudolph E. Tanzi and Dr. Doo Yeon Kim (Harvard University, Cambridge, MA) and generated as previously described (222).

2.4.4 Cell Culture

HEK293 cells were maintained in complete media containing DMEM/F12 with GlutaMAX (Fisher Scientific) and supplemented with 10% fetal bovine serum (ThermoFisher Scientific). Cells were maintained at 37°C and 5% CO_2. CHO-K1 βarr2 cells were maintained in F12 media supplemented with 10% heat-inactivated fetal bovine serum, 1x Pen-Strep-Glutamine, and 3μg/mL hygromycin. Cells were maintained at 37°C and 5% CO_2. Human fAD NPCs (ReNCell) were plated and maintained on Matrigel GFR matrix (Corning) – coated 6-well plates and T75 cell culture flasks, respectively. Human fAD NPCs were expanded in ReNCell proliferation media containing DMEM/F12 with GlutaMAX (Fisher Scientific) supplemented with 1x B-27 supplement (Gibco), 2 μg/mL heparin (StemCell Technologies), 20 ng/mL hEGF

(Millipore Sigma), 20 ng/mL bFGF (Millipore Sigma) and filtered through a 0.2 μm Fisherbrand disposable PES filter (Fisher Scientific). Human fAD NPCs were maintained at 37°C, 5% O_2, and 5% CO_2.

2.4.5 Generation of HEK293 GRK Knockout Monoclonal Cell lines by CRISPR/Cas9

Genetic deletion of *Adrbk1, Adrkb2*, *Grk5,* and *Grk6* was performed using the vector pSpCas9(BB)-2A-Puro (Px459v2.0; Addgene plasmid no. 62988; deposited by F. Zhang)(223). Two sets of forward and reverse, small guide RNAs (sgRNAs) were designed targeting exon 1 of the *Adrbk1* gene, exon 1 of the *Adrbk2* gene, exon 3 of the *Grk5* gene, and exon 2 of the *Grk6* gene. The DNA sequences for each sgRNA are as listed in Table 1. Underlined letters indicate additional nucleotides added to the sgRNA sequence corresponding to the Bbs1 restriction site. Each set of target sgRNAs was annealed at 37°C and cloned into the Px459v2.0 plasmid via the Bbs1 restriction site. Low passage HEK293 cells plated at a density of $1.4x10^6$ cells /well in 6-well plates were transfected with 1μg of each target plasmid (2μg DNA total/well) using X-tremeGENE HP DNA reagent (Sigma Aldrich) according to manufacturer's instructions. After 48 hours, medium supplemented with puromycin (3μg/mL) was added for 24 hours. Cells were washed with PBS and allowed to recover from puromycin for 24 hours in complete media. Cells were then serially diluted and plated in 96-well plates to generate individual clones. The CRISPR control cell line was generated by transfection with the empty Px459v2.0 plasmid. Successful deletion of *Adrbk1*, *Adrbk2, Grk5,* and *Grk6* was verified by Western blot analysis for GRK2, GRK3, GRK5, GRK6 and polymerase chain reaction genotyping using primers flanking exon 1, 1, 3, and 2 of *Adrbk1*, *Adrbk2, Grk5*, and *Grk6* respectfully listed in Table 2. gDNA was extracted using KAPA genotyping kit (Kapa Biosystems) according to manufacturer's instructions.

Monoclonal *Adrbk1-*, *Adrbk2-*, *Grk5-*, and *Grk6* –deleted cell lines were then expanded and used in subsequent assays.

2.4.6 Mass Spectrometry

Pelleted cells were solubilized in 10% SDS; 100mM TEAB, probe sonicated, vortexed, and centrifuged to remove insoluble material. Total protein was quantified by Micro BCA (Pierce). 1.5 mg protein was digested with trypsin on Straps (Protifi), desalted on Peptide Desalted Columns (Thermo). Phosphopeptides were enriched with Fe cartridges on an AssayMAP Bravo (Agilent). Phosphopeptide enrichments were loaded onto an EASY C18, 1.7µm 2.1x50cm column at 300 nL/min with an UltiMate™ 3000 RSLCnano HPLC system, eluted over a 120-min gradient and analyzed on Orbitrap Eclipse™. The instrument was operated in MS2. MS1 spectra were acquired at a resolving power of 120,000. MS2 spectra acquired in the Orbitrap with CID normalized collision energy = 38. Dynamic exclusion was enabled to minimize the redundant selection of peptides previously selected for MS/MS. Phosphopeptides were identified (FDR 0.05) and quantified in Proteome Discoverer (2.5).

2.4.7 Aβ enzyme-linked immunosorbent assay (ELISA)

$A\beta_{40}$ and $A\beta_{42}$ levels were determined by standard sandwich ELISA using end-specific antibodies provided by Janssen Pharmaceutica as previously described (207). Briefly, 96-well plates were coated and incubated overnight with monoclonal antibodies $JRFcAb_{40}/28$ and $JRFcAb_{42}/26$, which recognize the C terminus of Aβ species terminating at amino acid 40 or 42, respectively. Horseradish peroxidase (HRP)–conjugated JRFAbN/25 was used as the detection

antibodies for human Aβ. Culture media from HEK293 cell and ReNCell fAD neuronal culture experiments were subjected to $A\beta_{40}$ and $A\beta_{42}$ ELISA. Aβ levels in each condition were normalized to C99-FLAG expression.

2.4.8 β-arrestin PathHunter Assay

On day 1, the CHO-K1 β-arrestin cell line was seeded on black, clear bottom 96-well plates at a cell density of 30,000 cells per well. Two plates were plated per experiment – one for PathHunter assays and one in parallel Aβ ELISAs. On day 2, cells were transfected with wild-type or mutant pCMV-APH1A-PK1 and pCMV-C99-FLAG using X-tremeGENE HP DNA transfection reagent (Millipore Sigma) according to manufacturer's instructions. On day 3, media was changed to F12 media (serum-free) for 16h. On day 4, one plate of cells was rinsed with PBS and analyzed with the PathHunter β-arrestin assay from DiscoveRx according to the manufacturer's protocol. Media and cells were collected from the second plate for Aβ ELISA and Western blot analysis of APH1A-PK and C99. RLU values were normalized to APH1A-PK expression levels in each condition.

2.4.9 Co-immunoprecipitation Assays

On day 1, HEK293 cells were plated in 10cm dishes a density of $6x10^6$ cells/dish. On day 2, cells were transfected with 3xHA-βarr2 WT, S75R, or L72E mutant and APH1A cDNA using X-tremeGENE HP DNA transfection reagent (Millipore Sigma) according to manufacturer's instructions. On day 3, the culture media was refreshed. On day 4, cells were collected and pelleted via centrifugation at 4°C. Cell pellets were lysed on ice for 1 hour in 1mL of ice-cold lysis buffer

(1% octyl-β-D-glucopyranoside, 1x complete protease inhibitor cocktail (Roche), 1x phosphatase inhibitor cocktails 2 and 3 (Millipore Sigma) in 25mM HEPES/150mM NaCl/1mM EDTA buffer. 20µL of pre-washed Protein G Dynabeads (Invitrogen) were incubated in 3% BSA at 1hr at room temperature on a rotator with 2µg of HA.11 or negative control antibody. Following incubation, 500µg of sample lysate was added to the 20µL of pre-coupled Dynabeads and incubated with rotation at 4°C for 16 hours (overnight). On day 5 following overnight incubation, the unbound fraction was collected, and beads were washed 3 times with lysis buffer. Following the final wash, bound fractions were collected in 20µL of 0.1M Glycerol pH2.8. 10µL of 1M Tris pH8.0 was added to each sample to neutralize and 10µL 4x Laemmeli Sample Buffer (Bio-Rad) + 4% β-mercaptoethanol (Bio-Rad) was added to bring the final volume to 40 µL. Samples were then heated for 10 minutes at 70°C and separated by SDS-PAGE and transferred to 0.45µm nitrocellulose membranes (Bio-Rad) using the Power Blotter Station (Invitrogen). Membranes were blocked for 1 hour at room temperature with agitation in 5% milk and incubated overnight on a shaker in appropriate antibody dilutions. The following day, membranes were washed 3 times for 10 minutes in 1XTBS-Tween (0.1% v/v) and incubated in a goat anti-Rabbit IgG (H+L) HRP-conjugated secondary antibody (1:10,000, Bio-Rad) for 1 hour at room temperature. Membranes were washed for 10 minutes, 3 times in 1XTBS-Tween (0.1% v/v) and 5 minutes, 3 times in 1XTBS. Chemiluminescence was measured upon addition of Western Lightning Plus-ECL, Enhanced Chemiluminescence Substrate (Perkin Elmer).

2.4.10 Generation of a βarr2-APH1A complex based on structural alignment

As APH1A bears structural similarities to the GPCRs, our original model for βarr2-APH1A complex was based on the X-ray structure of rhodopsin-arrestin complex (PDB id 4zwj) (224). We

aligned the APH1A subunit from the cryo-EM resolved γ-secretase complex (PDB id 5fn5) (232) against rhodopsin and the βarr2 molecules (PDB id 3p2d) (233) against the arrestin chain, then built the 'alignment' model for the βarr2-APH1A complex with the aligned chains and further refinement by energy minimization and MD simulations (see Fig. 14).

2.4.11 Generation of structural models for βarr2-APH1A complex using docking simulations

We used the HADDOCK 2.2 Server (234,235) for docking βarr2 onto APH1A. APH1A subunit was taken from the relaxed cryo-EM structure of γ-secretase complex (PDB id 5fn2, chain C) (232) . Two independent dockings were performed based on the active and inactive states of arrestin, named as DOCK1 and DOCK2. The active state for Dock1 comes from the crystal structure of visual arrestin chain (PDB id: 5w0p, chain A) (120) bound to rhodopsin. Dock2 is performed with the inactive conformer of βarr2 (PDB id: 3p2d) (233) in the apo state. The finger loop adopts a helical conformation in the active state bound to rhodopsin, whereas it is unstructured in the apo βarr2. HADDOCK performs flexible protein-protein docking when the active residues, i.e., those involved in the protein-protein interaction, are provided. In our case, finger loop residues of arrestin and their counterparts in the APH1A were defined as active residues to allow for their conformational flexibility. As a result of each docking, 200 poses were produced and clustered. We use the best-scoring cluster/pose from DOCK1 and DOCK2 for further refinements by full atomic simulations (see below). The first cluster from DOCK1 contained 186 out of 200 generated poses (HADDOCK score: -89.2). Modeling was performed on this complex to convert the visual arrestin chain into βarr2. The first cluster from DOCK2 included 59 out of 200 generated poses with a HADDOCK score of -99.0.

2.4.12 MD simulations of the βarr2-APH1A complex (WT and mutated)

All atom MD systems with explicit membrane were set-up using GHARMM-GUI membrane builder (236) , and simulations were performed using NAMD (237) with the CHARMM36m force field (238) for proteins and the CHARMM36 lipids (239), and the TIP3P water model. We performed two independent runs on each model of the complex explained above, namely Alignment, DOCK1 and DOCK2. Typically, a given system comprised approximately 675 POPC lipid molecules, 78,080 water molecules, 215 Na^+ ions, and 228 Cl^- ions, i.e., a total of 340,560 atoms in a 160 Å x 160 Å x 142 Å box. We relaxed the systems using the equilibration steps in CHARMM-GUI and performed NPT dynamics for 40 ns with 2 fs time step. Nosé-Hoover constant pressure (1 bar) and temperature (310 K) were used. To study the effect of mutations on the complex, we generated three additional runs each containing one mutation (L72E and S75R in βarr2, and R184D in APH1A), for DOCK1 model and the same protocol as that described above. For trajectory analysis and visualization we used VMD (240) and Pymol (version 1.8).

Table 1 DNA sequences for each sgRNA used to generate the CRISPR GRK KO cell lines

Underlined letters indicate additional nucleotides added to the sgRNA sequence corresponding to the Bbs1 restriction site.

Gene	Target	Direction	sgRNA Sequence
Adrbk1	A	Fwd	5'-CACCGCGTCGGCCAGCACCGCCTCC-3'
		Rev	5'-AAACGGAGGCGGTGCTGGCCGACGC-3'
	B	Fwd	5'-CACCGGAGAAGAGCAAGGCCACGC-3'
		Rev	5'-AAACGCGTGGCCTTGCTCTTCTCC-3'
Adrbk2	A	Fwd	5'-CACCGGTCGCCTTGCTCTTCTCCA-3'
		Rev	5'-AAACTGGAGAAGAGCAAGGCGACC-3'
	B	Fwd	5'-CACCGCAGCAAGAGGATCGTCCTGC-3'
		Rev	5'-AAACGCAGGACGATCCTCTTGCTGC-3'
Grk5	A	Fwd	5'-CACCGCGGAAAAGCAGCCTCCCGAT-3'
		Rev	5'-AAACATCGGGAGGCTGCTTTTCCGC-3'
	B	Fwd	5'-CACCGCAGTTTTGTGAAACCAGGCC-3'
		Rev	5'-AAACGGCCTGGTTTCACAAAACTGC-3'
Grk6	A	Fwd	5'-CACCGCACTGCCTCAGAACTGCCTC-3'
		Rev	5'-AAACGAGGCAGTTCTGAGGCAGTGC-3'
	B	Fwd	5'-CACCGATTGCTCCCACAGGTGGCGG-3'
		Rev	5'-AAACCCGCCACCTGTGGGAGCAATC-3'

Table 2 Sequencing primers used to validate the CRISPR GRK KO cell lines

Gene	Exon	Direction	Primer Sequence
Adrbk1	1	Fwd	5'-CTGGTTCGGGGTCAGATT-3'
		Rev	5'-GTCTGGGGCTTAGGGTCT-3'
Adrbk2	1	Fwd	5'-AGGAAGAGGAGGAGGAGT-3'
		Rev	5'-ATTTCAGAGACTGGAACGAC-3'
Grk5	3	Fwd	5'-CACTGTAATCAGAGAATGTGATG-3'
		Rev	5'-CTCCACTTTATAGCAATAGCAAC-3'
Grk6	2	Fwd	5'-GTCCTTCTCCCCTTTCTTC-3'
		Rev	5'-CTCTCCTTTTCAAAGTGGAAT-3'

3.0 GRK2 orchestrates GPR3-mediated amyloid-β generation

3.1 Introduction

Alzheimer's disease (AD) is a progressive neurodegenerative disease characterized by two main pathological hallmarks – extracellular amyloid plaques composed of aggregated amyloid-β (Aβ) peptides and intraneuronal inclusions of post-translationally modified and misfolded microtubule-associated protein tau (18). The dyshomeostasis of Aβ and generation of amyloid plaques occurs prior to the onset of tau pathology, neuronal loss, and clinical dementia in AD (24). Thus, Aβ dyshomeostasis is hypothesized to be an initial trigger of AD pathogenesis. Aβ peptides are generated via proteolytic processing of the amyloid precursor protein (APP) by β-secretase (BACE1) and γ-secretase, a four-subunit protease complex consisting of nicastrin (NCT), anterior pharynx-defective 1 (APH1), presenilin-enhancer 2 (PEN2), and a catalytic presenilin-1 (PS1) or presenilin-2 (PS2) subunit (45,211). The activity of β-secretase and γ-secretase activity can be modulated by the activity of G protein-coupled receptors (GPCRs) (227,228,241,242). As such, GPCRs are intriguing, druggable targets to modulate Aβ homeostasis without directly inhibiting β- or γ-secretases, a therapeutic approach that has proven challenging given the many secretase substrates and significant off-target side-effects of secretase inhibition.

In particular, the orphan GPR3 is an interesting putative therapeutic target in AD. GPR3 is elevated in the AD brain and modulates γ-secretase activity and generation of Aβ peptides (205). Genetic deletion of *Gpr3* in multiple AD transgenic mouse models alleviates amyloid plaque burden and cognitive deficits observed in these mice (207). Mechanistically, the GPR3-mediated effect on γ-secretase activity and Aβ generation requires recruitment of the multifunctional GPCR

scaffolding protein β-arrestin 2 (βarr2) (208). β-arrestin recruitment to GPCRs is mediated by GPCR carboxy-terminal (C-terminal) and intracellular loop (ICL) phosphorylation, canonically by the family of kinases known as GPCR kinases (GRKs). Significantly, βarr2 recruitment to GPR3 and downstream GPR3-induced Aβ generation are reduced and ablated, respectively, following serine-to-alanine mutagenesis of six GPR3 C-terminal residues (208). Thus, GPR3 phosphorylation, putatively via specific GRKs, is a critical step in regulating Aβ generation in AD.

GRK2, GRK3, GRK5, and GRK6 are ubiquitously expressed throughout tissues and in the brain (144,219). However, in the cerebral cortex and hippocampus, two regions affected in AD brains with high Aβ burden, GRK2-family of GRKs (GRK2/GRK3) are more highly expressed than GRK5 and GRK6 (145). Furthermore, one previous study demonstrated an increase in GPR3 internalization following the expression of GRK2 and βarr2 (243), suggesting GRK2 may be responsible for GPR3 phosphorylation. Therefore, we hypothesized that GRK2 regulates GPR3-mediated γ-secretase activity and Aβ generation. Here, we show that the kinase activity of GRK2 indeed orchestrates GPR3-induced γ-secretase activity and Aβ generation by regulating βarr2 recruitment to GPR3. Furthermore, we demonstrate that a GPR3 mutant, which is biased towards βarr2 recruitment and signaling, increases direct βarr2-γ-secretase interaction. Collectively, our data suggest that developing biased GPR3 ligands that can reduce GRK2 phosphorylation of GPR3 may provide therapeutic benefit in preventing early Aβ dyshomeostasis in AD.

3.2 Results

3.2.1 GRK2 regulates GPR3-mediated Aβ generation in HEK293 cells

Previous studies from our lab have determined that C-terminal phosphorylation and βarr2 recruitment to GPR3 positively regulate γ-secretase processing of APP and generation of Aβ peptides (205,208). Another group demonstrated that co-expression of βarr2, GRK2, and GPR3 in HEK293 cells reduced cell-surface localization of GPR3, and co-expression of GRK2 and GPR3 was able to reduce constitutive cAMP generation in HEK293 cells (243). However, the authors did not directly measure the effect of GRK2 on βarr2 recruitment to GPR3 nor any downstream βarr2-signaling. Nonetheless, GRK2 was a likely candidate we suspected may regulate GPR3 phosphorylation, βarr2 recruitment to GPR3 and the GPR3-βarr2-mediated effect on γ-secretase activity. As such, we hypothesized that genetic deletion of the *Adrbk1* gene (GRK2 gene) would reduce GPR3-mediated Aβ generation in HEK293 cells.

Since GPR3 is an orphan GPCR and has no known ligand, we turned to a GPR3-overexpression system. We have previously shown that GRK2 KO cells exhibit increased constitutive γ-secretase activity and Aβ generation compared to control cells, independent of a specific receptor (Fig. 10A). However, because the cells here would be overexpressing GPR3, we could attribute any effect of GRK2 KO on γ-secretase activity and Aβ generation to altered GPR3 signaling and not an effect on GRK2 constitutive regulation of γ-secretase. To first determine if genetic deletion of *Adrbk1* affected GPR3-mediated Aβ generation, we expressed GPR3 and APP-C99 into HEK293 CRISPR control and GRK2 KO cells (Fig. 20), as previously described in Figs. 7 and 8, and measured secreted $A\beta_{40}$ and $A\beta_{42}$ from culture media using an ELISA. Interestingly, GPR3 expression in GRK2 KO cells leads to a significant decrease in $A\beta_{40}$ and $A\beta_{42}$ release than

the control cells (Fig. 21A). To further test whether GRK2 kinase activity regulated GPR3-mediated Aβ generation, we treated control cells or GRK2 KO cells with 10μM CMPD101, a selective GRK2/3 inhibitor, overnight and measured secreted $A\beta_{40}$ and $A\beta_{42}$ from culture media using an ELISA. Chemical inhibition of GRK2/3 with CMPD101 decreased $A\beta_{40}$ and $A\beta_{42}$ levels compared to vehicle-treated control cells and to a similar level as vehicle-treated GRK2 KO cells (Fig. 21A). Of significance, treatment of the GRK2 KO cells with CMPD101 did not further reduce Aβ generation compared to vehicle-treated GRK2 KO cells, suggesting that the inhibition of GRK2, and not GRK3, regulates GPR3-mediated Aβ generation (Fig. 21A).

To further evaluate whether GRK2 specifically regulates GPR3-mediated γ-secretase activity and Aβ generation, we performed Aβ ELISA in HEK293 CRISPR control and GRK2 KO cells co-expressing GPR3, APP-C99, and an empty vector control or GRK2 K220R, a kinase-dead dominant-negative mutant. Our ELISA data indicated that expression of GRK2 K220R mutant in control cells decreases $A\beta_{40}$ and $A\beta_{42}$ generation to a similar level as GRK2 KO cells with the empty-control plasmid (Fig. 21B). Similar to CMPD101 treatment, GRK2 K220R expression in GRK2 KO cells did not further reduce Aβ generation compared to GRK2 KO cells with the empty vector (Fig. 21B). Collectively, these data indicate that GRK2 kinase activity regulates GPR3-mediated γ-secretase activity and Aβ generation in HEK293 cells.

3.2.2 GRK2 regulates GPR3-mediated Aβ generation in fAD neurons

We next wanted to evaluate whether GRK2 regulates GPR3-mediated γ-secretase activity and Aβ generation in a more physiologically relevant model of AD. To do this, we turned to a human neural progenitor cell (NPC) line, ReN, that harbors familial AD (fAD) mutations in APP

(221,222) which we differentiated for 4 weeks into mature neuronal cultures (Fig. 22A). We expressed GPR3 into the 4 week-differentiated fAD neurons and treated overnight with vehicle or 10μM CMPD101 and used ELISAs to measure the amounts of secreted $A\beta_{40}$ (Fig. 22B) and $A\beta_{42}$ (Fig. 22C). As expected, overexpression of GPR3 in the fAD neurons increased the generation of $A\beta_{40}$ and $A\beta_{42}$. Furthermore, treatment of the fAD neurons with the GRK2/3 inhibitor significantly reduced the amount of Aβ generation. Overall, the data from HEK293 cells and fAD neurons suggest that GRK2 kinase activity regulates GPR3-mediated Aβ generation in multiple cellular models, including a physiologically relevant model of fAD.

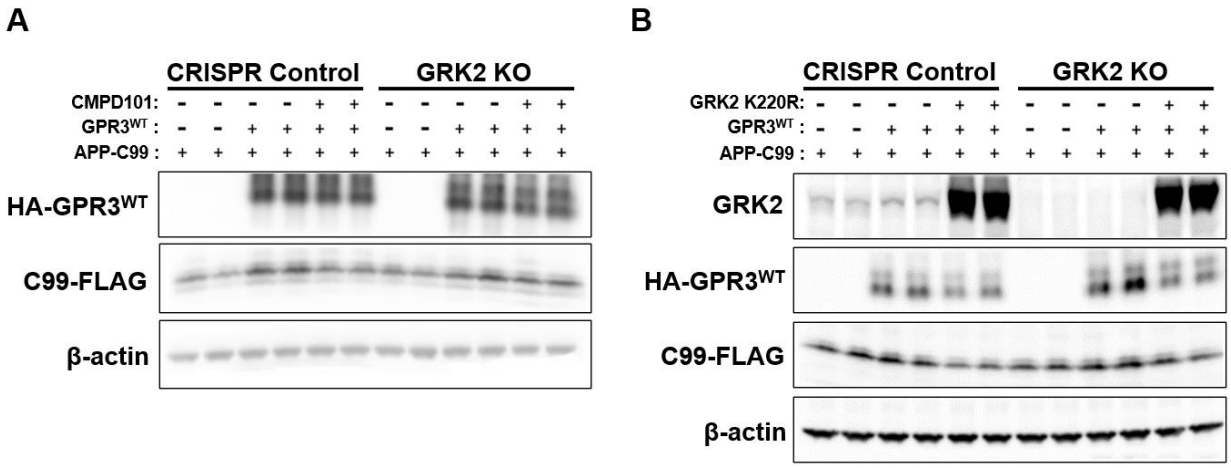

Figure 20. Representative Western blot images for Aβ ELISA assays corresponding to Figure 21.

(A) Representative Western blot of the HA-GPR3^{WT} and C99-FLAG transfection in HEK control and GRK2 KO cells ± 10μM CMPD101 treatment. **(B)** Representative Western blot of the HA-GPR3^{WT}, C99-FLAG, and GRK2 K220R transfection in HEK control and GRK2 KO cells.

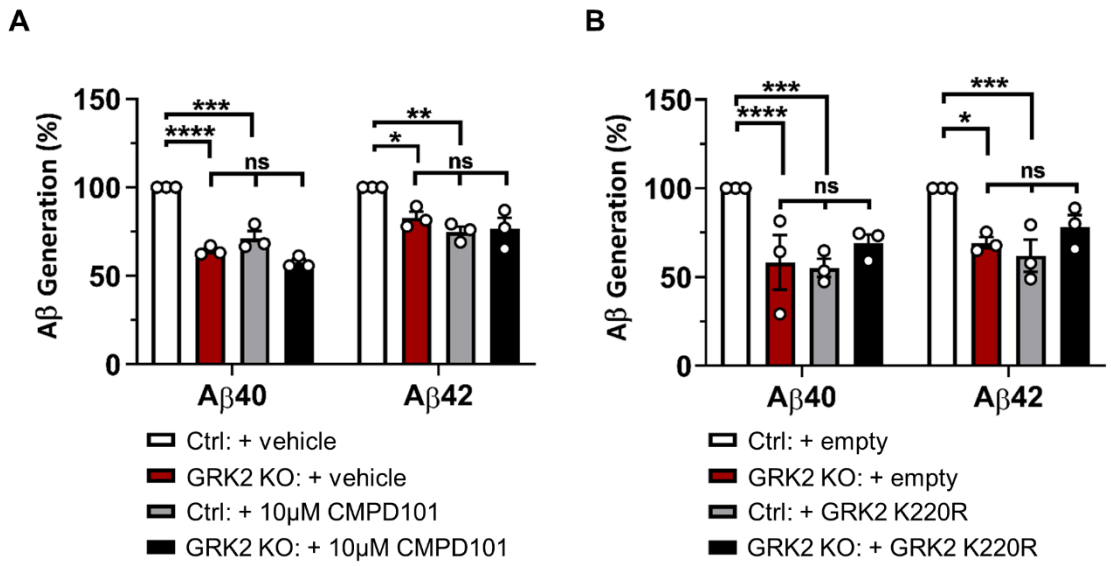

Figure 21. GRK2 regulates GPR3-mediated Aβ generation

(A) $A\beta_{40}$ and $A\beta_{42}$ generation in HEK293 CRISPR control and GRK2 KO cells expressing APP-C99 and HA-$GPR3^{WT}$ ± 10μM CMPD101. * P < 0.05, ** P < 0.01, *** P < 0.001, **** P < 0.0001 by ANOVA with Tukey's post-test. **(B)** $A\beta_{40}$ and $A\beta_{42}$ generation in HEK293 CRISPR control and GRK2 KO cells expressing APP-C99 and HA-$GPR3^{WT}$ ± GRK2 K220R. * P < 0.05, *** P < 0.001, **** P < 0.0001 by ANOVA with Tukey's post-test. Data represent means of 3 independent experiments (n = 3) performed in triplicate. In each independent experiment, the control condition was normalized to 100%.

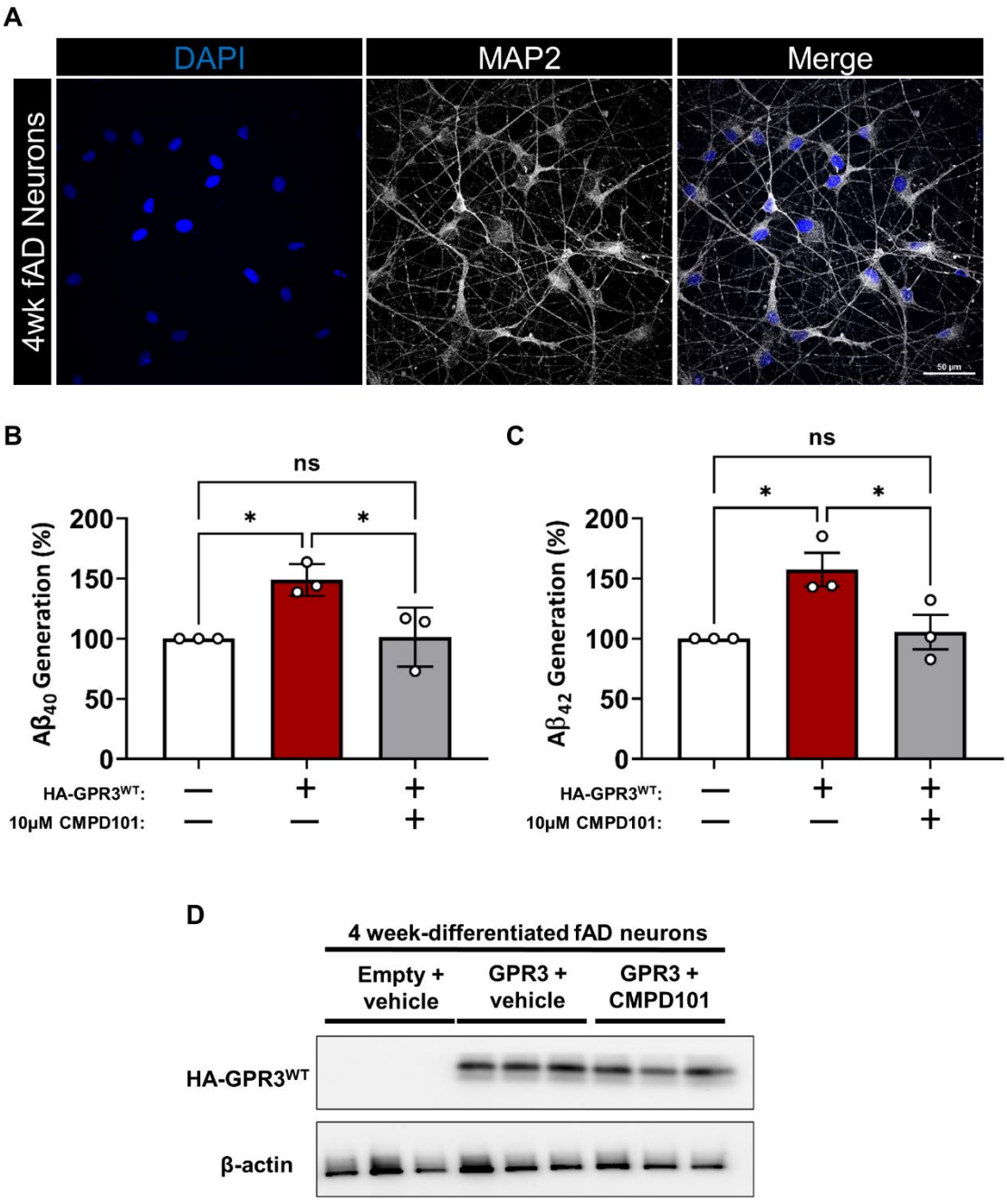

Figure 22. 4 week-differentiated fAD neuron characterization

(A) Confocal images of 4 week-differentiated fAD neurons stained with DAPI (*blue*) and the neuronal marker MAP2 (*white*). **(B)** $A\beta_{40}$ and **(C)** $A\beta_{42}$ generation in 4 week-differentiated fAD neurons expressing an empty-vector or HA-$GPR3^{WT}$ and treated with 0.1% DMSO vehicle or 10µM CMPD101. * $P < 0.05$ by ANOVA with Tukey's post-test. Data represent means of 3 independent experiments (n = 3) performed in triplicate. In each independent experiment,

the control condition was normalized to 100%. **(D)** Representative Western blot of HA-GPR3^{WT} transfection of 4 week-differentiated fAD neurons for an Aβ ELISA experiment.

3.2.3 GRK2 regulates βarr2 recruitment to GPR3

Given that GRK2 regulates GPR3-mediated Aβ generation and βarr2 recruitment to GPR3 is necessary for GPR3-mediated Aβ generation, we hypothesized that GRK2 regulates βarr2 recruitment to GPR3. To test this hypothesis, we utilized a bioluminescence resonance energy transfer (BRET) assay in HEK293 control and GRK2 KO cells to measure constitutive βarr2 interaction with GPR3. Control and GRK2 KO cells were transfected with GPR3 tagged with enhanced yellow fluorescent protein (GPR3^{EYFP}) and βarr2 tagged with Renilla luciferase (βarr2^{Rluc}). The GRK2 KO cells exhibited significantly reduced ΔBRET than control cells (Fig. 23A), suggesting that GRK2 indeed regulates βarr2 interaction with GPR3. Additionally, expressing the GRK2 K220R mutant into control cells significantly reduced ΔBRET compared to control cells without the GRK2 dominant-negative mutant. However, expression of GRK2 K220R did not reduce ΔBRET to the level of the GRK2 KO cells. This data suggests that GRK2 kinase activity may only be partially responsible for mediating βarr2 recruitment to GPR3.

To further confirm the functional role of GRK2 in mediating βarr2 recruitment and binding to GPR3, we utilized a co-immunoprecipitation (Co-IP) assay. In cross-linked HEK293 control or GRK2 KO cells, we and looked at the interaction between immunoprecipitated HA-tagged GPR3 and endogenous βarr2. The Western blot of the Co-IP experiment shows reduced βarr2 binding to GPR3 in GRK2 KO cells compared to control cells (Fig. 23B) and adds further support for a functional role of GRK2 in regulating βarr2 recruitment and binding to GPR3.

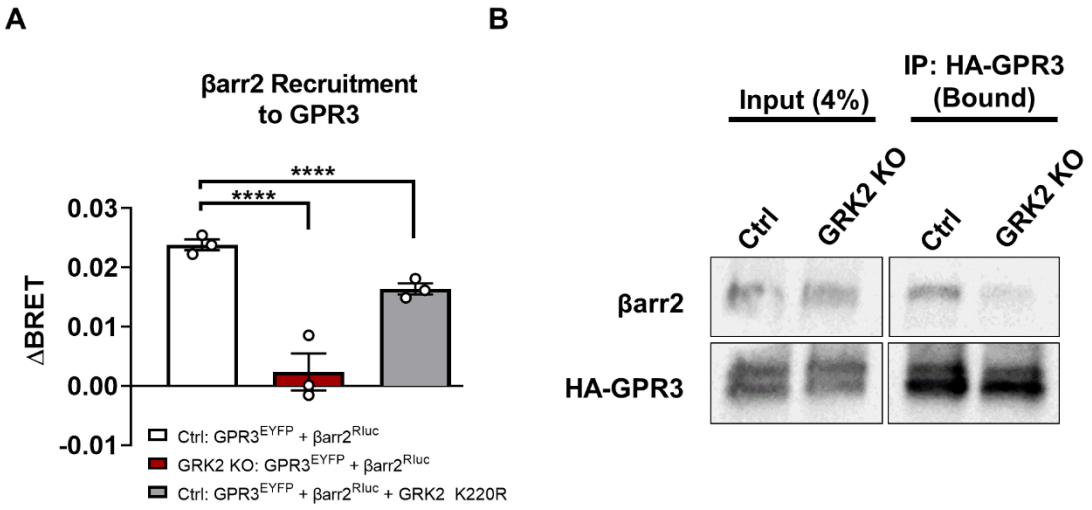

Figure 23. GRK2 regulates βarr2 recruitment to GPR3

(A) βarr2 recruitment to GPR3^{WT} was measured in HEK293 control ± GRK2 K220R and GRK2 KO cells via BRET assay. **** $P < 0.0001$ by ANOVA with Dunnett's multiple comparison test. Data represent means of 3 independent experiments (n = 3) performed in triplicate. In each independent experiment, the control condition was normalized to 100%. **(B)** Co-immunoprecipitation experiment in HEK293 control or GRK2 KO cells expressing HA-GPR3^{WT}.

3.2.4 GPR3-βarr2 signaling regulates βarr2 interaction with γ-secretase

Following βarr2 recruitment to GPR3, the subsequent steps in the signaling cascade that regulate γ-secretase activity and Aβ generation are relatively unknown. However, our lab has previously demonstrated that βarr2 interacts directly with the APH1A subunit of the γ-secretase complex to stabilize localization of all subunits into DRM domains and increase proteolytic cleavage of APP-C99 (208). Furthermore, genetic deletion of *Gpr3* in mice reduces amyloid plaque burden in AD transgenic mice and reduces direct βarr2-APH1A interaction in the cortex. Therefore, we hypothesized that GPR3-βarr2 signaling can regulate γ-secretase activity by

increasing βarr2 binding to the APH1A subunit of the γ-secretase complex. To test this hypothesis, we expressed APH1A^{WT} along with wild-type GPR3 (GPR3^{WT}), a GPR3 βarr2-biased mutant (GPR3^{DRY}), or a GPR3 G-protein-biased mutant (GPR3$^{S/A}$) in CHO-βarr2 cells and utilized a βarr2 PathHunter assay to measure βarr2 recruitment to APH1A (Fig. 5). We have previously shown that the GPR3^{DRY} mutant increases βarr2 recruitment to GPR3 and increases GPR3-mediated Aβ generation compared to GPR3^{WT}. Additionally, the GPR3$^{S/A}$ C-terminal phosphorylation-dead and G-protein-biased mutant reduces constitutive βarr2 recruitment to GPR3 and decreases GPR3-mediated Aβ generation compared to GPR3^{WT} (208). Interestingly, expression of the GPR3^{DRY} mutant increased βarr2 recruitment to APH1A by ~50% compared to the cells expressing GPR3^{WT} (Fig. 24). In contrast, the cells expressing the GPR3$^{S/A}$ C-terminal phosphorylation-dead mutant exhibited no difference in βarr2 recruitment to APH1A compared to the GPR3^{WT}-expressing condition (Fig. 24). Thus, we can conclude that decreasing constitutive βarr2 recruitment to GPR3 does not directly affect βarr2 interaction with APH1A, but biasing GPR3 towards a βarr2 signaling pathway significantly increases βarr2 interaction with APH1A.

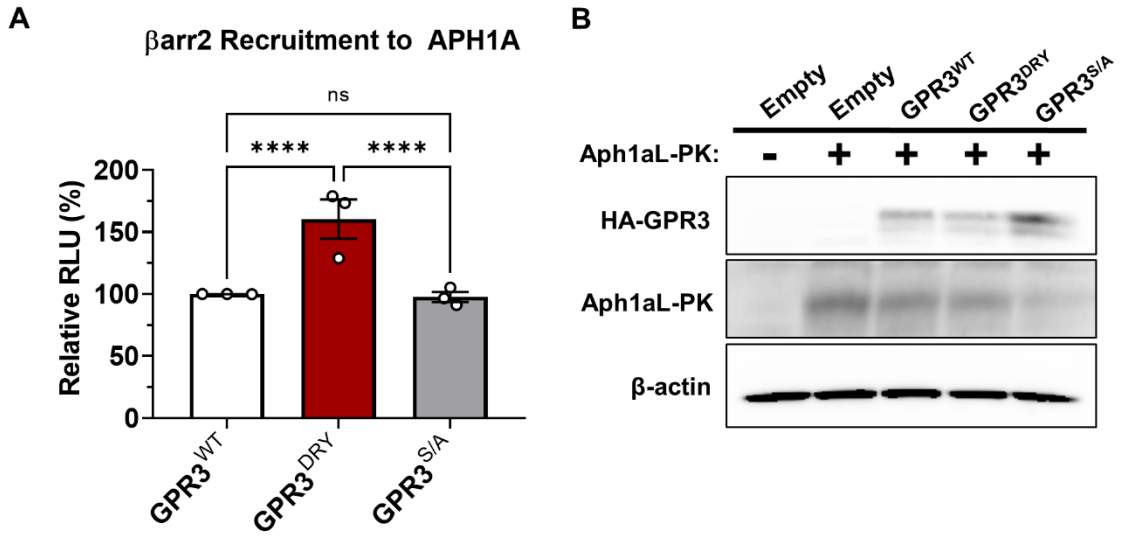

Figure 24. GPR3- βarr2 signaling regulates βarr2 interaction with γ-secretase

(A) βarr2 recruitment to APH1A in the CHO-βarr2 cell line expressing HA-GPR3^{WT}, HA-GPR3^{DRY}, or HA-GPR3$^{S/A}$. **** $P < 0.0001$ by ANOVA with Tukey's post-test. Data represent means of 3 independent experiments (n = 3) performed in triplicate. In each independent experiment, the control (GPR3^{WT}) condition was normalized to 100%. **(B)** Representative Western blot of APH1A-PK and HA-GPR3^{WT}/ HA-GPR3^{DRY}/ or HA-GPR3$^{S/A}$ transfection in CHO-βarr2 cells.

3.3 Discussion

The orphan GPCR GPR3 is a positive regulator of γ-secretase activity and the generation of Aβ peptides in AD (205,209). GPR3 regulation of γ-secretase requires the recruitment of the multifunctional scaffolding protein βarr2 and downstream β-arrestin-mediated signaling pathways (208). The family of kinases known as GRKs are canonical regulators of GPCR phosphorylation and β-arrestin recruitment to GPCRs. Furthermore, specific GRKs can differentially regulate distinct downstream signaling outcomes via unique phosphorylation patterns on the ICLs and C-

terminus of a GPCR (140,217). Thus, selective GPCR ligands that favor recruitment and phosphorylation by specific GRKs can differentially bias receptor signaling and physiological outcomes. Here, we uncover a role of GRK2 in modulating GPR3-mediated γ-secretase activity and Aβ generation. We determine that genetic deletion of *Adrbk1* (GRK2) or GRK2 inhibition are sufficient to significantly reduce GPR3-mediated Aβ generation in both HEK293 cells and in mature fAD neurons. Additionally, we determine that βarr2 recruitment to GPR3 is almost completely abolished in GRK2 KO cells; however, inhibiting GRK2 activity with a GRK2 dominant-negative mutant only partially inhibits βarr2 recruitment. Furthermore, we demonstrate that biasing GPR3 signaling towards increased βarr2 recruitment and signaling increases direct interaction between βarr2 and the APH1A subunit of the γ-secretase complex – an interaction previously demonstrated to regulate γ-secretase activity and proteolytic processing of APP (Fig. 19) (208,244). Intriguingly, preventing GPR3 C-terminal phosphorylation which has been shown to reduce βarr2 recruitment to GPR3 and GPR3-mediated Aβ generation (208) has no effect on βarr2-APH1A interaction suggesting that multiple possible mechanisms of GPR3 regulation of γ-secretase activity may exist. Collectively, these studies suggest a model whereby GRK2 orchestrates βarr2 recruitment to GPR3 and downstream signaling to regulate Aβ generation. Our data support the development of GPR3 biased ligands, against GRK2 phosphorylation, to prevent Aβ dyshomeostasis in the early stages of AD.

In both the HEK293 cells and mature fAD neurons, inhibiting GRK2 kinase activity with CMPD101 or GRK2 K220R is sufficient to reduce GPR3-mediated Aβ generation (Figs. 21 and 22). However, inhibiting GRK activity with the kinase-dead dominant-negative GRK2 K220R mutant only partially reduces βarr2 recruitment to GPR3 in the BRET assay (Fig. 23A). Therefore, GRK2 kinase activity is necessary for regulating GPR3-mediated Aβ generation but not sufficient

to prevent βarr2 interaction with GPR3. As such, GRK2 likely plays an additional role as a molecular scaffold, independent of kinase function, in recruiting βarr2 to GPR3. In fact, another group has shown that GRK2 can regulate GPR3 signaling independent of kinase function (243). Upon co-expression of GPR3 and the GRK2 K220R mutant, the authors measured a decrease in cAMP generation similar to when a wild-type GRK2 was co-expressed with GPR3. Nonetheless, the authors did note that GRK2 kinase activity was required to reduce GPR3 cell-surface localization. Because preventing GRK kinase activity alone results in the same decrease in GPR3-mediated Aβ generation as in the GRK2 KO cells (Fig. 21), GPR3-mediated Aβ generation most likely is dependent on a unique GRK2-mediated phosphorylation pattern on GPR3 to allow for a distinct GPR3-βarr2 conformation that functionally increases γ-secretase activity. Putatively, GPR3 internalization following GRK2 phosphorylation may be required for the positive regulatory effect on γ-secretase activity and Aβ generation as well. Additional quantitative mass spectrometry experiments measuring the changes in GPR3 phosphorylation in the GRK2 KO cells and upon GRK2 inhibition in control cells are necessary moving forward to identify the specific residues GRK2 may be responsible for phosphorylating to regulate Aβ generation.

Our lab previously demonstrated that direct βarr2 interaction with the APH1A subunit of the γ-secretase complex regulates Aβ generation via the extent of βarr2 interaction and putatively the conformation of the βarr2-APH1A complex (Fig. 19). In addition, we have previously shown that biasing GPR3 signaling towards βarr2 recruitment and signaling by preventing G-protein coupling with a $GPR3^{DRY}$ mutant increases GPR3-mediated Aβ generation (208). Interestingly, the same $GPR3^{DRY}$ mutant increased the interaction between βarr2 and APH1A by ~50% compared to cells expressing $GPR3^{WT}$ (Fig. 24). One potential mechanism for GPR3 signaling increasing the βarr2-APH1A interaction is via ‘activation’ of βarr2 following interaction with GPR3. Following

recruitment and interaction with GPR3, βarr2 may adopt an 'active' conformation that is maintained via interactions with plasma membrane phospholipids (245). In this 'active' conformation, βarr2 would be in a more favorable conformation to bind APH1A. A previous report suggests that arrestins can adopt a stable active conformation, maintained at the plasma membrane, following recruitment to a GPCR – a mechanism the authors describe as 'catalytic activation' of β-arrestins (245). Because we have demonstrated that βarr2 interaction with APH1A resembles a fully engaged GPCR-β-arrestin complex (Figs 15-17), βarr2 binding to GPR3 and subsequent release from GPR3 in this conformation would increase the probability of binding to APH1A. Further investigation into how GRK2 regulation of GPR3 signaling affects βarr2-APH1A interaction is needed to fully understand how GRK2 regulates GPR3-mediated Aβ generation. Surprisingly, serine-to-alanine mutagenesis of six GPR3 C-terminal serine residues ($GPR3^{S/A}$) did not affect the extent of βarr2-APH1A interaction (Fig. 24). This mutant has previously been shown to decrease βarr2 recruitment to GPR3 as well as GPR3-mediated Aβ generation (208). This new finding suggests that in addition to regulating βarr2 interaction with APH1A, GPR3 may regulate γ-secretase processing of APP via additional mechanisms. Overall, we identify GRK2 as a critical regulator of GPR3-mediated γ-secretase activity and Aβ generation. Designing GPR3 ligands to bias signaling way from GRK2 may provide therapeutic benefit in the early stages of AD.

3.4 Materials and Methods

3.4.1 Antibodies and Compounds

Rabbit polyclonal antibodies to human $APH1A_L$ (B82.3, 1:1,000) has been previously described and were the gift of Dr. Bart De Strooper (VIB and KU Leuven, Leuven, Belgium; UK Dementia Research Institute and University College London, London, United Kingdom)(230,231). Antibodies to the following were purchased: GRK2 (mouse, C-9, SantaCruz Biotechnology, 1:1000), βarr2 (mouse, H-9, SantaCruz Biotechnology, 1:1000), hemagglutinin (HA) (mouse, HA.11, BioLegend, 1:1000), hemagglutinin (HA) (rabbit, C29F4, Cell Signaling Technologies, 1:1000), MAP2 (Synaptic Systems, 1:500). Takeda Compound101 was purchased from Hello Bio, and octyl-β-D-glucopyranoside was purchased from EMD Millipore.

3.4.2 Plasmid Construction

All mutations in APH1A and βarr2 were generated with the XL II Site-Directed Mutagenesis Kit (Agilent Technologies) according to manufacturer's instructions.

3.4.3 Cell Lines

The HEK293 cell line was purchased from American Type Culture Collection. The GRK2 KO cells were generated using CRISPR/Cas9 genome-editing and described previously (Section 2.4.5). The CHO-KI β-arrestin 2 cell line (CHO-βarr2) was purchased from DiscoveRx. The

ReNCell GA2 familial Alzheimer's disease (fAD) human neural progenitor cell (hNPC) line was a kind gift From Dr. Rudolph E. Tanzi and Dr. Doo Yeon Kim (Harvard University, Cambridge, MA) and generated as previously described (222).

3.4.4 Cell Culture

HEK293 cells were maintained in complete media containing DMEM/F12 with GlutaMAX (Fisher Scientific) and supplemented with 10% fetal bovine serum (ThermoFisher Scientific). Cells were maintained at 37°C and 5% CO_2. CHO-K1 βarr2 cells were maintained in F12 media supplemented with 10% heat-inactivated fetal bovine serum, 1x Pen-Strep-Glutamine, and 3μg/mL hygromycin. Cells were maintained at 37°C and 5% CO_2. Human fAD NPCs (ReNCell) were plated and maintained on Matrigel GFR matrix (Corning) – coated 6-well plates and T75 cell culture flasks, respectively. Human fAD NPCs were expanded in ReNCell proliferation media containing DMEM/F12 with GlutaMAX (Fisher Scientific) supplemented with 1x B-27 supplement (Gibco), 2 μg/mL heparin (StemCell Technologies), 20 ng/mL hEGF (Millipore Sigma), 20 ng/mL bFGF (Millipore Sigma) and filtered through a 0.2 μm Fisherbrand disposable PES filter (Fisher Scientific). To differentiate the human fAD NPCs into neurons, media was changed to ReNCell differentiation media containing DMEM/F12 with GlutaMAX (Fisher Scientific) supplemented with 1x B-27 supplement (Gibco) and 2 μg/mL heparin (StemCell Technologies (no growth factors) and filtered through a 0.2 μm Fisherbrand disposable PES filter (Fisher Scientific). Cells underwent half-media changes over other day for 4 weeks until the time of experiment. Human fAD NPCs and differentiated neurons were maintained at 37°C, 5% O_2, and 5% CO_2.

3.4.5 Aβ enzyme-linked immunosorbent assay (ELISA)

$A\beta_{40}$ and $A\beta_{42}$ levels were determined by standard sandwich ELISA using end-specific antibodies provided by Janssen Pharmaceutica as previously described (207). Briefly, 96-well plates were coated and incubated overnight with monoclonal antibodies $JRFcAb_{40}$/28 and $JRFcAb_{42}$/26, which recognize the C terminus of Aβ species terminating at amino acid 40 or 42, respectively. Horseradish peroxidase (HRP)–conjugated JRFAbN/25 was used as the detection antibodies for human Aβ. Culture media from HEK293 cell and 4 week-differentiated ReNCell fAD neuronal culture experiments were subjected to $A\beta_{40}$ and $A\beta_{42}$ ELISA. Aβ levels in each condition were normalized to C99-FLAG expression.

3.4.6 Bioluminescence Resonance Energy Transfer (BRET) Assay

HEK293 CRISPR control and GRK2 KO cells plated in 6-well plates at a density of $1.4x10^6$ cells/well were transfected with 3xHA-$GPR3^{EYFP}$ and $\beta arr2^{Rluc}$ (ratio 4:1) using X-tremeGENE HP DNA reagent (Millipore Sigma) according to manufacturer's instructions. In all experiments, the total amount of DNA transfected was equalized between conditions by addition with empty pcDNA3.0 expression vector. An additional transfection condition was included for both CRISPR control and GRK2 KO cells with only the $\beta arr2^{Rluc}$ construct and empty expression vector. 24 hours after transfection, media was refreshed with 2mL of complete media (DMEM/F12 + GlutaMax +10% FBS) and incubated at 37°C for another 24 hours. Cells were then transferred to 96-well BRET assay plates (Costar #3917, Corning) at a density of 100,000 cells per well coated with 100μg/μL poly-L-lysine. Additional cells from each transfection condition were plated in a

non-coated, 96-well cell culture plate for $A\beta_{40}$ and $A\beta_{42}$ ELISA analysis the following day. After 24 hours, BRET assay cells were washed twice with PBS and coelentrazine-h (Promega) was added to a final concentration of 5 μM. Cells were incubated in the dark for 15 minutes at 37°C before BRET measurements were made on a BioTek synergy neo2 plate reader. BRET ratio was calculated as emission at 540nm/emission at 460nm. Delta BRET (ΔBRET) is defined as the 540nm/460nm BRET ratio of cells expressing both $\beta arr2^{Rluc}$ and 3xHA-$GPR3^{EYFP}$ minus the 540nm/460nm BRET ratio of cells expressing only the $\beta arr2^{Rluc}$ construct in the same cell line in the same experiment.

3.4.7 β-arrestin PathHunter Assay

On day 1, the CHO-K1 β-arrestin cell line was seeded on black, clear bottom 96-well plates at a cell density of 30,000 cells per well. Two plates were plated per experiment – one for PathHunter assays and one in parallel for Western blot analysis of plasmid expression. On day 2, cells were transfected with pCMV-APH1A-PK1 and pEZ-3xHA-$GPR3^{WT}$, pEZ-3xHA-$GPR3^{DRY}$, or pEZ-3xHA-$GPR3^{S/A}$ using X-tremeGENE HP DNA transfection reagent (Millipore Sigma) according to manufacturer's instructions. On day 3, media was changed to F12 media (serum-free) for 16h. On day 4, one plate of cells was rinsed with PBS and analyzed with the PathHunter β-arrestin assay from DiscoveRx according to the manufacturer's protocol. Cells were collected from the second plate for Western blot analysis of APH1A-PK and HA-GPR3. RLU values were normalized to APH1A-PK expression levels in each condition.

3.4.8 Co-immunoprecipitation Assay

On day 1, HEK293 cells were plated in 10cm dishes at a density of $6.5x10^6$ cells/dish and transfected with 3xHA-$GPR3^{WT}$ using X-tremeGENE HP DNA transfection reagent (Millipore Sigma) according to manufacturer's instructions. Complete media was refreshed after 24 hours in transfection media. 48 hours post-transfection, cells were washed twice with room-temperature reaction buffer (PBS, 30mM HEPES buffer, pH 7.4) and cross-linked with dithiobis(succinimidyl propionate) (DSP) for 30 minutes at room temperature with gentle agitation. Crosslinking was terminated through the addition of 20mM Tris, pH 7.5 for 15 minutes. Cross-linked cells were collected and pelleted via centrifugation at 4°C. Cell pellets were lysed on ice for 1 hour in 1mL of ice-cold lysis buffer (1% n-octyl-β-D-glucopyranoside, 1x complete protease inhibitor cocktail (Roche), 1x phosphatase inhibitor cocktails 2 and 3 (Millipore Sigma) and 0.1M phosphate buffer, pH 7.15) and cleared by centrifugation (*14,000 x g* for 20 min at 4°C). Lysate concentrations were determined via Bradford assay. 300µg of lysate was pre-cleared in 50µL of pre-washed, Protein G Sepharose 4 Fast Flow beads (GE Healthcare) for 2 hours on a rotator at 4°C. Samples were then centrifuged at *5,000 x g* for 5 min and sample supernatant was incubated in 1µg of anti HA.11 antibody or goat-serum negative control for 2 hours on a rotator at 4°C. Samples were then added to 30µL of pre-washed, Protein G Sepharose 4 Fast Flow beads and incubated overnight on a rotator at 4°C. The following day, samples were centrifuged at *5,000 x g* for 5 min and unbound fraction was collected. Protein G beads were vigorously washed 4 times in ice-cold lysis buffer. Following the final wash, bound fractions were collected as follows. 30µL of 2.5X Laemmeli Sample Buffer (Bio-Rad) + 2.5% β-mercaptoethanol (Bio-Rad) was added to washed beads and heated for 10 minutes at 70°C. Samples were centrifuged for 10 minutes at *10,000 x g* and supernatant/bound fraction was collected. Samples were separated by SDS-PAGE (4-20% mini-

PROTEAN TGX pre-cast gels, Bio-Rad) and transferred to 0.45μm nitrocellulose membranes (Bio-Rad) using the Trans-Blot Turbo Transfer System (Bio-Rad). Membranes were blocked for 1 hour at room temperature with agitation in 5% milk and incubated overnight on a shaker in βarr1/2 and anti HA (Cell Signaling Technology) antibodies. The following day, membranes were washed 3 times for 10 minutes in TBS-Tween (0.1% v/v) and incubated in a goat anti-Rabbit IgG (H+L) HRP-conjugated secondary antibody (1:10,000, Bio-Rad) for 1 hour at room temperature. Membranes were washed for 10 minutes, 3 times in TBS-Tween (0.1% v/v) and 5 minutes, 3 times in TBS. Chemiluminescence was measured upon addition of Western Lightning Plus-ECL, Enhanced Chemiluminescence Substrate (Perkin Elmer).

3.4.9 Immunostaining and Confocal Microscopy

Human fAD NPCs (ReNCell GA2) were plated at a density of $7x10^5$ cells/well on Matrigel-coated coverslips in a 6-well plate and differentiated for 4 weeks according to the protocol outlined in 3.4.4. After 4 weeks of differentiation, cells were transfected with 3xHA-$GPR3^{WT}$ or empty vector using LipofectamineSTEM (ThermoFisher) according to manufacturer's instructions at a ratio of 1:7 DNA:LipofectamineSTEM reagent in differentiation media (Day 1). On the day following transfection (Day 2), a half media change was done on each well and 0.1% vehicle or 10μM CMPD101 final concentration was added to each well. On Day 3, media was collected for ELISA assays and cells on the coverslips were fixed in a solution of 4% paraformaldehyde for 15min at room temperature and washed 3x with 1xPBS. Coverslips were then blocked with 5% normal donkey serum for 1 hour at room temperature and stained with MAP2 (Guinea Pig 1:5000) primary antibody overnight. The following day, cells were incubated for1 hour at room temperature with anti-guinea pig AlexaFluor647 secondary antibody and subsequently washed 3x

in 1x PBS. Cells were mounted onto coverslips with ProLong Diamond Antifade Mounting Media with DAPI, (Invitrogen) for visualization by Confocal microscopy. Images were obtained with a Nikon A1R HD25 confocal microscope.

4.0 Discussion

This dissertation uncovered a novel role of the GRK family of kinases in directly regulating γ-secretase activity and the generation of pathogenic Aβ peptides. Additionally, these findings highlight the role of a specific GRK, GRK2, in regulating γ-secretase activity and Aβ generation indirectly via canonical regulation of the GPCR GPR3. GRKs directly mediate γ-secretase activity via regulating distinct phosphorylation patterns, or barcodes, on the ICL2 and C-terminus of the APH1A subunit of the γ-secretase complex which in turn recruits the multifunctional GPCR scaffolding protein βarr2. This mechanism closely resembles the mechanism by which GRKs exert precise control of GPCR signaling and orchestrate distinct downstream signaling cascades following GPCR activation (217). Significantly, these findings highlight the βarr2-APH1A interaction as a potentially viable therapeutic target to regulate γ-secretase activity in disease. Furthermore, the work here expands upon the mechanism by which GPR3 signaling regulates γ-secretase activity and further illuminates GPR3 as a potential therapeutic target in AD. Collectively, these findings increase our understanding of the multifaceted roles of GRKs in regulating cellular signaling in human health and disease.

The results in Chapter 2 highlight the role of phosphorylation on the APH1A subunit of the γ-secretase complex and establish the existence of an APH1A phosphorylation barcode, mediated by the GRK family of kinases, which regulates direct interaction with the GPCR scaffolding protein βarr2 and functionally, γ-secretase cleavage of APP and generation of Aβ peptides. Phosphorylation of the NCT and PS1 subunits by members of the AGC family of kinases has been demonstrated previously (56,59,246,247); however, our work provides the first evidence of phosphorylation on the APH1A subunit. Utilizing label-free quantitative LC-MS/MS, we were

able to reproducibly measure high levels of phosphorylation on APH1A within ICL2 and the C-terminus in total HEK293 cell lysate overexpressing APH1A. Work from our lab (208) and another (244) have demonstrated that β-arrestins (βarr1 and βarr2) interact with APH1 to regulate active γ-secretase complex assembly and localization in DRM domains where proteolytic activity most efficiently occurs. Given the 7TM domain structure of APH1 resembles the 7TM domain structure of a GPCR and the common interaction with β-arrestins, we reasoned that APH1 phosphorylation may mediate APH1-β-arrestin interaction similarly to GPCR-β-arrestin interactions. Indeed, we found that the ubiquitously expressed GRKs regulate the phosphorylation of APH1A using genetically engineered GRK KO cell lines and label-free, quantitative LC-MS/MS. Functionally, we discovered that the genetic deletion of each *Grk* results in differential changes in γ-secretase proteolytic processing of APP-C99 and secretion of Aβ peptides. Guided by the mass spectrometry data in each GRK KO cell line, we generated phosphorylation-deficient and phosphorylation-mimetic APH1A mutants corresponding to specific phosphorylation changes in ICL2 and the C-terminus. We demonstrated that specific phosphorylation combinations or patterns from the mutants correspond to similar changes in γ-secretase activity as in the individual GRK KO cells. Additionally, we measure βarr2 recruitment to each APH1A mutant and demonstrate that the extent of βarr2 recruitment does not always parallel the extent of γ-secretase activity. This finding suggests that the functional effect of βarr2 binding to APH1A likely depends, at least partially, on the specific conformation that the APH1A-βarr2 complex adopts. These APH1A mutagenesis experiments act collectively as a proof-of-concept for the existence of an APH1A phosphorylation barcode, mediated by GRKs, to regulate Aβ generation. Based on our results, we propose a model of constitutive GRK regulation of γ-secretase activity and APP proteolytic processing. This model significantly expands the role of GRKs in health and disease, as γ-secretase has over 90 known

substrates and has been implicated in multiple diseases, in particular, AD and multiple types of cancer.

To gain a deeper understanding of the APH1A-βarr2 interaction and the functional effect on γ-secretase activity, we utilized computational docking and molecular dynamic simulations to predict the structure of APH1A-βarr2 and to gather insight into critical residues mediating interaction. Our computational modeling data revealed putative key residues within the βarr2 finger loop domain (L72 and S75) and the APH1A ICL3 (R184), which we further validate in *in vitro* cell-based assays to demonstrate these residues are in fact important for interaction as well as functionally affect γ-secretase activity and Aβ generation. These findings show that βarr2 binding to APH1A closely resembles a fully-engaged GPCR-βarr2 complex (175,178). Mutagenesis of the β-arrestin finger loop domain significantly hinders arrestin-GPCR interactions and functional downstream signaling from GPCRs and structural studies have highlighted this region in arrestin as functionally important for β-arrestins to adopt an 'active' conformation (121,178). Thus, we propose a model whereby the specific GRK-mediated APH1A phosphorylation barcode regulates γ-secretase activity by modulating distinct binding conformation(s) of βarr2 to APH1A which alter γ-secretase complex recognition of substrate (APP-C99) and/or proteolytic activity of the complex.

The results in Chapter 3 further elucidate the mechanisms by which the orphan GPCR GPR3 regulates γ-secretase activity and Aβ generation in AD. Our work demonstrates that GRK2 in particular is able to regulate βarr2 recruitment and binding to GPR3 and the downstream functional increase in γ-secretase activity and Aβ generation. Importantly, we discover that the kinase function of GRK2 is critical in regulating GPR3-mediated Aβ generation. We demonstrate that biasing GPR3 signaling towards a βarr2 pathway, in expense of the $G_{\alpha S}$ signaling pathway,

increases direct interaction between βarr2 and APH1A. However, preventing GPR3 C-terminal phosphorylation, which has been previously shown to reduce βarr2 recruitment and Aβ generation compared to $GPR3^{WT}$, has no effect on downstream APH1A-βarr2 interaction. Overall, these findings suggest that GPR3 may regulate γ-secretase activity and proteolytic processing of APP-C99 by multiple, distinct mechanisms. Further elaboration into these putative mechanisms will be explored later in this section.

4.1 APH1 C-terminal phosphorylation in β-arrestin binding and γ-secretase activity

One interesting question for further investigation is the functional role of APH1A C-terminal phosphorylation in regulating βarr2 binding and regulation of γ-secretase activity. Our data in Chapter 2 suggest that genetic deletion of each ubiquitously expressed GRK individually results in a decrease in phosphorylation at S251 and S257 on the C-terminus. Our APH1A mutagenesis data also suggest that loss of phosphorylation at both of these residues functionally results in reduced βarr2 interaction and γ-secretase processing of APP. However, when ICL2 residues are phosphorylated in conjunction with loss of C-terminal phosphorylation (GRK2 KO cells), γ-secretase activity is increased. Although this may indicate that ICL2 phosphorylation may be important for βarr2 to adopt an 'active' conformation that functionally results in increased Aβ generation, the C-terminus of APH1A could be involved in initial recognition and binding to β-arrestins. In fact, structural analysis of β-arrestin interactions with GPCRs demonstrates that GPCRs initially interact with the N-domain of β-arrestin, prior to finger loop domain engagement with the cytoplasmic core of the receptor, to allow arrestin to adopt an active conformation (175,177,179,180). In particular, GPCR C-terminal phosphorylation disrupts an 'ionic lock' on β-

arrestin to allow for the finger loop domain to swing outward and engage with a GPCR cytoplasmic core (178). Significantly, one study demonstrated that treatment of cells with APH1A or APH1B C-terminal peptides (ACT or BCT, respectively) concentration-dependently reduced γ-secretase activity and Aβ generation as well as interaction with βarr1 (244). Thus, inhibiting β-arrestin engagement with the APH1 C-terminus is sufficient to reduce γ-secretase cleavage of APP-C99. However, ICL2 phosphorylation also appears sufficient to overcome loss of APH1A C-terminal phosphorylation to allow for β-arrestin 2 to adopt an 'active' conformation to increase γ-secretase activity as demonstrated in the GRK2 KO cell line. A comprehensive analysis on how APH1 C-terminal peptides inhibit the interaction between both βarr1 or βarr2 and APH1A and APH1B is necessary moving forward to gain complete understanding of the functional significance of the APH1 C-terminal domain in regulating interaction with arrestin and γ-secretase activity.

One limitation to our experimental approach in Chapter 2 is our computational alignment and docking analysis was done modeling the APH1A-βarr2 interaction after the solved crystal structure of rhodopsin-bound arrestin1 (visual arrestin). In this solved structure (224), arrestin1 is fully engaged with the rhodopsin cytoplasmic core. Moving forward, completing docking experiments and MD simulations modeling APH1A-βarr2 interaction off of a partially engaged GPCR-β-arrestin complex would give additional mechanistic insights into initial modes of arrestin binding to the APH1A C-terminus and the role of phosphorylation in regulating this interaction. For example, the structure of the β_2V_2R chimeric GPCR bound to βarr1 in a partially engaged complex (175) could be a good starting point for additional computational experiments into the binding mechanism of APH1A and βarr2. Here, we would be able to assess whether initial βarr2 engagement with the APH1A C-terminus resembles initial arrestin recruitment to a phosphorylated GPCR. Furthermore, completing additional modeling experiments mimicking APH1A

phosphorylation (or phosphorylation deficiency) will provide additional and needed insights into the specific conformations both βarr2 and APH1A adopt upon binding and how these distinct conformations may regulate the recognition of γ-secretase substrates and γ-secretase proteolytic activity.

The predicted human APH1A structure from the open-source, structure prediction database AlphaFold 2.0 (248) exhibits high similarity to the solved structure of APH1A in complex with γ-secretase (249,250) and in our computational model in complex with βarr2, particularly within the TM domains, ICL2 and ICL3. However, the AlphaFold-predicted structure displays low confidence in the C-terminal structure following helix 8. Nonetheless, the AlphaFold-predicted structure of the C-terminus predicts a short α-helical structure containing both S251 and S257 – two residues on which we measure phosphorylation. GPCR C-termini are typically considered to be disordered, and we do not predict further secondary structure in the APH1A C-terminus following helix 8 in our computational models based off of the solved rhodopsin structure (Figs. 15 and 16). Therefore, phosphorylation changes at S251 or S257 could putatively alter a short helical structure of the C-terminus on APH1A to regulate binding to βarr2 and γ-secretase activity. Ultimately, further modeling and structural analysis of APH1A is necessary to elucidate the role of the C-terminus and C-terminal phosphorylation in regulating binding to βarr2 and γ-secretase function.

4.2 Mechanisms of GPR3-mediated γ-secretase activity and Aβ generation

The results in Chapter 3 present evidence that GRK2 kinase activity regulates GPR3-mediated Aβ generation through multiple mechanisms. Previous evidence suggests that GRK2 can

regulate GPR3 $G_{\alpha S}$ signaling independent of GRK2 kinase function. Our data also demonstrate that inhibiting GRK2 kinase activity by overexpression of a GRK2 K220R dominant negative still results in ~75% of βarr2 recruitment to GPR3 compared to cells not expressing the GRK2 dominant negative mutant (empty-vector-expressing cells). However, we demonstrate that regulation of GPR3-mediated Aβ generation by GRK2 is kinase dependent. Therefore, we hypothesize that βarr2 is able to bind to GPR3 in different conformations depending on whether GPR3 is phosphorylated by GRK2 (βarr2*) or GPR3 is not phosphorylated by GRK2 ($\beta arr2^{o}$). βarr2* represents an 'active' conformation of βarr2 that allows for downstream activation of γ-secretase and Aβ generation via 2 hypothesized mechanisms (Fig. 25A).

Our data in Chapter 3 demonstrate that biasing GPR3 towards the βarr2 pathway by expressing the $GPR3^{DRY}$ mutant increases direct βarr2 interaction with the APH1A subunit of the γ-secretase compared to cells expressing $GPR3^{WT}$. In our current model, we predict that increasing βarr2 recruitment to the $GRP3^{DRY}$ mutant increases the concentration of βarr2* (activated βarr2). Mechanistically, activated conformations of βarr2 have been shown to remain at the plasma membrane following dissociation from a class A GPCR (β_2AR) (245). This active conformation is stabilized via βarr2 C-domain interaction with plasma membrane phosphoinositides and inositol phosphates (particularly phosphatidylinositol 4,5 bisphosphate (PIP_2) and inositol hexaphosphate (IP6)) (251) and allows for βarr2 to interact with downstream effectors including binding to proteins in clathrin-coated structures. Disrupting interactions with the plasma membrane results in a reduced pool of active βarr2 and decreased downstream arrestin signaling. This mechanism has been termed 'catalytic activation' of β-arrestins, and we hypothesize that GRK2 phosphorylation of GPR3 allows βarr2 to adopt an activate conformation that is maintained at the plasma membrane following dissociation from GPR3 (βarr2*). We demonstrated in Chapter 2 that βarr2 engages with

the APH1A subunit of γ-secretase similarly to a fully engaged βarr2-GPCR complex involving finger loop domain residues. In our model, the βarr2* conformation adopted by βarr2 following binding to GRK2-phosphorylated GPR3 allows for more favorable binding to APH1A in the local DRM environment and increased γ-secretase proteolytic cleavage of APP-C99 and Aβ generation.

Additionally, our lab has previously demonstrated that GPR3 C-terminal serine-to-alanine mutagenesis ($GPR3^{S/A}$ mutant) reduces βarr2 recruitment to GPR3 and reduces GPR3-mediated Aβ generation compared to $GPR3^{WT}$ (208). Surprisingly, cells expressing the $GPR3^{S/A}$ mutant do not reduce βarr2-APH1A interaction compared to $GPR3^{WT}$-expressing cells. Thus, the $GPR3^{S/A}$ mutant likely reduces γ-secretase activity via a different mechanism than catalytic activation of βarr2. Previous work has shown that GRK2 kinase activity is necessary to reduce cell-surface localization of GPR3 despite not being required to halt G-protein signaling (243). Therefore, we hypothesize that GPR3 trafficking is also involved in regulating Aβ generation. Interesting unpublished data from out lab demonstrates that GPR3 strongly localizes to the Golgi compartment in cells and, within the Golgi, is co-localized with APP. However, the $GPR3^{S/A}$ mutant exhibits statistically significantly reduced Golgi localization and reduced Golgi co-localization and total-lysate co-immunoprecipitation with APP. Interestingly, GPR3-APP interaction has been shown to regulate Aβ generation, and reduced GPR3-APP interaction results in reduced Aβ secretion (209). Cells expressing $GPR3^{S/A}$ do not exhibit any changes in APP localization compared to $GPR3^{WT}$-expressing cells. Some early, preliminary data hint that GRK2 may regulate GPR3 localization to the Golgi and co-localization with APP (Appendix Fig. 1), although more experiments and replicates are needed to draw conclusions. Our working hypothesis is that from the Golgi, GPR3 traffics back to the plasma membrane with APP and can undergo additional signaling. Therefore, the $GPR3^{WT}$ turnover rate is greater than that of $GPR3^{S/A}$ and can undergo more rounds of

phosphorylation by GRK2, βarr2 recruitment and activation, and increased interaction with APH1A and γ-secretase activity. Thus, following inhibition of GRK2 kinase activity or in GRK2 KO cells, βarr2 can be recruited to GPR3 but adopts an 'inactive' conformation ($\beta arr2^{o}$) that is not catalytically activated by GPR3, does not undergo favorable interaction with APH1A, and does not interact with endocytosis and/or trafficking machinery to traffic to the Golgi where it interacts with APP and is recycled back to the plasma membrane to undergo additional signaling (Fig. 25B).

To continue to test our hypotheses regarding these mechanisms moving forward, I would first investigate whether βarr2 is indeed catalytically activated following binding to GPR3. To accomplish this, I would utilize the Co-IP assay expressing GPR3, APH1A, and either $\beta arr2^{WT}$ or a $\beta arr2^{KRK/Q}$ mutant. The $\beta arr2^{KRK/Q}$ mutant (K233Q, R237Q, K251Q) maintains recruitment to a GPCR, but not continued binding to IP6 at the plasma membrane following recruitment (245,251). The $\beta arr2^{KRK/Q}$ mutant does not translocate to clathrin-coated structures (CCS) at plasma membrane following recruitment to β_2AR and cannot mediate receptor endocytosis (245). Preventing the non-GPCR interactions at the plasma membrane (IP6) prevented βarr2 from interacting with downstream partners to mediate signaling. By immunoprecipitating βarr2 and measuring interaction with APH1A, I could determine if preventing βarr2-plasma membrane interactions affect downstream interaction with APH1A. Additionally, I could utilize the $GPR3^{DRY}$ mutant and/or GRK2 KO cells to test if biasing GPR3 signaling affects the βarr2-APH1A interaction and is dependent on maintaining an active conformation at the plasma membrane. Additionally, more immunostaining experiments in GRK2 KO cells need to be conducted to make conclusions about the effect of GRK2 on GPR3 Golgi localization, GPR3-APP co-localization at the Golgi, and GPR3 trafficking. Cell surface biotinylation assays or total internal reflection fluorescence (TIRF) microscopy can be used in control and GRK2 KO cells expressing $GPR3^{WT}$

or GPR3$^{S/A}$ to determine if the cell-surface expression and turnover rate of GPR3 is altered by preventing GPR3 C-terminal phosphorylation or by genetic deletion of *Adrbk1*.

It is important to note that in this study we only investigated the role of GRK2 in regulating GPR3-mediated Aβ generation. While some evidence presented here suggests that GRK3 kinase activity is not involved in regulating this pathway, we do not comprehensively analyze the role of each ubiquitously expressed GRK in regulating GPR3 signaling. Many GPCRs undergo phosphorylation by multiple GRKs, and we expect this to hold true for GPR3 as well. Moving forward, a comprehensive analysis of the roles of GRK3, GRK5, and GRK6 is needed to fully understand how GRK regulation of GPR3 phosphorylation, βarr2 recruitment to GPR3, and GPR3 trafficking regulate γ-secretase activity and Aβ generation.

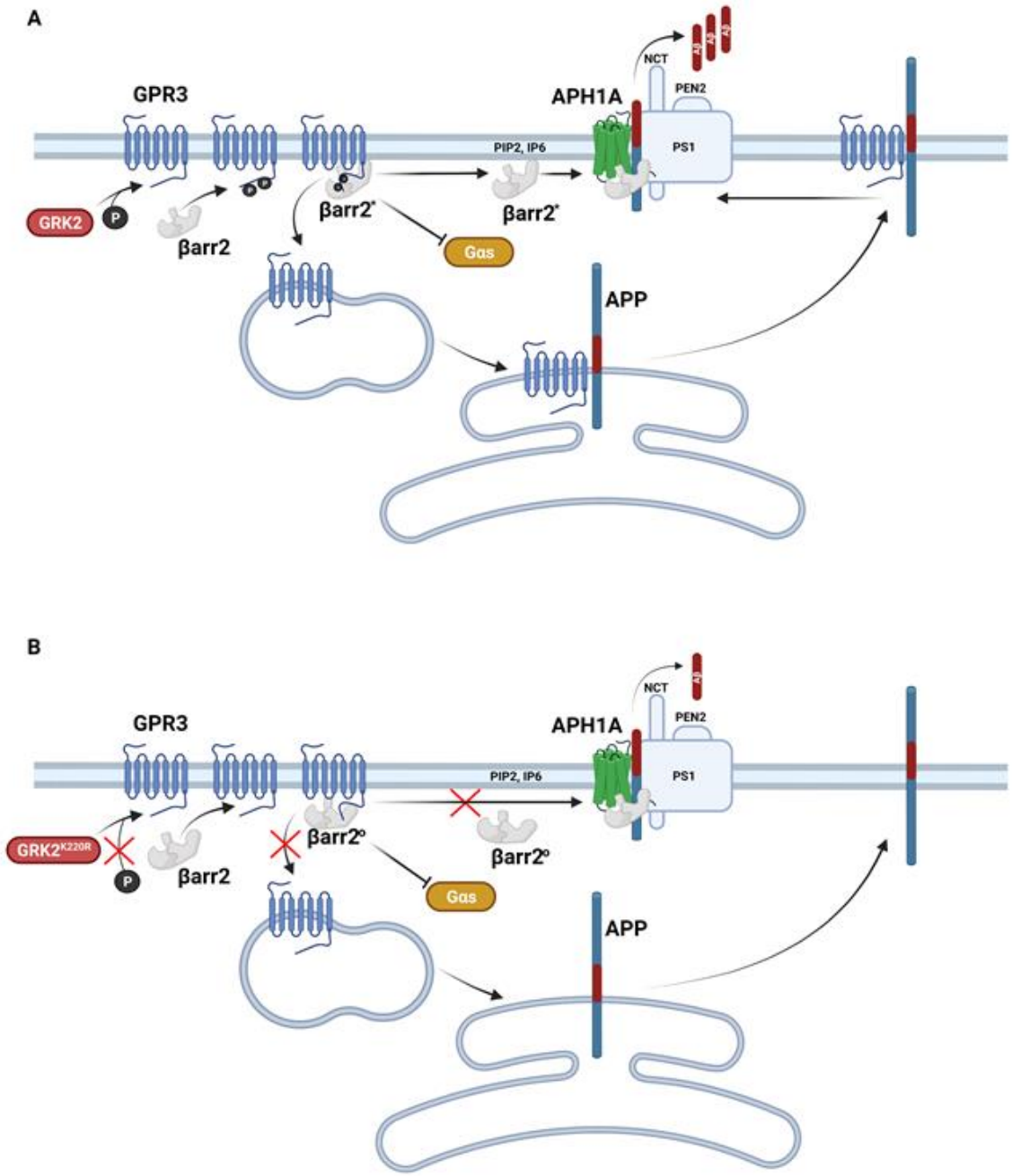

Figure 25. Proposed mechanism GPR3-mediated Aβ generation and regulation by GRK2

(A) GRK2 regulates βarr2 recruitment to GPR3. GRK2 kinase activity is not required to recruit βarr2 and prevent $G_{\alpha S}$ G-protein signaling but is necessary to internalize GPR3 and to initiate GPR3-dependent Aβ generation. We propose GPR3 regulates γ-secretase activity and Aβ generation by two distinct mechanisms. Firstly, GRK kinase activity allows for βarr2 to bind and adopt an 'active' conformation (βarr2*) that is maintained at the plasma membrane via non-GPCR interactions with the phosphoinositides and inositol phosphates (PIP_2 and IP6). βarr2* is in a conformation

favorable to bind with the APH1A subunit of the γ-secretase complex in the local DRM/lipid raft environment to stabilize the complex and increase proteolytic processing of APP. Secondly, GRK2 kinase activity regulates GPR3 internalization and trafficking to the Golgi, where it directly interacts with APP. GPR3-APP interaction at the Golgi increases GPR3 trafficking back to the plasma membrane, increasing GPR3 turnover and allowing additional βarr2 signaling cascades culminating in increased Aβ generation. **(B)** GRK2 K220R kinase dead mutant expression still allows for 75% of βarr2 recruitment to GPR3 and is able to prevent $G_{\alpha S}$ G-protein signaling downstream of GPR3. However, βarr2 adopts an 'inactive' conformation upon binding to non-GRK2-phosphorylated GPR3 (βarr2^{o}) which cannot be maintained at the plasma membrane and does not interact with APH1A. Additionally, βarr2^{o}-bound GPR3 does not initiate GPR3 internalization of trafficking and therefore GPR3 exhibits slower turnover and interaction with APP. In GRK2 KO cells, βarr2 recruitment to GPR3 is almost entirely abolished and results in reduced γ-secretase activity and Aβ generation.

4.3 Exploring GPR3 as a putative regulator of the APH1A phosphorylation barcode

The data presented in Chapter 2 suggest that GRKs exhibit a level of constitutive regulation of APH1A phosphorylation and γ-secretase activity. A significant unanswered question remaining is what induces changes in the APH1A phosphorylation barcode to alter γ-secretase proteolytic activity. As discussed previously, we hypothesize this may occur via 1) direct changes in GRK activity due to changes in expression level in specific cell types and/or regions of the brain with normal aging or in disease, or 2) via indirect changes in GRK activity due to altered GPCR signaling. Both GPCRs and the γ-secretase complex partition into DRM domains where signaling complexes are concentrated (206,252). Of particular interest, GPR3 presents an intriguing candidate receptor that may regulate the APH1A phosphorylation barcode. GPR3 expression is increased in the AD brain and modulates γ-secretase activity via βarr2 signaling (205,208). In Chapter 3 we demonstrate that biasing GPR3 signaling towards a βarr2 pathway by expressing the

GPR3^{DRY} mutant directly increases βarr2 interaction with APH1A. Furthermore, we demonstrate that GRK2 regulates βarr2 recruitment to GPR3 and downstream signaling. Interestingly, GRK2 is a critical regulator of constitutive APH1A phosphorylation (Chapter 2). Genetic deletion of *Adrbk1* (GRK2 KO) increases APH1A ICL2 phosphorylation and significantly increases constitutive γ-secretase activity and Aβ generation. Furthermore, GPR3-mediated γ-secretase activity is decreased in GRK2 KO cells compared to control cells. Therefore, we propose a model whereby increased GPR3 expression (or increased GPR3 activation) in AD competes as a substrate for GRK2 and reduces GRK2-mediated APH1A phosphorylation (Fig. 26). This effect would have two consequences. Firstly, GRK2 kinase activity mediates βarr2 recruitment to GPR3 – activating GPR3-βarr2 signaling cascades, increasing βarr2 interaction with APH1A and increasing γ-secretase activity and Aβ generation. Secondly, reduced GRK2 phosphorylation of APH1A would increase ICL2 phosphorylation and increase βarr2 recruitment to APH1A to allow for an APH1A-βarr2 conformation conducive for APP-C99 substrate recognition and proteolytic processing by the active γ-secretase complex. Overall, these two mechanisms combine to significantly increase Aβ generation and further highlight the development of GPR3 ligands to bias signaling away from GRK2 phosphorylation and βarr2 signaling.

The next steps to take in evaluating the role of GPR3 in modulating the APH1A phosphorylation barcode would be to directly measure APH1A phosphorylation following expression of GPR3 in both control cells and GRK2 KO cells. To do so, we can utilize a similar label-free quantitative LC-MS/MS approach as used in the experiments of this dissertation. We expect the overexpression of GPR3^{WT}, and GPR3^{DRY} to a greater extent, will increase APH1A phosphorylation at ICL2 in particular (S105 and S110). Furthermore, we hypothesize that this increase in APH1A ICL2 phosphorylation will be negated by the genetic deletion of *Adrbk1* in the

cells. Another interesting experiment would be to test the effect of GPR3aa18-27 on GPR3-mediated Aβ generation and a putative effect on regulating APH1A phosphorylation. In the recent study that characterized the N-terminal GPR3aa18-27 as a putative GPR3 ligand (201), the authors did not measure the effect on βarr2 recruitment to GPR3. By using a βarr2 PathHunter assay, BRET assay, or Co-IP assay, we can determine if GPR3aa18-27 has an effect on regulating βarr2 recruitment to GPR3. If so, we could then treat GPR3-expressing cells with GPR3aa18-27 and determine how modulating GPR3 signaling with GPR3aa18-27 alters APH1A phosphorylation as well as γ-secretase activity and Aβ generation.

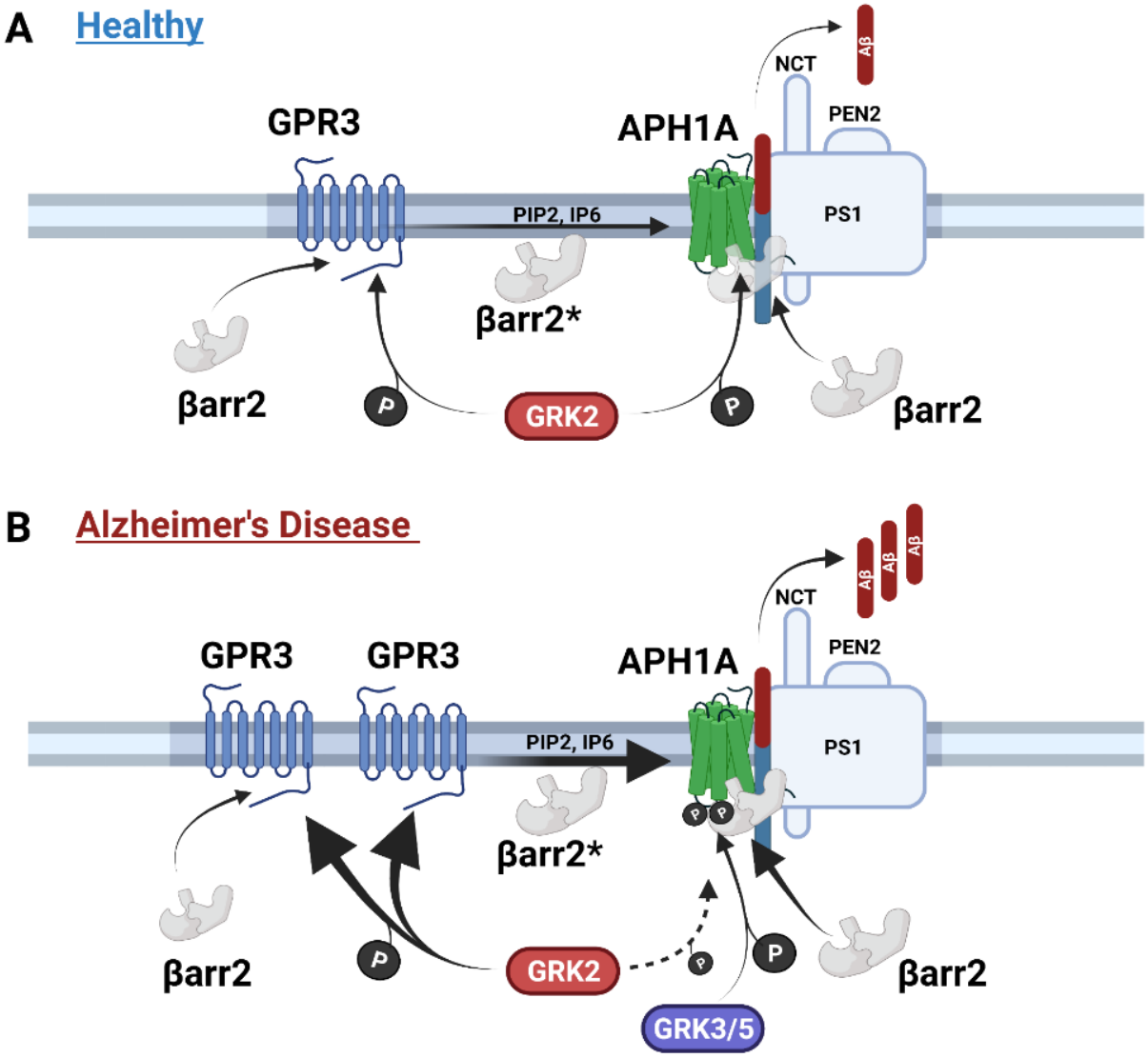

Figure 26. Proposed mechanism of GPR3 modulation of the APH1A phosphorylation barcode in normal physiology and in Alzheimer's disease and GRK2 regulation of these mechanisms

(A) GRK2 kinase activity is a constitutive regulator of both GPR3 signaling and APH1A phosphorylation. Under normal physiological conditions, GRK2 kinase activity regulates βarr2 recruitment to GPR3 to desensitize and internalize the receptor. Following binding to GPR3, βarr2 adopts an active conformation that is stabilized at the plasma membrane via phosphoinositide and inositol phosphate interactions (βarr2*) and allows for efficient binding to the APH1A subunit of γ-secretase to regulate basal proteolytic processing of APP. GRK2 also regulates APH1A

phosphorylation and acts to inhibit pathogenic APH1A phosphorylation, particularly at S105 and S110 in ICL2. GRK2 negatively regulates constitutive γ-secretase activity and results in a basal level of Aβ generation. **(B)** GPR3 expression is increased in the AD brain. Increased GPR3 expression outcompetes with APH1A for GRK2 phosphorylation. As a consequence, there is an increased amount of active βarr2* to bind to APH1A and stabile the γ-secretase in DRM domains where it is most catalytically active. Additionally, the reduced GRK2 regulation of APH1A (*dashed line*) allows for increased ICL2 pathogenic phosphorylation (putatively via GRK3 and GRK5) and exacerbates the effect on βarr2 binding, γ-secretase activity, and increased Aβ generation.

4.4 Evaluating the APH1A-βarr2 interaction as a therapeutic target

The γ-secretase complex has over 90 known substrates including APP and Notch1, a single-pass transmembrane protein involved in cell proliferation and tumorigenesis in multiple cancers (41,54). As such, targeting γ-secretase therapeutically has been investigated in both AD and cancer, yet no drug has been FDA approved to date in part by the many off-target effects of γ-secretase modulation (253,254). In AD, γ-secretase inhibitors (GSIs) have failed in clinical trials due to liver toxicity and worsening of cognition, hypothesized to be due to impaired Notch cleavage and accumulation of substrates that results in non-AD neurodegeneration (46). More recent clinical trials investigating Notch-sparing, γ-secretase modulators (GSMs) have also failed for similar reasons, suggesting other mechanisms of γ-secretase are affected (255). However, some of these failures may be due to the later stages of clinical dementia the patients in clinical trials were at, and the pathological alterations and cellular dysfunction caused by Aβ dyshomeostasis had already occurred at the time of GSI/GSM administration and were not affected by γ-secretase modulation. Therefore, a reasonable approach to targeting γ-secretase activity and Aβ in AD may be to target a cellular pathway or pathways upregulated in AD which increases γ-secretase activity

and Aβ generation, without directly targeting the γ-secretase complex itself and to administer this treatment at the earliest signs of AD progression based on biomarker analysis. Ultimately, a combination of approaches will likely be needed to address the multifaceted origins and cellular dysfunctions in AD.

The APH1A-βarr2 interaction is an intriguing putative therapeutic target in AD. Both βarr1 and βarr2 are upregulated in the AD brain, and interaction between both β-arrestins and APH1A has been shown to increase γ-secretase activity and cleavage of APP (208,244). One study showed that in cells, treatment with the APH1A or APH1B C-terminal peptides (ACT and BCT, respectively) concentration-dependently reduced Aβ generation without affecting Notch1 cleavage (244). However, these peptides are relatively large and would be difficult to administer into the brain of AD patients. Our computational analysis and *in vitro* validation of the βarr2-APH1A binding interface provides an excellent starting point to perform computational drug screens for small molecules to target and disrupt the interaction between β-arrestins and APH1A. Putative hit compounds can be tested using the βarr2 PathHunter assay coupled to an Aβ ELISA as performed in Chapter 2. Hits can further be validated as putative drug candidates by determining if they inhibit γ-secretase cleavage of substrates other than APP, such as Notch1, N-cadherin, and RAGE. Ideal compounds would specifically inhibit γ-secretase cleavage of APP.

Another interesting drug candidate screen would be for putative extracellular APH1A ligands. Although APH1A has no known ligand and is not classified as a receptor, it is capable of binding to β-arrestin in a similar manner as a GPCR. GPCR ligands can alter receptor conformation in ways to bias against β-arrestin binding and downstream signaling. It is therefore reasonable to believe that small molecules exist or can be designed to bind to the extracellular APH1A interface to alter APH1A conformation in a way that prevents βarr2 binding or recognition of APP-C99 as

substrate. Indeed, other 7TM proteins can only couple to β-arrestins and exhibit no G-protein binding or activation. A recent paper has characterized two non-canonical 7TM receptors as 'arrestin-coupled receptors' – the decoy 6 receptor (D6R) and the complement C5a receptor subtype 2 (C5aR2) (256). Each of these 7TM proteins has an endogenous ligand, CCL7 and C5a for the D6R and C5aR2, respectively, and displays distinct β-arrestin binding profiles mediated by distinct GRKs. This raises the interesting question as to whether APH1A may have an endogenous ligand or, at a minimum, could be modulated pharmacologically to direct GRK-mediated phosphorylation, β-arrestin binding, and γ-secretase activity. Additional computational screening of small molecules could provide a starting point for APH1A biased-ligand development.

Beyond AD, targeting the APH1A-βarr2 interaction could also provide therapeutic benefit in multiple cancers as well. Not only is increased γ-secretase activity and cleavage of Notch1 implicated in increased tumorigenesis in breast, lung, ovarian, and pancreatic cancer (among others) (253,257–259), these types of cancers are also associated with expression level changes in the ubiquitously expressed GRKs (260). Therefore, alterations in GRK expression in cancer could be a potential driver of increased Notch1 cleavage, cell proliferation, and a worse prognosis in patients. Therefore, targeting the APH1A-βarr2 interaction may be beneficial to prevent putative changes in activity caused by GRK-mediated APH1A phosphorylation in cancers as well as AD.

4.5 Concluding Remarks

The dyshomeostasis of Aβ peptides is an initial driver of the pathogenic cascade of cellular events culminating in Alzheimer's disease. Despite years of drug development, no successful disease-modifying therapeutic has been developed. As such, research seeking to understand basic

disease-driving mechanisms is paramount to better focus drug discovery efforts and to identify novel and beneficial therapeutic targets in AD. The work in this dissertation represents efforts to understand a basic, cellular mechanism regulating γ-secretase activity and Aβ generation. This dissertation reveals a novel mechanism of constitutive regulation of APH1A phosphorylation, βarr2 interaction, and γ-secretase activity by the GRK family of kinases. The work here broadens the functional role of GRKs in mediating phosphorylation barcodes to direct distinct signaling pathways in normal physiology and disease. Additionally, the work here further elucidates the mechanism of GPR3-mediated Aβ generation. Collectively, our work suggests that targeting the APH1A-βarr2 interface with small molecules may be a putative therapeutic target in AD, and further highlights the development of GPR3 biased ligands to reduce GRK2-mediated phosphorylation and βarr2 signaling in AD.

Appendix A

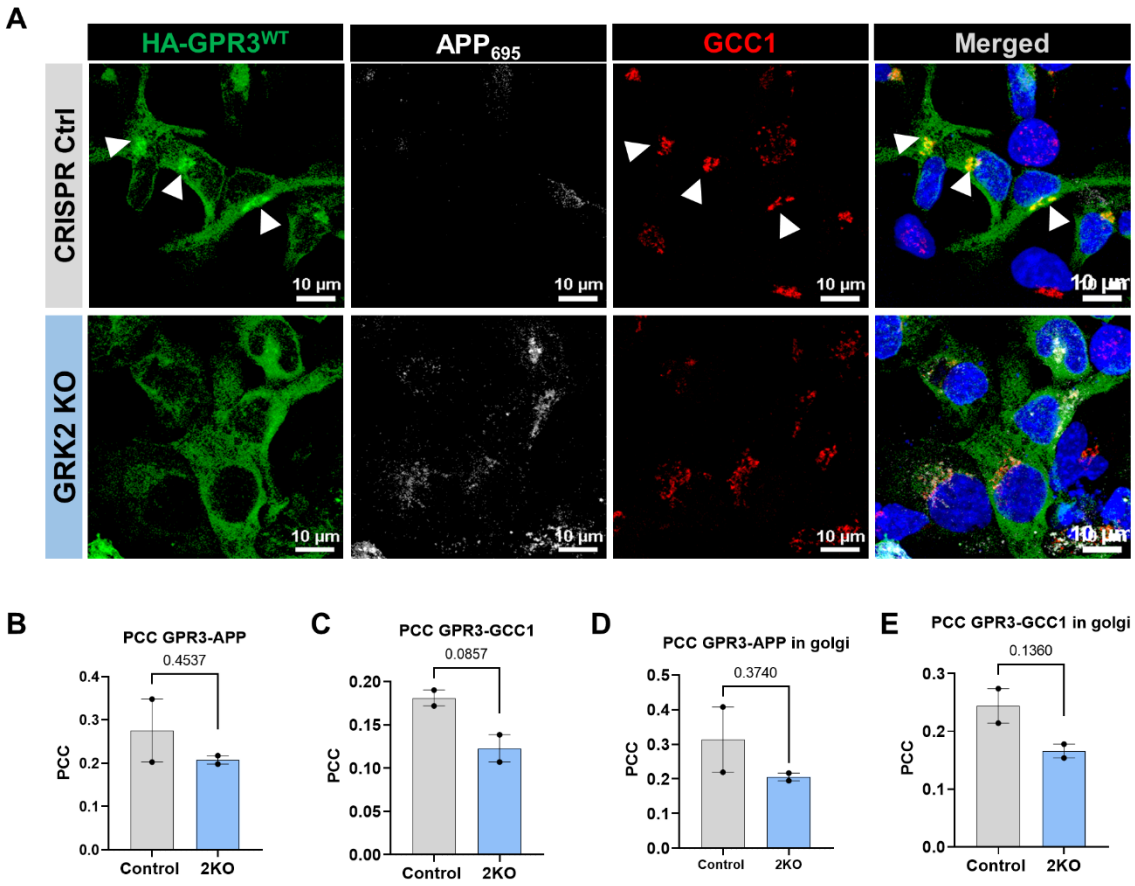

Appendix Figure 1. Preliminary evidence of reduced GPR3 Golgi localization and co-localization with APP in a GRK2 KO cell line.

(A) Confocal microscopy images of HEK293 control and GRK2 KO cells expressing HA-GPR3^{WT} and APP$_{695}$ and immunostained for HA-GPR3^{WT} (*green*), APP (*white*), and the Golgi marker GCC1 (*red*). White arrowheads indicate the Golgi and GPR3 localization in the Golgi. **(B-E)** Pearson correlation coefficients determining the extent of co-localization between **(B)** GPR3 and APP in the whole cell, **(C)** GPR3 and GCC1 in the whole cell, **(D)** GPR3 and APP in the Golgi, and **(E)** GPR3 and GCC1 in the Golgi. Data represent individual coverslips (black circles) from 1 experiment (n = 1) ± SEM. P-values are from unpaired t-test.

Appendix B

Contribution of GPCRs to Cognitive and Neuropsychiatric Symptoms of AD

Section 1.3.1 includes modified text from:
Y. Huang, **N. Todd**, A. Thathiah, The role of GPCRs in neurodegenerative diseases: avenues for therapeutic intervention. Curr. Opin. Pharmacol. 32, 96–110 (2017).

GPCRs and cognitive deficits in AD

AD leads to significant degeneration of various brain regions and the alteration of multiple neurochemical pathways. Magnetic resonance imaging (MRI) studies have shown that a reduction in the volume of the hippocampus and entorhinal cortex, which are affected early in disease progression (18,261), and cortical thickness of the medial temporal, inferior temporal, temporal pole, angular gyrus, superior parietal, superior frontal, and inferior frontal cortex correlate with the cognitive deficits observed in AD patients (262). Furthermore, changes in multiple neurochemical pathways, including the acetylcholine, serotonin, adenosine pathways have been shown to be involved in the cognitive impairments observed in AD.

Currently, there is no effective treatment for AD. Levels of acetylcholine are reduced in the brains of AD patients (263). As such, acetylcholinesterase inhibitors have been shown to temporarily ameliorate disease symptoms (264) by decreasing acetylcholine breakdown, which results in an increase in cholinergic neurotransmission and a mild improvement in cognitive function. Excitotoxicity due to overstimulation of glutamatergic neurotransmission (265) is also associated with the pathophysiology of AD (266). Memantine is an N-methyl-D-aspartate (NMDA) receptor antagonist that inhibits NMDA receptor-mediated calcium influx into neurons (267) and protects excessive glutamate-induced neuronal death and excitotoxicity (266), providing

temporary improvement in cognitive function (268). Until recently, acetylcholinesterase inhibitors and memantine were the only available symptomatic treatments that slow the decline in cognitive function in individuals with AD (264). Recently, the monoclonal Aβ antibody aducanumab (Aduhelm) received FDA approval for use in patients with MCI or mild dementia, although there is still much debate over whether administration to patients delays cognitive decline (269). This section highlights some of the GPCRs that have been rigorously evaluated in the modulation of cognitive function in AD mouse models in recent literature.

Glutamate receptors mediate most of the excitatory neurotransmission in the mammalian brain (270). The metabotropic glutamate receptor (mGluR) family mediate glutamate neurotransmission. mGluR5 has been shown to be involved in cognitive function and Aβ generation. Genetic deletion of mGluR5 has been shown to alleviate cognitive impairment and Aβ production in an APPswe/PSEN1ΔE9 AD mouse model, which overexpresses human APP harboring the Swedish mutation and human presenilin-1 lacking exon 9 (271). Interestingly, pharmacological inhibition of mGluR5 with 3-[(2-methyl-1,3-thiazol-4-yl)ethynyl]-pyridine (MTEP), an antagonist, has also been shown to alleviate the cognitive deficits in the same AD mouse model (272). Similarly, treatment with the mGluR5 negative allosteric modulator 2-chloro-4-((2,5-dimethyl-1-(4-(trifluoromethoxy)phenyl)1H-imidazol-4-yl)ethynyl) pyridine (CTEP) alleviates the cognitive deficits and reduces the amyloid plaque burden in two AD mouse models (273). These studies suggest that allosteric modulators of mGluR5 may be an effective therapeutic strategy for some AD cases.

Extensive serotonergic denervation of the neocortex and hippocampus has been observed in AD patients. Reduction in 5-hydroxytryptamine (5-HT, serotonin) and 5HT1A, 5-HT2A, 5-HT4, and 5-HT6 receptor levels have been reported in the hippocampus and/or prefrontal cortex

of AD patients. In rodent models, activation of 5-HT2A and 5-HT4 receptors leads to an improvement in hippocampal-dependent learning and memory (274,275) via G protein- or β-arrestin-dependent activation of extracellular signal-regulated kinase (ERK) (276,277). In contrast, antagonism of the 5-HT1A and the least studied 5-HT5A receptors has been shown to ameliorate the memory deficits in a rat AD model (278,279), possibly through an inhibition of $G_{\alpha i}$ signaling which leads to the activation of the NMDA receptor (280,281). Interestingly, both 5-HT6 receptor agonists and antagonists enhance learning and memory (282) through potentially different mechanisms of action. Activation of the 5-HT6 receptor has been shown to stimulate $G_{\alpha s}$ protein-dependent brain-derived neurotrophic factor (BDNF) mRNA expression and Fyn kinase-dependent activation of ERK1/2 in wild-type rats (283). Both BDNF and ERK1/2 have been shown to be associated with cognitive function (284,285). In contrast, 5-HT6 receptor antagonists have been shown to stimulate glutamate and acetylcholine release in rat brains, which has been shown to improve scopolamine- and MK-801-induced deficits in associative learning (285). These studies support the potential benefit of selective modulation of the 5-HT receptor subtypes for AD therapy.

Expression of the adenosine A1and A2A receptors (A1R and A2AR) has been reported to be elevated in the frontal cortex of the human AD brain (286). Caffeine, a nonselective adenosine receptor inhibitor, has been shown to enhance memory consolidation in humans (287) and reduce Aβ levels and improve cognitive function in an AD mouse model (288). Similarly, caffeine and the A2AR antagonist SCH58261 has been shown to be protective against Aβ-induced cognitive impairment (289). Interestingly, conditional deletion of astrocytic A2ARs has been shown to enhance alleviate the memory deficits in AD transgenic mice through $G_{\alpha s}$-coupled signaling (290), whereas activation of the $G_{\alpha i}$-coupled A1R and inhibition of PKA has been shown enhance long-term depression (LTD) (291). These studies potentially suggest that activation of $G_{\alpha s}$-coupled

receptors, such as the A2AR, which activates PKA, may suppress LTD and promote long-term potentiation (LTP), whereas $G_{\alpha i}$-coupled receptors, such as the A1R may be involved in the induction of LTD.

In addition to GPCRs with identified ligands, the orphan GPCR GPR3 has been shown to modulate Aβ generation and cognitive function *in vivo*. Levels of GPR3 are elevated in the human AD brain (205,208). Genetic deletion of Gpr3 has been shown to alleviate the learning and memory deficits in an AD mouse model and reduce amyloid pathology in four AD mouse models (207). The GPR3-mediated effect on amyloid pathology involves β-arrestin recruitment, independently of $G_{\alpha s}$ coupling (208). GRP3 will be discussed in further detail in section 1.3.4. Together, mGluRs, 5-HT receptors, adenosine receptors, and other GPCRs such as GPR3 that are involved in affected neurochemical pathways in AD suggest viable therapeutic avenues for the treatment of cognitive deficits in AD.

GPCRs and neuropsychiatric symptoms in AD

The corticotrophin-releasing hormone (CRH) receptor 1 and 2 (CRHR1 and CRHR2) are GPCRs associated with depression (292,293). Interestingly, a greater density of amyloid plaques has been observed in the hippocampus of AD patients with a previous history of major depression (294). Reports also show that genetic deletion of *Crhr1* in the *PSAPP* AD mouse model, which overexpress a chimeric mouse/human APP gene with human APP Swedish mutation and human presenilin-1 lacking exon 9, leads to a reduction in amyloid pathology (295). Pharmacological studies in the Tg2576 AD mouse model, which overexpresses human APP with the Swedish mutation, with the CRHR1 antagonist antalarmin in acutely (7days) or in chronically (9-months) stressed mice reduces Aβ production and involves the $G_{\alpha s}$ signaling pathway (296); however, pre-treatment with antalarmin failed to inhibit an increase in Aβ levels in acutely (3-hours) stressed

wild-type mice. *In vitro* cell-free γ-secretase activity assays with the CRHR1 antagonists astressin, antalarmin, and NBI-27914 have been shown to modulate Aβ generation in the absence of CRHR1, suggesting that the compounds tested may have CRHR1-independent effects on the modulation of γ-secretase activity (293). Treatment of wild-type mice with the CRHR1 antagonist antalarmin reduces depression-like behaviors, whereas genetic deficiency of *Crhr2* leads to an increase in depression-like behaviors (297). Although both receptors have considerable sequence similarity, the two receptors have different expression patterns in the brain and affinities for CRH (298). Interestingly, CRHR1 is more abundantly expressed in the pituitary gland, and atrophy of this region is associated with the neuropsychiatric symptoms in AD (299). The *in vivo* studies suggest that a highly selective antagonist specific for CRHR1 may be beneficial for the symptoms of depression in AD; however, careful monitoring of Aβ levels would also be necessary to fully assess the therapeutic potential.

References

1. Alzheimer’s Facts and Figures Report | Alzheimer's Association [Internet]. [cited 2020 Apr 3]. Available from: https://www.alz.org/alzheimers-dementia/facts-figures
2. Mendez MF. Early-Onset Alzheimer Disease. Neurol Clin. 2017 May;35(2):263–281.
3. McKhann GM, Knopman DS, Chertkow H, Hyman BT, Jack CR, Kawas CH, et al. The diagnosis of dementia due to Alzheimer’s disease: recommendations from the National Institute on Aging-Alzheimer's Association workgroups on diagnostic guidelines for Alzheimer's disease. Alzheimers Dement. 2011 May;7(3):263–269.
4. Jack CR, Bennett DA, Blennow K, Carrillo MC, Dunn B, Haeberlein SB, et al. NIA-AA Research Framework: Toward a biological definition of Alzheimer’s disease. Alzheimers Dement. 2018 Apr;14(4):535–562.
5. Jack CR, Albert MS, Knopman DS, McKhann GM, Sperling RA, Carrillo MC, et al. Introduction to the recommendations from the National Institute on Aging-Alzheimer’s Association workgroups on diagnostic guidelines for Alzheimer's disease. Alzheimers Dement. 2011 May;7(3):257–262.
6. Ryan NS, Nicholas JM, Weston PSJ, Liang Y, Lashley T, Guerreiro R, et al. Clinical phenotype and genetic associations in autosomal dominant familial Alzheimer’s disease: a case series. Lancet Neurol. 2016 Dec;15(13):1326–1335.
7. Edwards Iii GA, Gamez N, Escobedo G, Calderon O, Moreno-Gonzalez I. Modifiable risk factors for alzheimer’s disease. Front Aging Neurosci. 2019 Jun 24;11:146.
8. Crous-Bou M, Minguillón C, Gramunt N, Molinuevo JL. Alzheimer’s disease prevention: from risk factors to early intervention. Alzheimers Res Ther. 2017 Sep 12;9(1):71.

9. Liu C-C, Liu C-C, Kanekiyo T, Xu H, Bu G. Apolipoprotein E and Alzheimer disease: risk, mechanisms and therapy. Nat Rev Neurol. 2013 Feb;9(2):106–118.

10. Corder EH, Saunders AM, Strittmatter WJ, Schmechel DE, Gaskell PC, Small GW, et al. Gene dose of apolipoprotein E type 4 allele and the risk of Alzheimer's disease in late onset families. Science. 1993 Aug 13;261(5123):921–923.

11. Liao F, Yoon H, Kim J. Apolipoprotein E metabolism and functions in brain and its role in Alzheimer's disease. Curr Opin Lipidol. 2017 Feb;28(1):60–67.

12. Liu C-C, Zhao N, Fu Y, Wang N, Linares C, Tsai C-W, et al. Apoe4 accelerates early seeding of amyloid pathology. Neuron. 2017 Dec 6;96(5):1024–1032.e3.

13. Albert MS, DeKosky ST, Dickson D, Dubois B, Feldman HH, Fox NC, et al. The diagnosis of mild cognitive impairment due to Alzheimer's disease: recommendations from the National Institute on Aging-Alzheimer's Association workgroups on diagnostic guidelines for Alzheimer's disease. Alzheimers Dement. 2011 May;7(3):270–279.

14. De Strooper B, Karran E. The cellular phase of alzheimer's disease. Cell. 2016 Feb 11;164(4):603–615.

15. Dubois B, Hampel H, Feldman HH, Scheltens P, Aisen P, Andrieu S, et al. Preclinical Alzheimer's disease: Definition, natural history, and diagnostic criteria. Alzheimers Dement. 2016 Mar;12(3):292–323.

16. Querfurth HW, LaFerla FM. Alzheimer's disease. N Engl J Med. 2010 Jan 28;362(4):329–344.

17. Craft S, Peskind E, Schwartz MW, Schellenberg GD, Raskind M, Porte D. Cerebrospinal fluid and plasma insulin levels in Alzheimer's disease: relationship to severity of dementia and apolipoprotein E genotype. Neurology. 1998 Jan;50(1):164–168.

18. Serrano-Pozo A, Frosch MP, Masliah E, Hyman BT. Neuropathological alterations in Alzheimer disease. Cold Spring Harb Perspect Med. 2011 Sep;1(1):a006189.

19. Perl DP. Neuropathology of Alzheimer's disease. Mt Sinai J Med. 2010 Feb;77(1):32–42.

20. Hyman BT, Phelps CH, Beach TG, Bigio EH, Cairns NJ, Carrillo MC, et al. National Institute on Aging-Alzheimer's Association guidelines for the neuropathologic assessment of Alzheimer's disease. Alzheimers Dement. 2012 Jan;8(1):1–13.

21. Jellinger KA. Alpha-synuclein pathology in Parkinson's and Alzheimer's disease brain: incidence and topographic distribution--a pilot study. Acta Neuropathol. 2003 Sep;106(3):191–201.

22. Thomas DX, Bajaj S, McRae-McKee K, Hadjichrysanthou C, Anderson RM, Collinge J. Association of TDP-43 proteinopathy, cerebral amyloid angiopathy, and Lewy bodies with cognitive impairment in individuals with or without Alzheimer's disease neuropathology. Sci Rep. 2020 Sep 3;10(1):14579.

23. DeTure MA, Dickson DW. The neuropathological diagnosis of Alzheimer's disease. Mol Neurodegener. 2019 Aug 2;14(1):32.

24. Jack CR, Knopman DS, Jagust WJ, Petersen RC, Weiner MW, Aisen PS, et al. Tracking pathophysiological processes in Alzheimer's disease: an updated hypothetical model of dynamic biomarkers. Lancet Neurol. 2013 Feb;12(2):207–216.

25. Hardy JA, Higgins GA. Alzheimer's disease: the amyloid cascade hypothesis. Science. 1992 Apr 10;256(5054):184–185.

26. Sleegers K, Brouwers N, Gijselinck I, Theuns J, Goossens D, Wauters J, et al. APP duplication is sufficient to cause early onset Alzheimer's dementia with cerebral amyloid angiopathy. Brain. 2006 Nov;129(Pt 11):2977–2983.

27. Selkoe DJ, Hardy J. The amyloid hypothesis of Alzheimer's disease at 25 years. EMBO Mol Med. 2016 Jun 1;8(6):595–608.

28. Wang X, Zhou X, Li G, Zhang Y, Wu Y, Song W. Modifications and trafficking of APP in the pathogenesis of alzheimer's disease. Front Mol Neurosci. 2017 Sep 15;10:294.

29. Lichtenthaler SF. Alpha-secretase cleavage of the amyloid precursor protein: proteolysis regulated by signaling pathways and protein trafficking. Curr Alzheimer Res. 2012 Feb;9(2):165–177.

30. Chasseigneaux S, Allinquant B. Functions of Aβ, sAPPα and sAPPβ : similarities and differences. J Neurochem. 2012 Jan;120 Suppl 1:99–108.

31. Nabers A, Perna L, Lange J, Mons U, Schartner J, Güldenhaupt J, et al. Amyloid blood biomarker detects Alzheimer's disease. EMBO Mol Med. 2018;10(5).

32. Lesné SE, Sherman MA, Grant M, Kuskowski M, Schneider JA, Bennett DA, et al. Brain amyloid-β oligomers in ageing and Alzheimer's disease. Brain. 2013 May;136(Pt 5):1383–1398.

33. Viola KL, Klein WL. Amyloid β oligomers in Alzheimer's disease pathogenesis, treatment, and diagnosis. Acta Neuropathol. 2015 Feb;129(2):183–206.

34. D'Andrea MR, Nagele RG. Morphologically distinct types of amyloid plaques point the way to a better understanding of Alzheimer's disease pathogenesis. Biotech Histochem. 2010 Apr;85(2):133–147.

35. Abd-Elrahman KS, Albaker A, de Souza JM, Ribeiro FM, Schlossmacher MG, Tiberi M, et al. Aβ oligomers induce pathophysiological mGluR5 signaling in Alzheimer's disease model mice in a sex-selective manner. Sci Signal. 2020 Dec 15;13(662).

36. Hamilton A, Zamponi GW, Ferguson SSG. Glutamate receptors function as scaffolds for the regulation of β-amyloid and cellular prion protein signaling complexes. Mol Brain. 2015 Mar 24;8:18.

37. Chen G-F, Xu T-H, Yan Y, Zhou Y-R, Jiang Y, Melcher K, et al. Amyloid beta: structure, biology and structure-based therapeutic development. Acta Pharmacol Sin. 2017 Sep;38(9):1205–1235.

38. Briner A, Götz J, Polanco JC. Fyn kinase controls tau aggregation in vivo. Cell Rep. 2020 Aug 18;32(7):108045.

39. Smith LM, Kostylev MA, Lee S, Strittmatter SM. Systematic and standardized comparison of reported amyloid-β receptors for sufficiency, affinity, and Alzheimer's disease relevance. J Biol Chem. 2019 Apr 12;294(15):6042–6053.

40. Mroczko B, Groblewska M, Litman-Zawadzka A, Kornhuber J, Lewczuk P. Cellular receptors of amyloid β oligomers (aβos) in alzheimer's disease. Int J Mol Sci. 2018 Jun 27;19(7).

41. Haapasalo A, Kovacs DM. The many substrates of presenilin/γ-secretase. J Alzheimers Dis. 2011;25(1):3–28.

42. Wouters R, Michiels C, Sannerud R, Kleizen B, Dillen K, Vermeire W, et al. Assembly of γ-secretase occurs through stable dimers after exit from the endoplasmic reticulum. J Cell Biol. 2021 Sep 6;220(9).

43. Vetrivel KS, Cheng H, Lin W, Sakurai T, Li T, Nukina N, et al. Association of gamma-secretase with lipid rafts in post-Golgi and endosome membranes. J Biol Chem. 2004 Oct 22;279(43):44945–44954.

44. Haass C, Kaether C, Thinakaran G, Sisodia S. Trafficking and proteolytic processing of APP. Cold Spring Harb Perspect Med. 2012 May;2(5):a006270.

45. Dries DR, Yu G. Assembly, maturation, and trafficking of the gamma-secretase complex in Alzheimer's disease. Curr Alzheimer Res. 2008 Apr;5(2):132–146.

46. Acx H, Serneels L, Radaelli E, Muyldermans S, Vincke C, Pepermans E, et al. Inactivation of γ-secretases leads to accumulation of substrates and non-Alzheimer neurodegeneration. EMBO Mol Med. 2017 Aug;9(8):1088–1099.

47. Yonemura Y, Futai E, Yagishita S, Kaether C, Ishiura S. Specific combinations of presenilins and Aph1s affect the substrate specificity and activity of γ-secretase. Biochem Biophys Res Commun. 2016 Sep 30;478(4):1751–1757.

48. Shirotani K, Edbauer D, Prokop S, Haass C, Steiner H. Identification of distinct gamma-secretase complexes with different APH-1 variants. J Biol Chem. 2004 Oct 1;279(40):41340–41345.

49. Serneels L, Dejaegere T, Craessaerts K, Horré K, Jorissen E, Tousseyn T, et al. Differential contribution of the three Aph1 genes to gamma-secretase activity in vivo. Proc Natl Acad Sci USA. 2005 Feb 1;102(5):1719–1724.

50. Acx H, Chávez-Gutiérrez L, Serneels L, Lismont S, Benurwar M, Elad N, et al. Signature amyloid β profiles are produced by different γ-secretase complexes. J Biol Chem. 2014 Feb 14;289(7):4346–4355.

51. Pardossi-Piquard R, Yang S-P, Kanemoto S, Gu Y, Chen F, Böhm C, et al. APH1 polar transmembrane residues regulate the assembly and activity of presenilin complexes. J Biol Chem. 2009 Jun 12;284(24):16298–16307.

52. Chen AC, Guo LY, Ostaszewski BL, Selkoe DJ, LaVoie MJ. Aph-1 associates directly with full-length and C-terminal fragments of gamma-secretase substrates. J Biol Chem. 2010 Apr 9;285(15):11378–11391.

53. Chiang P-M, Fortna RR, Price DL, Li T, Wong PC. Specific domains in anterior pharynx-defective 1 determine its intramembrane interactions with nicastrin and presenilin. Neurobiol Aging. 2012 Feb;33(2):277–285.

54. Wolfe MS. Substrate recognition and processing by γ-secretase. Biochim Biophys Acta Biomembr. 2020 Jan 1;1862(1):183016.

55. Mo J-S, Yoon J-H, Hong J-A, Kim M-Y, Ann E-J, Ahn J-S, et al. Phosphorylation of nicastrin by SGK1 leads to its degradation through lysosomal and proteasomal pathways. PLoS One. 2012 May 10;7(5):e37111.

56. Jo E-H, Ahn J-S, Mo J-S, Yoon J-H, Ann E-J, Baek H-J, et al. Akt1 phosphorylates Nicastrin to regulate its protein stability and activity. J Neurochem. 2015 Sep;134(5):799–810.

57. Kim S-K, Park H-J, Hong HS, Baik EJ, Jung MW, Mook-Jung I. ERK1/2 is an endogenous negative regulator of the gamma-secretase activity. FASEB J. 2006 Jan;20(1):157–159.

58. Matz A, Halamoda-Kenzaoui B, Hamelin R, Mosser S, Alattia J-R, Dimitrov M, et al. Identification of new Presenilin-1 phosphosites: implication for γ-secretase activity and Aβ production. J Neurochem. 2015 May;133(3):409–421.

59. Maesako M, Horlacher J, Zoltowska KM, Kastanenka KV, Kara E, Svirsky S, et al. Pathogenic PS1 phosphorylation at Ser367. Elife. 2017 Jan 30;6.

60. Bustos V, Pulina MV, Kelahmetoglu Y, Sinha SC, Gorelick FS, Flajolet M, et al. Bidirectional regulation of Aβ levels by Presenilin 1. Proc Natl Acad Sci USA. 2017 Jul 3;114(27):7142–7147.

61. Braak H, Braak E. Neuropathological stageing of Alzheimer-related changes. Acta Neuropathol. 1991;82(4):239–259.

62. Braak H, Alafuzoff I, Arzberger T, Kretzschmar H, Del Tredici K. Staging of Alzheimer disease-associated neurofibrillary pathology using paraffin sections and immunocytochemistry. Acta Neuropathol. 2006 Oct;112(4):389–404.

63. Liu F, Gong C-X. Tau exon 10 alternative splicing and tauopathies. Mol Neurodegener. 2008 Jul 10;3:8.

64. Wang Y, Mandelkow E. Tau in physiology and pathology. Nat Rev Neurosci. 2016 Jan;17(1):5–21.

65. Greenwood JA, Johnson GV. Localization and in situ phosphorylation state of nuclear tau. Exp Cell Res. 1995 Oct;220(2):332–337.

66. Hanger DP, Lau DHW, Phillips EC, Bondulich MK, Guo T, Woodward BW, et al. Intracellular and extracellular roles for tau in neurodegenerative disease. J Alzheimers Dis. 2014;40 Suppl 1:S37–45.

67. Rai SK, Savastano A, Singh P, Mukhopadhyay S, Zweckstetter M. Liquid-liquid phase separation of tau: From molecular biophysics to physiology and disease. Protein Sci. 2021 Jul;30(7):1294–1314.

68. Wegmann S, Eftekharzadeh B, Tepper K, Zoltowska KM, Bennett RE, Dujardin S, et al. Tau protein liquid-liquid phase separation can initiate tau aggregation. EMBO J. 2018 Apr 3;37(7).

69. DeVos SL, Corjuc BT, Oakley DH, Nobuhara CK, Bannon RN, Chase A, et al. Synaptic tau seeding precedes tau pathology in human alzheimer's disease brain. Front Neurosci. 2018 Apr 24;12:267.

70. Jucker M, Walker LC. Propagation and spread of pathogenic protein assemblies in neurodegenerative diseases. Nat Neurosci. 2018 Sep 26;21(10):1341–1349.

71. Hallinan GI, Vargas-Caballero M, West J, Deinhardt K. Tau Misfolding Efficiently Propagates between Individual Intact Hippocampal Neurons. J Neurosci. 2019 Nov 27;39(48):9623–9632.

72. Ahmed Z, Cooper J, Murray TK, Garn K, McNaughton E, Clarke H, et al. A novel in vivo model of tau propagation with rapid and progressive neurofibrillary tangle pathology: the pattern of spread is determined by connectivity, not proximity. Acta Neuropathol. 2014 May;127(5):667–683.

73. Liu L, Drouet V, Wu JW, Witter MP, Small SA, Clelland C, et al. Trans-synaptic spread of tau pathology in vivo. PLoS One. 2012 Feb 1;7(2):e31302.

74. van der Kant R, Goldstein LSB, Ossenkoppele R. Amyloid-β-independent regulators of tau pathology in Alzheimer disease. Nat Rev Neurosci. 2020 Jan;21(1):21–35.

75. Santa-María I, Pérez M, Hernández F, Avila J, Moreno FJ. Characteristics of the binding of thioflavin S to tau paired helical filaments. J Alzheimers Dis. 2006 Aug;9(3):279–285.

76. Despres C, Byrne C, Qi H, Cantrelle F-X, Huvent I, Chambraud B, et al. Identification of the Tau phosphorylation pattern that drives its aggregation. Proc Natl Acad Sci USA. 2017 Aug 22;114(34):9080–9085.

77. Hanger DP, Anderton BH, Noble W. Tau phosphorylation: the therapeutic challenge for neurodegenerative disease. Trends Mol Med. 2009 Mar;15(3):112–119.

78. Cavallini A, Brewerton S, Bell A, Sargent S, Glover S, Hardy C, et al. An unbiased approach to identifying tau kinases that phosphorylate tau at sites associated with Alzheimer disease. J Biol Chem. 2013 Aug 9;288(32):23331–23347.

79. La Joie R, Visani AV, Baker SL, Brown JA, Bourakova V, Cha J, et al. Prospective longitudinal atrophy in Alzheimer's disease correlates with the intensity and topography of baseline tau-PET. Sci Transl Med. 2020 Jan 1;12(524).

80. Mandelkow EM, Biernat J, Drewes G, Gustke N, Trinczek B, Mandelkow E. Tau domains, phosphorylation, and interactions with microtubules. Neurobiol Aging. 1995 Jun;16(3):355–62; discussion 362.

81. Cowan CM, Mudher A. Are tau aggregates toxic or protective in tauopathies? Front Neurol. 2013 Aug 13;4:114.

82. Wang Y, Zhang Y, Hu W, Xie S, Gong C-X, Iqbal K, et al. Rapid alteration of protein phosphorylation during postmortem: implication in the study of protein phosphorylation. Sci Rep. 2015 Oct 29;5:15709.

83. Sohn PD, Tracy TE, Son H-I, Zhou Y, Leite REP, Miller BL, et al. Acetylated tau destabilizes the cytoskeleton in the axon initial segment and is mislocalized to the somatodendritic compartment. Mol Neurodegener. 2016 Jun 29;11(1):47.

84. Zempel H, Dennissen FJA, Kumar Y, Luedtke J, Biernat J, Mandelkow E-M, et al. Axodendritic sorting and pathological missorting of Tau are isoform-specific and determined by axon initial segment architecture. J Biol Chem. 2017 Jul 21;292(29):12192–12207.

85. Rane JS, Kumari A, Panda D. An acetylation mimicking mutation, K274Q, in tau imparts neurotoxicity by enhancing tau aggregation and inhibiting tubulin polymerization. Biochem J. 2019 May 21;476(10):1401–1417.

86. He Z, Guo JL, McBride JD, Narasimhan S, Kim H, Changolkar L, et al. Amyloid-β plaques enhance Alzheimer's brain tau-seeded pathologies by facilitating neuritic plaque tau aggregation. Nat Med. 2018 Jan;24(1):29–38.

87. Shin WS, Di J, Cao Q, Li B, Seidler PM, Murray KA, et al. Amyloid β-protein oligomers promote the uptake of tau fibril seeds potentiating intracellular tau aggregation. Alzheimers Res Ther. 2019 Oct 18;11(1):86.

88. Gomes LA, Hipp SA, Rijal Upadhaya A, Balakrishnan K, Ospitalieri S, Koper MJ, et al. Aβ-induced acceleration of Alzheimer-related τ-pathology spreading and its association with prion protein. Acta Neuropathol. 2019 Aug 14;138(6):913–941.

89. Umeda T, Maekawa S, Kimura T, Takashima A, Tomiyama T, Mori H. Neurofibrillary tangle formation by introducing wild-type human tau into APP transgenic mice. Acta Neuropathol. 2014 May;127(5):685–698.

90. Tackenberg C, Grinschgl S, Trutzel A, Santuccione AC, Frey MC, Konietzko U, et al. NMDA receptor subunit composition determines beta-amyloid-induced neurodegeneration and synaptic loss. Cell Death Dis. 2013 Apr 25;4:e608.

91. Ghosh S, Wu MD, Shaftel SS, Kyrkanides S, LaFerla FM, Olschowka JA, et al. Sustained interleukin-1β overexpression exacerbates tau pathology despite reduced amyloid burden in an Alzheimer's mouse model. J Neurosci. 2013 Mar 13;33(11):5053–5064.

92. Kitazawa M, Cheng D, Tsukamoto MR, Koike MA, Wes PD, Vasilevko V, et al. Blocking IL-1 signaling rescues cognition, attenuates tau pathology, and restores neuronal β-catenin

pathway function in an Alzheimer's disease model. J Immunol. 2011 Dec 15;187(12):6539–6549.

93. Bolmont T, Clavaguera F, Meyer-Luehmann M, Herzig MC, Radde R, Staufenbiel M, et al. Induction of tau pathology by intracerebral infusion of amyloid-beta -containing brain extract and by amyloid-beta deposition in APP x Tau transgenic mice. Am J Pathol. 2007 Dec;171(6):2012–2020.

94. Stancu I-C, Vasconcelos B, Terwel D, Dewachter I. Models of β-amyloid induced Tau-pathology: the long and "folded" road to understand the mechanism. Mol Neurodegener. 2014 Nov 18;9:51.

95. Shin WS, Di J, Murray KA, Sun C, Li B, Bitan G, et al. Different Amyloid-β Self-Assemblies Have Distinct Effects on Intracellular Tau Aggregation. Front Mol Neurosci. 2019 Nov 8;12:268.

96. Ittner LM, Ke YD, Delerue F, Bi M, Gladbach A, van Eersel J, et al. Dendritic function of tau mediates amyloid-beta toxicity in Alzheimer's disease mouse models. Cell. 2010 Aug 6;142(3):387–397.

97. Fredriksson R, Schiöth HB. The repertoire of G-protein-coupled receptors in fully sequenced genomes. Mol Pharmacol. 2005 May;67(5):1414–1425.

98. Wootten D, Christopoulos A, Marti-Solano M, Babu MM, Sexton PM. Mechanisms of signalling and biased agonism in G protein-coupled receptors. Nat Rev Mol Cell Biol. 2018 Oct;19(10):638–653.

99. Schiöth HB, Fredriksson R. The GRAFS classification system of G-protein coupled receptors in comparative perspective. Gen Comp Endocrinol. 2005 May 15;142(1-2):94–101.

100. Huang Y, Todd N, Thathiah A. The role of GPCRs in neurodegenerative diseases: avenues for therapeutic intervention. Curr Opin Pharmacol. 2017 Feb;32:96–110.

101. Che T. Advances in the treatment of chronic pain by targeting gpcrs. Biochemistry. 2021 May 11;60(18):1401–1412.

102. Dorsam RT, Gutkind JS. G-protein-coupled receptors and cancer. Nat Rev Cancer. 2007 Feb;7(2):79–94.

103. Wang J, Gareri C, Rockman HA. G-Protein-Coupled Receptors in Heart Disease. Circ Res. 2018 Aug 31;123(6):716–735.

104. Chidambaram H, Chinnathambi S. G-Protein Coupled Receptors and Tau-different Roles in Alzheimer's Disease. Neuroscience. 2020 Jul 1;438:198–214.

105. Leysen H, van Gastel J, Hendrickx JO, Santos-Otte P, Martin B, Maudsley S. G Protein-Coupled Receptor Systems as Crucial Regulators of DNA Damage Response Processes. Int J Mol Sci. 2018 Sep 26;19(10).

106. Vroon A, Heijnen CJ, Kavelaars A. GRKs and arrestins: regulators of migration and inflammation. J Leukoc Biol. 2006 Dec;80(6):1214–1221.

107. Sriram K, Insel PA. G Protein-Coupled Receptors as Targets for Approved Drugs: How Many Targets and How Many Drugs? Mol Pharmacol. 2018 Apr;93(4):251–258.

108. Hauser AS, Attwood MM, Rask-Andersen M, Schiöth HB, Gloriam DE. Trends in GPCR drug discovery: new agents, targets and indications. Nat Rev Drug Discov. 2017 Dec;16(12):829–842.

109. Latorraca NR, Venkatakrishnan AJ, Dror RO. GPCR dynamics: structures in motion. Chem Rev. 2017 Jan 11;117(1):139–155.

110. Hilger D, Masureel M, Kobilka BK. Structure and dynamics of GPCR signaling complexes. Nat Struct Mol Biol. 2018 Jan 8;25(1):4–12.

111. Strasser A, Wittmann H-J, Seifert R. Binding kinetics and pathways of ligands to gpcrs. Trends Pharmacol Sci. 2017 Jun 20;38(8):717–732.

112. Sanchez-Soto M, Verma RK, Willette BKA, Gonye EC, Moore AM, Moritz AE, et al. A structural basis for how ligand binding site changes can allosterically regulate GPCR signaling and engender functional selectivity. Sci Signal. 2020 Feb 4;13(617).

113. Preininger AM, Meiler J, Hamm HE. Conformational flexibility and structural dynamics in GPCR-mediated G protein activation: a perspective. J Mol Biol. 2013 Jul 10;425(13):2288–2298.

114. Inoue A, Raimondi F, Kadji FMN, Singh G, Kishi T, Uwamizu A, et al. Illuminating G-Protein-Coupling Selectivity of GPCRs. Cell. 2019 Jun 13;177(7):1933–1947.e25.

115. Smrcka AV. G protein βγ subunits: central mediators of G protein-coupled receptor signaling. Cell Mol Life Sci. 2008 Jul;65(14):2191–2214.

116. Ribas C, Penela P, Murga C, Salcedo A, García-Hoz C, Jurado-Pueyo M, et al. The G protein-coupled receptor kinase (GRK) interactome: role of GRKs in GPCR regulation and signaling. Biochim Biophys Acta. 2007 Apr;1768(4):913–922.

117. Watari K, Nakaya M, Kurose H. Multiple functions of G protein-coupled receptor kinases. J Mol Signal. 2014 Mar 6;9(1):1.

118. Parruti G, Peracchia F, Sallese M, Ambrosini G, Masini M, Rotilio D, et al. Molecular analysis of human beta-arrestin-1: cloning, tissue distribution, and regulation of expression. Identification of two isoforms generated by alternative splicing. J Biol Chem. 1993 May 5;268(13):9753–9761.

119. Attramadal H, Arriza JL, Aoki C, Dawson TM, Codina J, Kwatra MM, et al. Beta-arrestin2, a novel member of the arrestin/beta-arrestin gene family. J Biol Chem. 1992 Sep 5;267(25):17882–17890.

120. Zhou XE, He Y, de Waal PW, Gao X, Kang Y, Van Eps N, et al. Identification of Phosphorylation Codes for Arrestin Recruitment by G Protein-Coupled Receptors. Cell. 2017 Jul 27;170(3):457–469.e13.

121. Latorraca NR, Masureel M, Hollingsworth SA, Heydenreich FM, Suomivuori C-M, Brinton C, et al. How GPCR Phosphorylation Patterns Orchestrate Arrestin-Mediated Signaling. Cell. 2020 Dec 23;183(7):1813–1825.e18.

122. van Gastel J, Hendrickx JO, Leysen H, Santos-Otte P, Luttrell LM, Martin B, et al. β-Arrestin Based Receptor Signaling Paradigms: Potential Therapeutic Targets for Complex Age-Related Disorders. Front Pharmacol. 2018 Nov 28;9:1369.

123. Seyedabadi M, Ghahremani MH, Albert PR. Biased signaling of G protein coupled receptors (GPCRs): Molecular determinants of GPCR/transducer selectivity and therapeutic potential. Pharmacol Ther. 2019 May 8;200:148–178.

124. Zidar DA, Violin JD, Whalen EJ, Lefkowitz RJ. Selective engagement of G protein coupled receptor kinases (GRKs) encodes distinct functions of biased ligands. Proc Natl Acad Sci USA. 2009 Jun 16;106(24):9649–9654.

125. Rankovic Z, Brust TF, Bohn LM. Biased agonism: An emerging paradigm in GPCR drug discovery. Bioorg Med Chem Lett. 2016 Jan 15;26(2):241–250.

126. Crilly SE, Puthenveedu MA. Compartmentalized GPCR Signaling from Intracellular Membranes. J Membr Biol. 2020 Nov 24;

127. White AD, Jean-Alphonse FG, Fang F, Peña KA, Liu S, König GM, et al. Gq/11-dependent regulation of endosomal cAMP generation by parathyroid hormone class B GPCR. Proc Natl Acad Sci USA. 2020 Mar 31;117(13):7455–7460.

128. Pavlos NJ, Friedman PA. GPCR signaling and trafficking: the long and short of it. Trends Endocrinol Metab. 2017 Mar;28(3):213–226.

129. Nguyen AH, Thomsen ARB, Cahill TJ, Huang R, Huang L-Y, Marcink T, et al. Structure of an endosomal signaling GPCR-G protein-β-arrestin megacomplex. Nat Struct Mol Biol. 2019 Dec;26(12):1123–1131.

130. Irannejad R, Tomshine JC, Tomshine JR, Chevalier M, Mahoney JP, Steyaert J, et al. Conformational biosensors reveal GPCR signalling from endosomes. Nature. 2013 Mar 28;495(7442):534–538.

131. Tsvetanova NG, Trester-Zedlitz M, Newton BW, Peng GE, Johnson JR, Jimenez-Morales D, et al. Endosomal cAMP production broadly impacts the cellular phosphoproteome. J Biol Chem. 2021 Jul;297(1):100907.

132. Smith JS, Lefkowitz RJ, Rajagopal S. Biased signalling: from simple switches to allosteric microprocessors. Nat Rev Drug Discov. 2018 Apr;17(4):243–260.

133. Jacobson KA. New paradigms in GPCR drug discovery. Biochem Pharmacol. 2015 Dec 15;98(4):541–555.

134. Kenakin T. Agonist-receptor efficacy. II. Agonist trafficking of receptor signals. Trends Pharmacol Sci. 1995 Jul;16(7):232–238.

135. Schönegge A-M, Gallion J, Picard L-P, Wilkins AD, Le Gouill C, Audet M, et al. Evolutionary action and structural basis of the allosteric switch controlling β2AR functional selectivity. Nat Commun. 2017 Dec 18;8(1):2169.

136. Liu JJ, Horst R, Katritch V, Stevens RC, Wüthrich K. Biased signaling pathways in β2-adrenergic receptor characterized by 19F-NMR. Science. 2012 Mar 2;335(6072):1106–1110.

137. Peng Y, McCorvy JD, Harpsøe K, Lansu K, Yuan S, Popov P, et al. 5-HT2C Receptor Structures Reveal the Structural Basis of GPCR Polypharmacology. Cell. 2018 Feb 8;172(4):719–730.e14.

138. Tan L, Yan W, McCorvy JD, Cheng J. Biased Ligands of G Protein-Coupled Receptors (GPCRs): Structure-Functional Selectivity Relationships (SFSRs) and Therapeutic Potential. J Med Chem. 2018 Nov 21;61(22):9841–9878.

139. Yang Z, Yang F, Zhang D, Liu Z, Lin A, Liu C, et al. Phosphorylation of G Protein-Coupled Receptors: From the Barcode Hypothesis to the Flute Model. Mol Pharmacol. 2017 Feb 28;92(3):201–210.

140. Nobles KN, Xiao K, Ahn S, Shukla AK, Lam CM, Rajagopal S, et al. Distinct phosphorylation sites on the β(2)-adrenergic receptor establish a barcode that encodes differential functions of β-arrestin. Sci Signal. 2011 Aug 9;4(185):ra51.

141. Premont RT. Keys to the Kingdom: GPCR phosphorylation patterns direct β-arrestin. EMBO Rep. 2020 Sep 3;21(9):e51249.

142. Rapacciuolo A, Suvarna S, Barki-Harrington L, Luttrell LM, Cong M, Lefkowitz RJ, et al. Protein kinase A and G protein-coupled receptor kinase phosphorylation mediates beta-1 adrenergic receptor endocytosis through different pathways. J Biol Chem. 2003 Sep 12;278(37):35403–35411.

143. Luo J, Busillo JM, Stumm R, Benovic JL. G Protein-Coupled Receptor Kinase 3 and Protein Kinase C Phosphorylate the Distal C-Terminal Tail of the Chemokine Receptor CXCR4 and Mediate Recruitment of β-Arrestin. Mol Pharmacol. 2017 Jun;91(6):554–566.

144. Gurevich EV, Tesmer JJG, Mushegian A, Gurevich VV. G protein-coupled receptor kinases: more than just kinases and not only for GPCRs. Pharmacol Ther. 2012 Jan;133(1):40–69.

145. Matthees ESF, Haider RS, Hoffmann C, Drube J. Differential Regulation of GPCRs-Are GRK Expression Levels the Key? Front Cell Dev Biol. 2021 May 24;9:687489.

146. Rafael Guimarães T, Swanson E, Kofler J, Thathiah A. G protein-coupled receptor kinases are associated with Alzheimer's disease pathology. Neuropathol Appl Neurobiol. 2021 Jun 23;

147. Boguth CA, Singh P, Huang C, Tesmer JJG. Molecular basis for activation of G protein-coupled receptor kinases. EMBO J. 2010 Oct 6;29(19):3249–3259.

148. Chen Q, Plasencia M, Li Z, Mukherjee S, Patra D, Chen C-L, et al. Structures of rhodopsin in complex with G-protein-coupled receptor kinase 1. Nature. 2021 Jul 14;595(7868):600–605.

149. Hildreth KL, Wu J-H, Barak LS, Exum ST, Kim LK, Peppel K, et al. Phosphorylation of the platelet-derived growth factor receptor-beta by G protein-coupled receptor kinase-2 reduces receptor signaling and interaction with the Na(+)/H(+) exchanger regulatory factor. J Biol Chem. 2004 Oct 1;279(40):41775–41782.

150. Pitcher JA, Hall RA, Daaka Y, Zhang J, Ferguson SS, Hester S, et al. The G protein-coupled receptor kinase 2 is a microtubule-associated protein kinase that phosphorylates tubulin. J Biol Chem. 1998 May 15;273(20):12316–12324.

151. Martini JS, Raake P, Vinge LE, DeGeorge BR, Chuprun JK, Harris DM, et al. Uncovering G protein-coupled receptor kinase-5 as a histone deacetylase kinase in the nucleus of cardiomyocytes. Proc Natl Acad Sci USA. 2008 Aug 26;105(34):12457–12462.

152. Lafarga V, Mayor F, Penela P. The interplay between G protein-coupled receptor kinase 2 (GRK2) and histone deacetylase 6 (HDAC6) at the crossroads of epithelial cell motility. Cell Adh Migr. 2012 Dec;6(6):495–501.

153. Chen X, Zhu H, Yuan M, Fu J, Zhou Y, Ma L. G-protein-coupled receptor kinase 5 phosphorylates p53 and inhibits DNA damage-induced apoptosis. J Biol Chem. 2010 Apr 23;285(17):12823–12830.

154. Carman CV, Parent JL, Day PW, Pronin AN, Sternweis PM, Wedegaertner PB, et al. Selective regulation of Galpha(q/11) by an RGS domain in the G protein-coupled receptor kinase, GRK2. J Biol Chem. 1999 Nov 26;274(48):34483–34492.

155. Ribeiro FM, Ferreira LT, Paquet M, Cregan T, Ding Q, Gros R, et al. Phosphorylation-independent regulation of metabotropic glutamate receptor 5 desensitization and internalization by G protein-coupled receptor kinase 2 in neurons. J Biol Chem. 2009 Aug 28;284(35):23444–23453.

156. Sorriento D, Ciccarelli M, Santulli G, Campanile A, Altobelli GG, Cimini V, et al. The G-protein-coupled receptor kinase 5 inhibits NFkappaB transcriptional activity by inducing nuclear accumulation of IkappaB alpha. Proc Natl Acad Sci USA. 2008 Nov 18;105(46):17818–17823.

157. Cheng J, Lucas PC, McAllister-Lucas LM. Canonical and Non-Canonical Roles of GRK2 in Lymphocytes. Cells. 2021 Feb 3;10(2).

158. Suo WZ, Li L. Dysfunction of G protein-coupled receptor kinases in Alzheimer's disease. ScientificWorldJournal. 2010 Aug 17;10:1667–1678.

159. van Gastel J, Leysen H, Boddaert J, Vangenechten L, Luttrell LM, Martin B, et al. Aging-related modifications to G protein-coupled receptor signaling diversity. Pharmacol Ther. 2021 Jul;223:107793.

160. Yu S, Sun L, Jiao Y, Lee LTO. The Role of G Protein-coupled Receptor Kinases in Cancer. Int J Biol Sci. 2018 Feb 5;14(2):189–203.

161. Murga C, Arcones AC, Cruces-Sande M, Briones AM, Salaices M, Mayor F. G Protein-Coupled Receptor Kinase 2 (GRK2) as a Potential Therapeutic Target in Cardiovascular and Metabolic Diseases. Front Pharmacol. 2019 Feb 19;10:112.

162. Sato PY, Chuprun JK, Schwartz M, Koch WJ. The evolving impact of g protein-coupled receptor kinases in cardiac health and disease. Physiol Rev. 2015 Apr;95(2):377–404.

163. Busillo JM, Armando S, Sengupta R, Meucci O, Bouvier M, Benovic JL. Site-specific phosphorylation of CXCR4 is dynamically regulated by multiple kinases and results in differential modulation of CXCR4 signaling. J Biol Chem. 2010 Mar 5;285(10):7805–7817.

164. Butcher AJ, Prihandoko R, Kong KC, McWilliams P, Edwards JM, Bottrill A, et al. Differential G-protein-coupled receptor phosphorylation provides evidence for a signaling bar code. J Biol Chem. 2011 Apr 1;286(13):11506–11518.

165. Just S, Illing S, Trester-Zedlitz M, Lau EK, Kotowski SJ, Miess E, et al. Differentiation of opioid drug effects by hierarchical multi-site phosphorylation. Mol Pharmacol. 2013 Mar;83(3):633–639.

166. Kaya AI, Perry NA, Gurevich VV, Iverson TM. Phosphorylation barcode-dependent signal bias of the dopamine D1 receptor. Proc Natl Acad Sci USA. 2020 Jun 23;117(25):14139–14149.

167. Kim O-J, Gardner BR, Williams DB, Marinec PS, Cabrera DM, Peters JD, et al. The role of phosphorylation in D1 dopamine receptor desensitization: evidence for a novel mechanism of arrestin association. J Biol Chem. 2004 Feb 27;279(9):7999–8010.

168. Ohguro H, Palczewski K, Ericsson LH, Walsh KA, Johnson RS. Sequential phosphorylation of rhodopsin at multiple sites. Biochemistry. 1993 Jun 1;32(21):5718–5724.

169. Palmer TM, Stiles GL. Identification of threonine residues controlling the agonist-dependent phosphorylation and desensitization of the rat A(3) adenosine receptor. Mol Pharmacol. 2000 Mar;57(3):539–545.

170. Kouhen OM, Wang G, Solberg J, Erickson LJ, Law PY, Loh HH. Hierarchical phosphorylation of delta-opioid receptor regulates agonist-induced receptor desensitization and internalization. J Biol Chem. 2000 Nov 24;275(47):36659–36664.

171. Gurevich EV, Gurevich VV. Grks as modulators of neurotransmitter receptors. Cells. 2020 Dec 31;10(1).

172. Mueller W, Schütz D, Nagel F, Schulz S, Stumm R. Hierarchical organization of multi-site phosphorylation at the CXCR4 C terminus. PLoS One. 2013 May 29;8(5):e64975.

173. Kim D, Castaño M, Lujan LK, Woo JA, Liggett SB. The short third intracellular loop and cytoplasmic tail of bitter taste receptors provide functionally relevant GRK phosphorylation sites in TAS2R14. J Biol Chem. 2021 Jun;296:100216.

174. Yin W, Li Z, Jin M, Yin Y-L, de Waal PW, Pal K, et al. A complex structure of arrestin-2 bound to a G protein-coupled receptor. Cell Res. 2019 Dec;29(12):971–983.

175. Shukla AK, Westfield GH, Xiao K, Reis RI, Huang L-Y, Tripathi-Shukla P, et al. Visualization of arrestin recruitment by a G-protein-coupled receptor. Nature. 2014 Aug 14;512(7513):218–222.

176. Kumari P, Srivastava A, Banerjee R, Ghosh E, Gupta P, Ranjan R, et al. Functional competence of a partially engaged GPCR-β-arrestin complex. Nat Commun. 2016 Nov 9;7:13416.

177. Ranjan R, Dwivedi H, Baidya M, Kumar M, Shukla AK. Novel Structural Insights into GPCR-β-Arrestin Interaction and Signaling. Trends Cell Biol. 2017 Jun 23;27(11):851–862.

178. Sente A, Peer R, Srivastava A, Baidya M, Lesk AM, Balaji S, et al. Molecular mechanism of modulating arrestin conformation by GPCR phosphorylation. Nat Struct Mol Biol. 2018 Jun 5;25(6):538–545.

179. Chen Q, Perry NA, Vishnivetskiy SA, Berndt S, Gilbert NC, Zhuo Y, et al. Structural basis of arrestin-3 activation and signaling. Nat Commun. 2017 Nov 10;8(1):1427.

180. Latorraca NR, Wang JK, Bauer B, Townshend RJL, Hollingsworth SA, Olivieri JE, et al. Molecular mechanism of GPCR-mediated arrestin activation. Nature. 2018 May 2;557(7705):452–456.

181. He Q-T, Xiao P, Huang S-M, Jia Y-L, Zhu Z-L, Lin J-Y, et al. Structural studies of phosphorylation-dependent interactions between the V2R receptor and arrestin-2. Nat Commun. 2021 Apr 22;12(1):2396.

182. Suo Z, Wu M, Citron BA, Wong GT, Festoff BW. Abnormality of G-protein-coupled receptor kinases at prodromal and early stages of Alzheimer's disease: an association with early beta-amyloid accumulation. J Neurosci. 2004 Mar 31;24(13):3444–3452.

183. Almonte AG, Qadri LH, Sultan FA, Watson JA, Mount DJ, Rumbaugh G, et al. Protease-activated receptor-1 modulates hippocampal memory formation and synaptic plasticity. J Neurochem. 2013 Jan;124(1):109–122.

184. Liu J, Rasul I, Sun Y, Wu G, Li L, Premont RT, et al. GRK5 deficiency leads to reduced hippocampal acetylcholine level via impaired presynaptic M2/M4 autoreceptor desensitization. J Biol Chem. 2009 Jul 17;284(29):19564–19571.

185. Cheng S, Li L, He S, Liu J, Sun Y, He M, et al. GRK5 deficiency accelerates {beta}-amyloid accumulation in Tg2576 mice via impaired cholinergic activity. J Biol Chem. 2010 Dec 31;285(53):41541–41548.

186. Zhang Y, Zhao J, Yin M, Cai Y, Liu S, Wang Y, et al. The influence of two functional genetic variants of GRK5 on tau phosphorylation and their association with Alzheimer's disease risk. Oncotarget. 2017 Sep 22;8(42):72714–72726.

187. Takeuchi T, Fujinami K, Goto H, Fujita A, Taketo MM, Manabe T, et al. Roles of M2 and M4 muscarinic receptors in regulating acetylcholine release from myenteric neurons of mouse ileum. J Neurophysiol. 2005 May;93(5):2841–2848.

188. Davis AA, Fritz JJ, Wess J, Lah JJ, Levey AI. Deletion of M1 muscarinic acetylcholine receptors increases amyloid pathology in vitro and in vivo. J Neurosci. 2010 Mar 24;30(12):4190–4196.

189. Li L, Liu J, Suo WZ. GRK5 deficiency exaggerates inflammatory changes in TgAPPsw mice. J Neuroinflammation. 2008 Jun 3;5:24.

190. Suo Z, Cox AA, Bartelli N, Rasul I, Festoff BW, Premont RT, et al. GRK5 deficiency leads to early Alzheimer-like pathology and working memory impairment. Neurobiol Aging. 2007 Dec;28(12):1873–1888.

191. Zhao J, Li X, Chen X, Cai Y, Wang Y, Sun W, et al. GRK5 influences the phosphorylation of tau via GSK3β and contributes to Alzheimer's disease. J Cell Physiol. 2019 Jul;234(7):10411–10420.

192. Takahashi M, Uchikado H, Caprotti D, Weidenheim KM, Dickson DW, Ksiezak-Reding H, et al. Identification of G-protein coupled receptor kinase 2 in paired helical filaments and neurofibrillary tangles. J Neuropathol Exp Neurol. 2006 Dec;65(12):1157–1169.

193. Wu H, Wei S, Huang Y, Chen L, Wang Y, Wu X, et al. Aβ monomer induces phosphorylation of Tau at Ser-214 through β2AR-PKA-JNK signaling pathway. FASEB J. 2020 Feb 17;

194. Bychkov ER, Gurevich VV, Joyce JN, Benovic JL, Gurevich EV. Arrestins and two receptor kinases are upregulated in Parkinson's disease with dementia. Neurobiol Aging. 2008 Mar;29(3):379–396.

195. Tanaka S, Ishii K, Kasai K, Yoon SO, Saeki Y. Neural expression of G protein-coupled receptors GPR3, GPR6, and GPR12 up-regulates cyclic AMP levels and promotes neurite outgrowth. J Biol Chem. 2007 Apr 6;282(14):10506–10515.

196. Martin AL, Steurer MA, Aronstam RS. Constitutive Activity among Orphan Class-A G Protein Coupled Receptors. PLoS One. 2015 Sep 18;10(9):e0138463 (1–12).

197. Ikawa F, Tanaka S, Harada K, Hide I, Maruyama H, Sakai N. Detailed neuronal distribution of GPR3 and its co-expression with EF-hand calcium-binding proteins in the mouse central nervous system. Brain Res. 2021 Jan 1;1750:147166.

198. Iismaa TP, Kiefer J, Liu ML, Baker E, Sutherland GR, Shine J. Isolation and chromosomal localization of a novel human G-protein-coupled receptor (GPR3) expressed predominantly in the central nervous system. Genomics. 1994 Nov 15;24(2):391–394.

199. Saeki Y, Ueno S, Mizuno R, Nishimura T, Fujimura H, Nagai Y, et al. Molecular cloning of a novel putative G protein-coupled receptor (GPCR21) which is expressed predominantly in mouse central nervous system. FEBS Lett. 1993 Dec 27;336(2):317–322.

200. Freudzon L, Norris RP, Hand AR, Tanaka S, Saeki Y, Jones TLZ, et al. Regulation of meiotic prophase arrest in mouse oocytes by GPR3, a constitutive activator of the Gs G protein. J Cell Biol. 2005 Oct 24;171(2):255–265.

201. Sveidahl Johansen O, Ma T, Hansen JB, Markussen LK, Schreiber R, Reverte-Salisa L, et al. Lipolysis drives expression of the constitutively active receptor GPR3 to induce adipose thermogenesis. Cell. 2021 Jun 24;184(13):3502–3518.e33.

202. Ledent C, Demeestere I, Blum D, Petermans J, Hämäläinen T, Smits G, et al. Premature ovarian aging in mice deficient for Gpr3. Proc Natl Acad Sci USA. 2005 Jun 21;102(25):8922–8926.

203. Tourino C, Valjent E, Ruiz-Medina J, Herve D, Ledent C, Valverde O. The orphan receptor GPR3 modulates the early phases of cocaine reinforcement. Br J Pharmacol. 2012 Oct;167(4):892–904.

204. Valverde O, Célérier E, Baranyi M, Vanderhaeghen P, Maldonado R, Sperlagh B, et al. GPR3 receptor, a novel actor in the emotional-like responses. PLoS One. 2009 Mar 4;4(3):e4704.

205. Thathiah A, Spittaels K, Hoffmann M, Staes M, Cohen A, Horré K, et al. The orphan G protein-coupled receptor 3 modulates amyloid-beta peptide generation in neurons. Science. 2009 Feb 13;323(5916):946–951.

206. Hur J-Y, Welander H, Behbahani H, Aoki M, Frånberg J, Winblad B, et al. Active gamma-secretase is localized to detergent-resistant membranes in human brain. FEBS J. 2008 Mar;275(6):1174–1187.

207. Huang Y, Skwarek-Maruszewska A, Horré K, Vandewyer E, Wolfs L, Snellinx A, et al. Loss of GPR3 reduces the amyloid plaque burden and improves memory in Alzheimer's disease mouse models. Sci Transl Med. 2015 Oct 14;7(309):309ra164.

208. Thathiah A, Horré K, Snellinx A, Vandewyer E, Huang Y, Ciesielska M, et al. β-arrestin 2 regulates Aβ generation and γ-secretase activity in Alzheimer's disease. Nat Med. 2013 Jan;19(1):43–49.

209. Nelson CD, Sheng M. Gpr3 stimulates Aβ production via interactions with APP and β-arrestin2. PLoS One. 2013 Sep 12;8(9):e74680.

210. Mucke L, Selkoe DJ. Neurotoxicity of amyloid β-protein: synaptic and network dysfunction. Cold Spring Harb Perspect Med. 2012 Jul;2(7):a006338.

211. Zhang Y, Thompson R, Zhang H, Xu H. APP processing in Alzheimer's disease. Mol Brain. 2011 Jan 7;4:3.

212. De Strooper B. Aph-1, Pen-2, and Nicastrin with Presenilin generate an active gamma-Secretase complex. Neuron. 2003 Apr 10;38(1):9–12.

213. DeWire SM, Ahn S, Lefkowitz RJ, Shenoy SK. Beta-arrestins and cell signaling. Annu Rev Physiol. 2007;69:483–510.

214. Lefkowitz RJ, Shenoy SK. Transduction of receptor signals by beta-arrestins. Science. 2005 Apr 22;308(5721):512–517.

215. Ren X-R, Reiter E, Ahn S, Kim J, Chen W, Lefkowitz RJ. Different G protein-coupled receptor kinases govern G protein and beta-arrestin-mediated signaling of V2 vasopressin receptor. Proc Natl Acad Sci USA. 2005 Feb 1;102(5):1448–1453.

216. Choi M, Staus DP, Wingler LM, Ahn S, Pani B, Capel WD, et al. G protein-coupled receptor kinases (GRKs) orchestrate biased agonism at the β2-adrenergic receptor. Sci Signal. 2018 Aug 21;11(544).

217. Gurevich VV, Gurevich EV. GPCR signaling regulation: the role of grks and arrestins. Front Pharmacol. 2019 Feb 19;10:125.

218. Blom N, Gammeltoft S, Brunak S. Sequence and structure-based prediction of eukaryotic protein phosphorylation sites. J Mol Biol. 1999 Dec 17;294(5):1351–1362.

219. Komolov KE, Benovic JL. G protein-coupled receptor kinases: Past, present and future. Cell Signal. 2018 Jan;41:17–24.

220. Thal DM, Yeow RY, Schoenau C, Huber J, Tesmer JJG. Molecular mechanism of selectivity among G protein-coupled receptor kinase 2 inhibitors. Mol Pharmacol. 2011 Aug;80(2):294–303.

221. Kim YH, Choi SH, D'Avanzo C, Hebisch M, Sliwinski C, Bylykbashi E, et al. A 3D human neural cell culture system for modeling Alzheimer's disease. Nat Protoc. 2015 Jul;10(7):985–1006.

222. Choi SH, Kim YH, Hebisch M, Sliwinski C, Lee S, D'Avanzo C, et al. A three-dimensional human neural cell culture model of Alzheimer's disease. Nature. 2014 Nov 13;515(7526):274–278.

223. Ran FA, Hsu PD, Wright J, Agarwala V, Scott DA, Zhang F. Genome engineering using the CRISPR-Cas9 system. Nat Protoc. 2013 Nov;8(11):2281–2308.

224. Kang Y, Zhou XE, Gao X, He Y, Liu W, Ishchenko A, et al. Crystal structure of rhodopsin bound to arrestin by femtosecond X-ray laser. Nature. 2015 Jul 30;523(7562):561–567.

225. Drube J, Haider RS, Matthees ESF, Reichel M, Zeiner J, Fritzwanker S, et al. GRK2/3/5/6 knockout: The impact of individual GRKs on arrestin-binding and GPCR regulation. BioRxiv. 2021 Feb 13;

226. Onorato JJ, Palczewski K, Regan JW, Caron MG, Lefkowitz RJ, Benovic JL. Role of acidic amino acids in peptide substrates of the beta-adrenergic receptor kinase and rhodopsin kinase. Biochemistry. 1991 May 28;30(21):5118–5125.

227. Thathiah A, De Strooper B. The role of G protein-coupled receptors in the pathology of Alzheimer's disease. Nat Rev Neurosci. 2011 Feb;12(2):73–87.

228. Teng L, Zhao J, Wang F, Ma L, Pei G. A GPCR/secretase complex regulates beta- and gamma-secretase specificity for Abeta production and contributes to AD pathogenesis. Cell Res. 2010 Feb;20(2):138–153.

229. Villar VAM, Cuevas S, Zheng X, Jose PA. Localization and signaling of GPCRs in lipid rafts. Methods Cell Biol. 2016 Feb 10;132:3–23.

230. Annaert WG, Esselens C, Baert V, Boeve C, Snellings G, Cupers P, et al. Interaction with telencephalin and the amyloid precursor protein predicts a ring structure for presenilins. Neuron. 2001 Nov 20;32(4):579–589.

231. Esselens C, Oorschot V, Baert V, Raemaekers T, Spittaels K, Serneels L, et al. Presenilin 1 mediates the turnover of telencephalin in hippocampal neurons via an autophagic degradative pathway. J Cell Biol. 2004 Sep 27;166(7):1041–1054.

232. Bai X, Rajendra E, Yang G, Shi Y, Scheres SHW. Sampling the conformational space of the catalytic subunit of human γ-secretase. Elife. 2015 Dec 1;4:e11182.

233. Zhan X, Gimenez LE, Gurevich VV, Spiller BW. Crystal structure of arrestin-3 reveals the basis of the difference in receptor binding between two non-visual subtypes. J Mol Biol. 2011 Feb 25;406(3):467–478.

234. Dominguez C, Boelens R, Bonvin AMJJ. HADDOCK: a protein-protein docking approach based on biochemical or biophysical information. J Am Chem Soc. 2003 Feb 19;125(7):1731–1737.

235. van Zundert GCP, Rodrigues JPGLM, Trellet M, Schmitz C, Kastritis PL, Karaca E, et al. The HADDOCK2.2 Web Server: User-Friendly Integrative Modeling of Biomolecular Complexes. J Mol Biol. 2016 Feb 22;428(4):720–725.

236. Jo S, Lim JB, Klauda JB, Im W. CHARMM-GUI Membrane Builder for mixed bilayers and its application to yeast membranes. Biophys J. 2009 Jul 8;97(1):50–58.

237. Phillips JC, Braun R, Wang W, Gumbart J, Tajkhorshid E, Villa E, et al. Scalable molecular dynamics with NAMD. J Comput Chem. 2005 Dec;26(16):1781–1802.

238. Huang J, Rauscher S, Nawrocki G, Ran T, Feig M, de Groot BL, et al. CHARMM36m: an improved force field for folded and intrinsically disordered proteins. Nat Methods. 2017 Jan;14(1):71–73.

239. Klauda JB, Venable RM, Freites JA, O'Connor JW, Tobias DJ, Mondragon-Ramirez C, et al. Update of the CHARMM all-atom additive force field for lipids: validation on six lipid types. J Phys Chem B. 2010 Jun 17;114(23):7830–7843.

240. Humphrey W, Dalke A, Schulten K. VMD: visual molecular dynamics. J Mol Graph. 1996 Feb;14(1):, 27.

241. Cochet M, Donneger R, Cassier E, Gaven F, Lichtenthaler SF, Marin P, et al. 5-HT4 receptors constitutively promote the non-amyloidogenic pathway of APP cleavage and interact with ADAM10. ACS Chem Neurosci. 2013 Jan 16;4(1):130–140.

242. Zhao J, Deng Y, Jiang Z, Qing H. G Protein-Coupled Receptors (GPCRs) in Alzheimer's Disease: A Focus on BACE1 Related GPCRs. Front Aging Neurosci. 2016 Mar 24;8:58.

243. Lowther KM, Uliasz TF, Götz KR, Nikolaev VO, Mehlmann LM. Regulation of Constitutive GPR3 Signaling and Surface Localization by GRK2 and β-arrestin-2 Overexpression in HEK293 Cells. PLoS One. 2013 Jun 27;8(6):e65365.

244. Liu X, Zhao X, Zeng X, Bossers K, Swaab DF, Zhao J, et al. β-arrestin1 regulates γ-secretase complex assembly and modulates amyloid-β pathology. Cell Res. 2013 Mar;23(3):351–365.

245. Eichel K, Jullié D, Barsi-Rhyne B, Latorraca NR, Masureel M, Sibarita J-B, et al. Catalytic activation of β-arrestin by GPCRs. Nature. 2018 May 2;557(7705):381–386.

246. Bustos V, Pulina MV, Bispo A, Lam A, Flajolet M, Gorelick FS, et al. Phosphorylated Presenilin 1 decreases β-amyloid by facilitating autophagosome-lysosome fusion. Proc Natl Acad Sci USA. 2017 Jul 3;114(27):7148–7153.

247. Ledo JH, Liebmann T, Zhang R, Chang JC, Azevedo EP, Wong E, et al. Presenilin 1 phosphorylation regulates amyloid-β degradation by microglia. Mol Psychiatry. 2020 Aug 13;

248. Jumper J, Evans R, Pritzel A, Green T, Figurnov M, Ronneberger O, et al. Highly accurate protein structure prediction with AlphaFold. Nature. 2021 Aug;596(7873):583–589.

249. Yang G, Zhou R, Shi Y. Cryo-EM structures of human γ-secretase. Curr Opin Struct Biol. 2017 Oct;46:55–64.

250. Sun L, Zhao L, Yang G, Yan C, Zhou R, Zhou X, et al. Structural basis of human γ-secretase assembly. Proc Natl Acad Sci USA. 2015 May 12;112(19):6003–6008.

251. Gaidarov I, Krupnick JG, Falck JR, Benovic JL, Keen JH. Arrestin function in G protein-coupled receptor endocytosis requires phosphoinositide binding. EMBO J. 1999 Feb 15;18(4):871–881.

252. Civciristov S, Ellisdon AM, Suderman R, Pon CK, Evans BA, Kleifeld O, et al. Preassembled GPCR signaling complexes mediate distinct cellular responses to ultralow ligand concentrations. Sci Signal. 2018 Oct 9;11(551).

253. McCaw TR, Inga E, Chen H, Jaskula-Sztul R, Dudeja V, Bibb JA, et al. Gamma secretase inhibitors in cancer: A current perspective on clinical performance. Oncologist. 2021 Apr;26(4):e608–e621.

254. Long JM, Holtzman DM. Alzheimer disease: an update on pathobiology and treatment strategies. Cell. 2019 Oct 3;179(2):312–339.

255. Bursavich MG, Harrison BA, Blain J-F. Gamma secretase modulators: new alzheimer's drugs on the horizon? J Med Chem. 2016 Aug 25;59(16):7389–7409.

256. Pandey S, Kumari P, Baidya M, Kise R, Cao Y, Dwivedi-Agnihotri H, et al. Intrinsic bias at non-canonical, β-arrestin-coupled seven transmembrane receptors. Mol Cell. 2021 Sep;

257. Pine SR. Rethinking Gamma-secretase Inhibitors for Treatment of Non-small-Cell Lung Cancer: Is Notch the Target? Clin Cancer Res. 2018 Dec 15;24(24):6136–6141.

258. Jia H, Wang Z, Zhang J, Feng F. γ-Secretase inhibitors for breast cancer and hepatocellular carcinoma: From mechanism to treatment. Life Sci. 2021 Mar 1;268:119007.

259. Jeon YH, Ha M, Kim SW, Kim MJ, Lee C-S, Oh C-K, et al. Evaluation of the prognostic significances of γ-secretase genes in pancreatic cancer. Oncol Lett. 2019 May;17(5):4614–4620.

260. Sun W-Y, Wu J-J, Peng W-T, Sun J-C, Wei W. The role of G protein-coupled receptor kinases in the pathology of malignant tumors. Acta Pharmacol Sin. 2018 Nov;39(11):1699–1705.

261. Du AT, Schuv N, Amend D, Laakso MP, Hsu YY, Jagust WJ, et al. Magnetic resonance imaging of the entorhinal cortex and hippocampus in mild cognitive impairment and Alzheimer's disease. J Neurol Neurosurg Psychiatry. 2001;71:441–447.

262. Dickerson BC, Bakkour A, Salat DH, Feczko E, Pacheco J, Greve DN, et al. The cortical signature of Alzheimer's disease: regionally specific cortical thinning relates to symptom severity in very mild to mild AD dementia and is detectable in asymptomatic amyloid-positive individuals. Cereb Cortex. 2009 Mar;19(3):497–510.

263. Colović MB, Krstić DZ, Lazarević-Pašti TD, Bondžić AM, Vasić VM. Acetylcholinesterase inhibitors: pharmacology and toxicology. Curr Neuropharmacol. 2013 May;11(3):315–335.

264. Selkoe DJ. The therapeutics of Alzheimer's disease: where we stand and where we are heading. Ann Neurol. 2013 Sep;74(3):328–336.

265. Dong X, Wang Y, Qin Z. Molecular mechanisms of excitotoxicity and their relevance to pathogenesis of neurodegenerative diseases. Acta Pharmacol Sin. 2009 Apr;30(4):379–387.

266. Porsteinsson AP, Cosman KM. Memantine in the treatment of Alzheimer's disease. Aging Health. 2006 Dec;2(6):891–904.

267. Danysz W, Parsons CG, Mobius HJ, Stoffler A, Quack G. Neuroprotective and symptomatological action of memantine relevant for Alzheimer's disease--a unified glutamatergic hypothesis on the mechanism of action. Neurotox Res. 2000;2(2-3):85–97.

268. Reisberg B, Doody R, Stöffler A, Schmitt F, Ferris S, Möbius HJ, et al. Memantine in moderate-to-severe Alzheimer's disease. N Engl J Med. 2003 Apr 3;348(14):1333–1341.

269. Alexander GC, Knopman DS, Emerson SS, Ovbiagele B, Kryscio RJ, Perlmutter JS, et al. Revisiting FDA approval of aducanumab. N Engl J Med. 2021 Aug 26;385(9):769–771.

270. Willard SS, Koochekpour S. Glutamate, glutamate receptors, and downstream signaling pathways. Int J Biol Sci. 2013 Sep 22;9(9):948–959.

271. Hamilton A, Esseltine JL, DeVries RA, Cregan SP, Ferguson SSG. Metabotropic glutamate receptor 5 knockout reduces cognitive impairment and pathogenesis in a mouse model of Alzheimer's disease. Mol Brain. 2014 May 29;7:40.

272. Um JW, Kaufman AC, Kostylev M, Heiss JK, Stagi M, Takahashi H, et al. Metabotropic glutamate receptor 5 is a coreceptor for Alzheimer aβ oligomer bound to cellular prion protein. Neuron. 2013 Sep 4;79(5):887–902.

273. Hamilton A, Vasefi M, Vander Tuin C, McQuaid RJ, Anisman H, Ferguson SSG. Chronic Pharmacological mGluR5 Inhibition Prevents Cognitive Impairment and Reduces Pathogenesis in an Alzheimer Disease Mouse Model. Cell Rep. 2016 May 31;15(9):1859–1865.

274. Lo AC, De Maeyer JH, Vermaercke B, Callaerts-Vegh Z, Schuurkes JAJ, D'Hooge R. SSP-002392, a new 5-HT4 receptor agonist, dose-dependently reverses scopolamine-induced learning and memory impairments in C57Bl/6 mice. Neuropharmacology. 2014 Oct;85:178–189.

275. Zhang G, Ásgeirsdóttir HN, Cohen SJ, Munchow AH, Barrera MP, Stackman RW. Stimulation of serotonin 2A receptors facilitates consolidation and extinction of fear memory in C57BL/6J mice. Neuropharmacology. 2013 Jan;64:403–413.

276. Barthet G, Framery B, Gaven F, Pellissier L, Reiter E, Claeysen S, et al. 5-hydroxytryptamine 4 receptor activation of the extracellular signal-regulated kinase pathway depends on Src activation but not on G protein or beta-arrestin signaling. Mol Biol Cell. 2007 Jun;18(6):1979–1991.

277. Göőz M, Göőz P, Luttrell LM, Raymond JR. 5-HT2A receptor induces ERK phosphorylation and proliferation through ADAM-17 tumor necrosis factor-alpha-converting enzyme (TACE) activation and heparin-bound epidermal growth factor-like growth factor (HB-EGF) shedding in mesangial cells. J Biol Chem. 2006 Jul 28;281(30):21004–21012.

278. Misane I, Ogren SO. Selective 5-HT1A antagonists WAY 100635 and NAD-299 attenuate the impairment of passive avoidance caused by scopolamine in the rat. Neuropsychopharmacology. 2003 Feb;28(2):253–264.

279. Yamazaki M, Okabe M, Yamamoto N, Yarimizu J, Harada K. Novel 5-HT5A receptor antagonists ameliorate scopolamine-induced working memory deficit in mice and reference memory impairment in aged rats. J Pharmacol Sci. 2015 Mar;127(3):362–369.

280. Francken BJ, Jurzak M, Vanhauwe JF, Luyten WH, Leysen JE. The human 5-ht5A receptor couples to Gi/Go proteins and inhibits adenylate cyclase in HEK 293 cells. Eur J Pharmacol. 1998 Nov 20;361(2-3):299–309.

281. Gonzalez R, Chávez-Pascacio K, Meneses A. Role of 5-HT5A receptors in the consolidation of memory. Behav Brain Res. 2013 Sep 1;252:246–251.

282. Woods S, Clarke NN, Layfield R, Fone KCF. 5-HT(6)' ' receptor agonists and antagonists enhance learning and memory in a conditioned emotion response paradigm by modulation of cholinergic and glutamatergic mechanisms. Br J Pharmacol. 2012 Sep;167(2):436–449.

283. Ramírez MJ. 5-HT6 receptors and Alzheimer's disease. Alzheimers Res Ther. 2013 Apr 22;5(2):15.

284. Lu B, Nagappan G, Lu Y. BDNF and synaptic plasticity, cognitive function, and dysfunction. Handb Exp Pharmacol. 2014;220:223–250.

285. Marcos B, Cabero M, Solas M, Aisa B, Ramirez MJ. Signalling pathways associated with 5-HT6 receptors: relevance for cognitive effects. Int J Neuropsychopharmacol. 2010 Jul;13(6):775–784.

286. Albasanz JL, Perez S, Barrachina M, Ferrer I, Martín M. Up-regulation of adenosine receptors in the frontal cortex in Alzheimer's disease. Brain Pathol. 2008 Apr;18(2):211–219.

287. Borota D, Murray E, Keceli G, Chang A, Watabe JM, Ly M, et al. Post-study caffeine administration enhances memory consolidation in humans. Nat Neurosci. 2014 Feb;17(2):201–203.

288. Arendash GW, Schleif W, Rezai-Zadeh K, Jackson EK, Zacharia LC, Cracchiolo JR, et al. Caffeine protects Alzheimer's mice against cognitive impairment and reduces brain beta-amyloid production. Neuroscience. 2006 Nov 3;142(4):941–952.

289. Dall'Igna OP, Fett P, Gomes MW, Souza DO, Cunha RA, Lara DR. Caffeine and adenosine A(2a) receptor antagonists prevent beta-amyloid (25-35)-induced cognitive deficits in mice. Exp Neurol. 2007 Jan;203(1):241–245.

290. Orr AG, Hsiao EC, Wang MM, Ho K, Kim DH, Wang X, et al. Astrocytic adenosine receptor A2A and Gs-coupled signaling regulate memory. Nat Neurosci. 2015 Mar;18(3):423–434.

291. Santschi LA, Zhang X, Stanton PK. Activation of receptors negatively coupled to adenylate cyclase is required for induction of long-term synaptic depression at Schaffer collateral-CA1 synapses. J Neurobiol. 2006 Feb 15;66(3):205–219.

292. Ishitobi Y, Nakayama S, Yamaguchi K, Kanehisa M, Higuma H, Maruyama Y, et al. Association of CRHR1 and CRHR2 with major depressive disorder and panic disorder in a Japanese population. Am J Med Genet B, Neuropsychiatr Genet. 2012 Jun;159B(4):429–436.

293. Park H-J, Ran Y, Jung JI, Holmes O, Price AR, Smithson L, et al. The stress response neuropeptide CRF increases amyloid-β production by regulating γ-secretase activity. EMBO J. 2015 Jun 12;34(12):1674–1686.

294. Rapp MA, Schnaider-Beeri M, Grossman HT, Sano M, Perl DP, Purohit DP, et al. Increased hippocampal plaques and tangles in patients with Alzheimer disease with a lifetime history of major depression. Arch Gen Psychiatry. 2006 Feb;63(2):161–167.

295. Campbell SN, Zhang C, Roe AD, Lee N, Lao KU, Monte L, et al. Impact of CRFR1 Ablation on Amyloid-β Production and Accumulation in a Mouse Model of Alzheimer's Disease. J Alzheimers Dis. 2015;45(4):1175–1184.

296. Dong H, Wang S, Zeng Z, Li F, Montalvo-Ortiz J, Tucker C, et al. Effects of corticotrophin-releasing factor receptor 1 antagonists on amyloid-β and behavior in Tg2576 mice. Psychopharmacology. 2014 Dec;231(24):4711–4722.

297. Bale TL, Vale WW. Increased depression-like behaviors in corticotropin-releasing factor receptor-2-deficient mice: sexually dichotomous responses. J Neurosci. 2003 Jun 15;23(12):5295–5301.

298. Reul JMHM, Holsboer F. On the role of corticotropin-releasing hormone receptors in anxiety and depression. Dialogues Clin Neurosci. 2002 Mar;4(1):31–46.

299. Chalmers DT, Lovenberg TW, De Souza EB. Localization of novel corticotropin-releasing factor receptor (CRF2) mRNA expression to specific subcortical nuclei in rat brain: comparison with CRF1 receptor mRNA expression. J Neurosci. 1995 Oct;15(10):6340–6350.